Experimental Design of a Solar-Heated Water Displacement Pump

José Reis

Master Thesis
MSc Integrated Product Design

Supervisors
Sepideh Ghodrat
Joost Alferink
Hubert Linssen

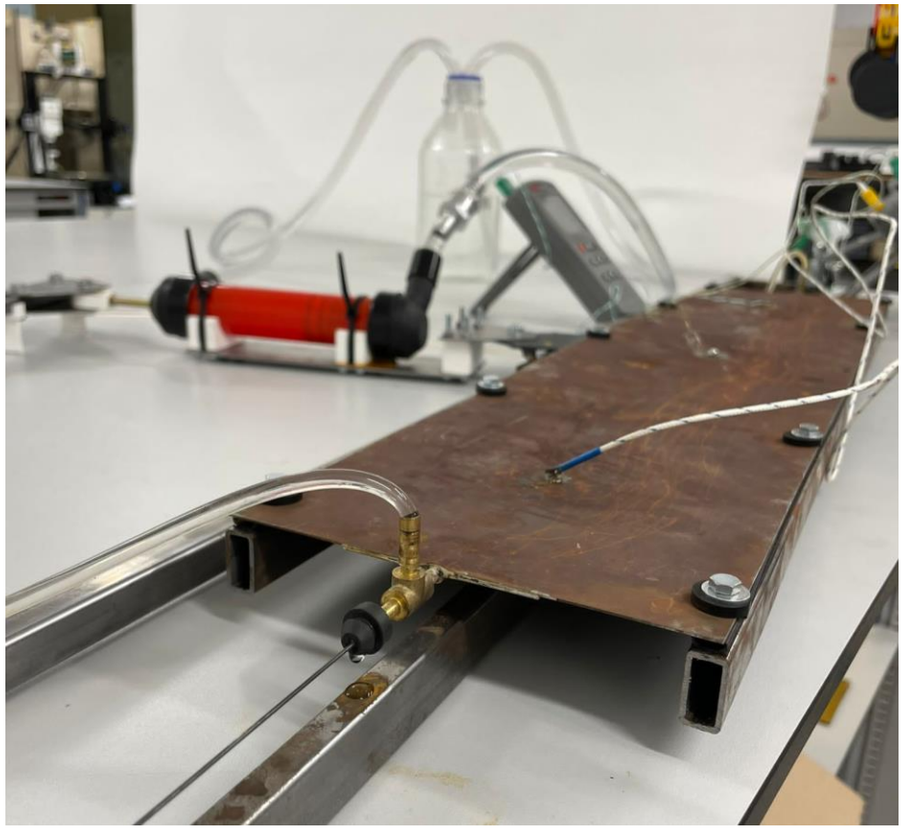

January 2024

Experimental Design of a Solar-Heated Water Displacement Pump

José Reis

MSc Integrated Product Design
Faculty of Industrial Design Engineering
Delft University of Technology

Supervisors
Sepideh Ghodrat
Joost Alferink
Hubert Linssen

TU Delft

Preface

This project comes about as the final and graduating project of the Master's of Integrated Product Design at the Faculty of Industrial Design Engineering of TU Delft, which is an advanced design programme that integrates design, technology, and research to enable students to develop new perspectives on product design.

The faculty stands for its mission to Design for Our Future and challenge students to shape innovative, sustainable, and ethical products that benefit people, society, and the planet, which this present work reflects.

In fact, the assignment of designing an affordable, robust, and scalable solar-heated water displacement pump focused on its implementation in areas lacking access to safe drinking water by conducting extensive research, investigating working principles and innovative materials, creatively thinking about applications, and applying advanced design methodologies to create an efficient and sustainable water transportation solution is a great challenge worth the level of a Master's thesis that aligns with the faculty's learning objectives of:

- *Creating innovative and responsible products and product services that balance the interests of people, organisations, and the environment.*
- *Mastering the use of design and engineering methods, tools, and technologies to shape product design processes effectively.*
- *Developing technical prototyping skills and experimentation to bring creative ideas to life.*
- *Integrating technology and design to create impactful solutions through emerging fields like digital innovation, sustainability principles and novel materials.*

With this, TU Delft trains a new generation of designers who create a positive impact in Our future which justified my decision to come to the Netherlands and pursue this transformative experience.

Acknowledgements

First and foremost, I would like to express my gratitude to my supervisory team Sepideh Ghodrat, Joost Alferink and Hubert Linssen, for placing your trust in me and giving me the opportunity to develop such a project. Your patience, enthusiasm and guidance throughout this challenging journey have truly contributed to its results.

A heartfelt thank you goes to my whole family. Especially to my Mother, Father, and brothers Manel and Afonso, for your unconditional love, belief, support and guidance and for being the greatest and most vivid example of service I have known. To my Aunt Salette and Uncle José Fernando, I thank you for the huge help in the proofreading and final efforts of this project through your hospitality, support, patience, knowledge, and willingness to push me to my best.

Lastly, I would like to thank all my friends. Special thanks to my friends João, Miguel, Niyaz, Serrita and Tomás for your friendship, emotional support, contagious happiness and example. To Diogo for your companionship beyond the prototyping workshops and for the fruitful discussions, knowledge, and support during this project. To my Formula Student friends for making my summer break so memorable. Last but not least, I would like to express my deep gratitude to all my friends in Delft, especially the Portuguese family, my housemates and Leafy, for sharing this incredible and memorable journey with me and making me feel at home in Delft. I will always carry your friendships, sense of humour and our memories in my heart with me on my future adventures.

Figure 1: Men collecting water from a dug well in Africa. Photographed by Giulio Napolitano.

Executive Summary

The report at hand is a comprehensive summary of the conducted research and consequent developments in the experimental design of a solar-heated water displacement pump focused on its implementation in areas lacking access to safe drinking water, particularly in developing countries.

The research begins by examining the dire situation faced by the two billion people lacking safely managed drinking water (WHO/UNICEF JMP, 2023). This is done by looking closer at the factors influencing water supply, considering needs and the context in which these affected people live.

This contextual analysis motivated the need to develop a solar-powered water pump system designed to effectively, reliably and sustainably bring safe drinking water from improved water sources to households in the most affected regions of the world.

To address this need, existing pumping systems that are currently used or have the potential to mitigate this problem were studied and evaluated.

By carefully examining the most recent advancements in relevant water pumping technologies for this contextual application, the opportunity to use Shape Memory Alloys (SMAs) for converting low-grade heat energy into mechanical energy was identified.

Having identified the problem and understood its context, analysed the existing solutions and identified a potentially disruptive hypothesis, an innovative system of an affordable, robust, and scalable solar-heated water displacement pump was designed.

In addition, the design was validated with a high-fidelity prototype with which experiments were done to successfully prove the concept's working principle.

This prototype elegantly integrates a Shape Memory Alloy in a solar collector using the absorbed heat to contract the wire. This elongation is associated with a force that is used to drive the piston of a displacement pump to pump water. To do this cycle repeatedly, a fraction of the pumped water is used to cool the Shape Memory Alloy, making it reversibly return to its initial state and restarting the cycle.

The successful proof of concept aligns with the established objectives of simplicity and accessibility. In fact, the water pump prototype was created on a minimal budget, making use of simple and accessible tools and materials, highlighting its potential for scalable cost-effective manufacturing.

This report provides a comprehensive analysis of the performance of the prototype, along with the theoretical design considerations that influenced its development. As a result, it serves as an experimental logbook that also offers insights into the existing water crisis and contributes to a better understanding of it. Thus, the present work lays the foundation for future research and developments on this innovative working principle, making it a valuable contribution to this life-changing field.

Figure 2: Preview of the prototyped proof of concept.

Contents

Brief
Preface . . . i
Acknowledgements . . . ii
Executive Summary . . . iv
Contents . . . vi
Introduction . . . 1

Context
Global Overview . . . 5
Problem and its Evolution – Call for Action . . . 7
Zooming In . . . 9
Decentralised Solutions Powered by Solar Energy . . . 15

State-of-the-art
Solar-Powered Water Pumps Overview . . . 19
Thermodynamic Cycles . . . 21
Photovoltaic Panels . . . 23
Augmenting the State-of-the-art . . . 25
Opportunity – Shape Memory Alloys . . . 27

Design Direction
Design Challenge . . . 31
Requirements . . . 31
Design Direction – Approach . . . 32
Conversion of Heat into Mechanical Energy . . . 33
Shape Memory Alloy-Driven Pumping Element . . . 34
Heating and Cooling of the Shape Memory Alloy . . . 35
Integration of the Subsystems . . . 37

Experimental Design
Approach . . . 41
Validation of Shape Memory Alloy and Concept Potential . . . 43
Design Iteration . . . 53
Design Iteration Validation . . . 63

Conclusion
Conclusions . . . 79
Future Recommendations . . . 80

References . . . 81

Appendixes
Appendix A . . . 85
Appendix B . . . 95
Appendix C . . . 101
Appendix D . . . 115
Appendix E . . . 121
Appendix F . . . 131

Introduction

The goal of this master's graduation project is to perform an experimental design of a Shape Memory Alloy (SMA) driven solar-heated water displacement pump focused on its implementation in areas lacking access to safe drinking water, particularly in developing countries.

This is motivated by the identified opportunity of using Shape Memory Alloys as the working medium to transform low-grade heat energy into mechanical energy.

In fact, Shape Memory Alloys have the particular characteristic of changing their crystalline organisation at low temperatures. This phase transformation is associated with a change in macroscopic shape that is paired with a significant tension. This tension and paired strain together are output mechanical labour that can be used to pump water.

Thus, heating the SMA above the phase transformation temperature, which usually varies from ambient temperature up to 100ºC, makes the SMA deform and produce output work. If then cooled down, the SMA can be reversibly deformed, which means that the cycle can be started again. By heating and cooling the SMA repeatedly, the output work can be used to power a water pump.

If SMAs are integrated into such a system that heats and cools the SMA alternately with the heat collected from the sun, a valuable solar-heated water pump is created.

Hence, the goal of this project is to design an affordable, robust, and scalable solar-heated water displacement pump. This will be done by conducting extensive research, investigating innovative materials and working principles, creatively thinking about applications, and applying advanced design methodologies to create an efficient and sustainable water transportation solution.

Thus, extensive research was first done to motivate this endeavour and understand the potential of such a pump. The chapter Context alerts for the two billion people without access to safely managed drinking water at their premises(WHO/UNICEF JMP,2023). This is prevalent in less developed regions, particularly in Sub-Saharan Africa.

As identified, the issue has little to do with a lack of water resources but rather results from the lack of water infrastructure. Following the example of more developed regions, such as Europe or North America, it is clear that proper and sustainable infrastructure mitigates the issue (Tortajada, 2014).

A key element needed for sustainable water infrastructure is a cheap, reliable, scalable and robust water pump that is powered by renewable and locally harnessed energy.

Among the various energy sources available, solar energy is the one with the most potential to universally contribute to mitigating the issue in the most affected regions of the world.

In fact, the areas where access to water is least available and where water pumps are most needed coincidently have the highest solar exposure (World Bank Group, 2020).

Thus, a solar-powered water pump has immense value in mitigating the issue. However, due to the economic situation of such regions, the pump system has to be as cheap as possible.

That is the point where the SMAs come into play. A simpler and minimally efficient pumping principle based on SMA can potentially disrupt the state-of-the-art of solar pump technology and thus contribute significantly to sustainable water infrastructure and provide water to the premises of the immense number of people in need.

Since SMAs have not yet been integrated into a solar-powered displacement pump, this project is an experimental exploration of the potential of this innovative system, never losing the focus on how the studied principles can be integrated into a feasible and viable system.

Thus, after the motivation and implementation context of this project, the report highlights the main findings and necessary background knowledge, as well as analysing relevant existing technologies.

With these findings, a design direction is defined, and the experimental design phase is started. In this report, the steps and experiments performed are thoroughly showcased, supporting the developments and allowing a well-based extrapolation of the state of the pump by the end of this project.

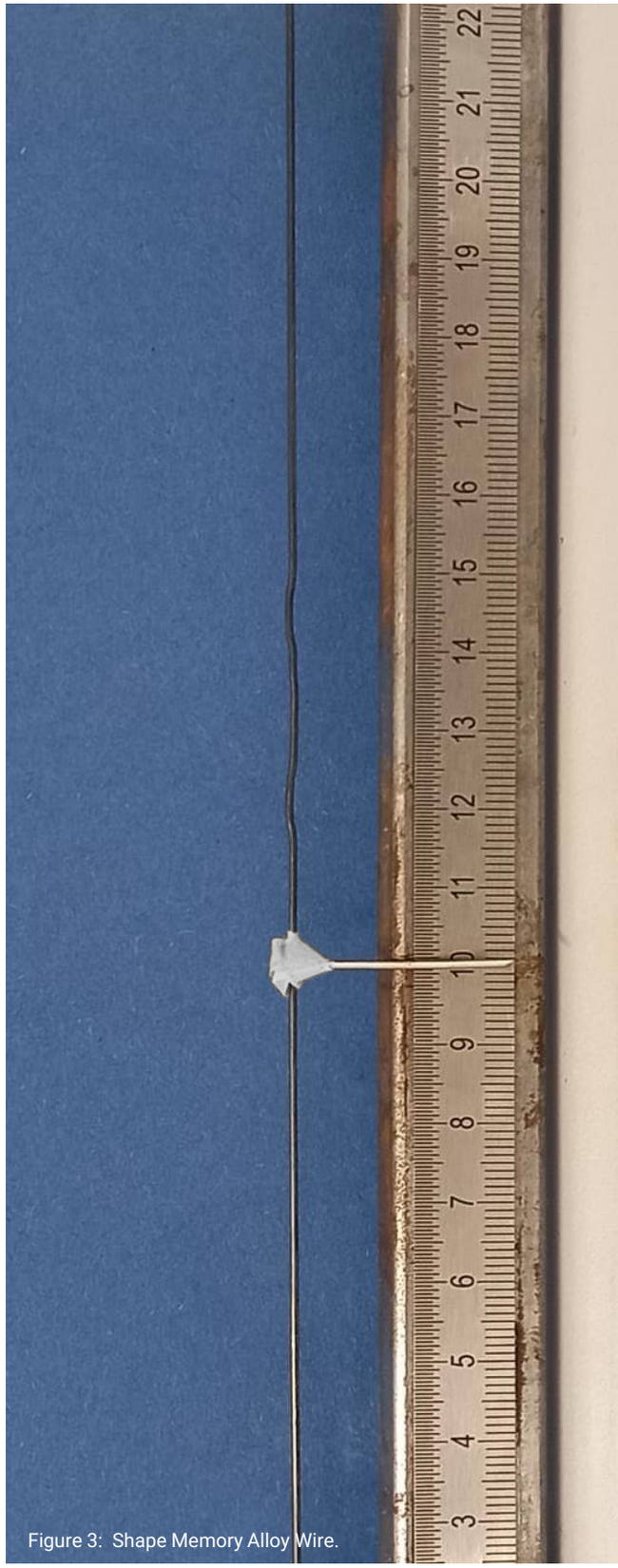

Figure 3: Shape Memory Alloy Wire.

Context

This chapter explores the context behind the lack of access to safe drinking water. This is done by delving through the layers of this urgent and complex global issue.

Through mapping and quantification, and through the identification of the multiple aspects that influence access to water, the solution scope is defined.

Contents

- Global Overview
- Problem and its Evolution – Call for Action
- Zooming In
- Decentralised Solutions Powered by Solar Energy

Photography Credit: John Phillips

Global Overview

In the present day, two billion people lack access to safely managed drinking water (WHO/UNICEF JMP, 2023).

This means that one out of every four people in the world lacks access to "*drinking water from an improved source that is accessible on premises, available when needed and free from faecal and priority chemical contamination*" (WHO/UNICEF JMP, 2023).

Moreover, and breaking down the substantial number, out of the 2 billion people affected, 1.6 billion have access to drinking water from an improved water source - *"that includes piped water, boreholes or tubewells, protected dug wells, protected springs, rainwater, and packaged or delivered water"* (WHO/UNICEF JMP, 2023) - but that is not available at their premises (Figure 4).

Consequently, for 1.6 billion people, collecting water is a task that is part of the daily routine of the members of their households.

Furthermore, for 300 million of these people, each walk for the collection of water from the water source to their homes takes more than half an hour, which often has to be done multiple times a day to meet the needs of their communities (WHO/UNICEF JMP, 2023).

In principle, providing means of water transportation from the improved water sources to their premises would replace each roundtrip and solve the issue for these affected people. Unfortunately, due to the scale, depth, and urgency of the problem, in practice, it is not that simple.

As known, the United Nations, in 2015, agreed on a set of global objectives that are a universal call for action to provide access to basic needs, protect the planet, and ensure prosperity for all by 2030. One of these Sustainable Development Goals is SDG 6 – *ensuring the availability and sustainable management of water and sanitation for all* (A/RES/70/1, 2015).

Therefore, to meet the set SDG 6, these two billion people without this basic need must have access to safe drinking water before 2030.

However, despite the ongoing global effort, this dire situation persists without significant improvement for a quarter of the world's population (United Nations Department of Economic and Social Affairs, 2023).

Thus, to gain a deeper insight into the reasons behind this persistent challenge, this chapter extensively explores the layers of the problem.

This chapter's research aims to:

- Acknowledge the evolution of the present problem and understand the urgency of it – Appendix A.
- Analyse the regions where the problem is most severe, relating demographical, geographical, and economic factors – Appendix B.
- Understand the local challenges, struggles and needs regarding water supply.
- Frame a solution scope for mitigating the issue and goals for this project.

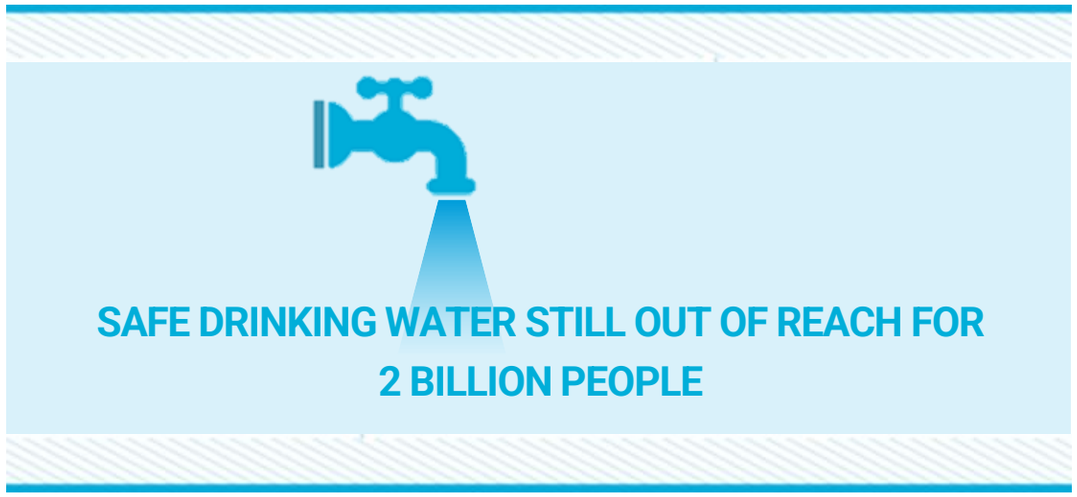

Figure 4: Infographic of global water access context (WHO/UNICEF JMP, 2023).

Problem and its Evolution – Call for Action

The global overview quantifies the severity of the water problem our society is facing, highlighting that there has been a considerably significant global effort aimed at making the Sustainable Development Goals a worldwide reality.

Remarkably, since the settlement of the SDGs in 2015, an average of ten billion dollars have been disbursed annually to assist the development of the water sector (WHO/UNICEF JMP, 2023).

However, despite these substantial efforts, the pace of progress and the evolution of the global situation, as seen in Figure 5, remain insufficient to meet the ultimately settled goal.

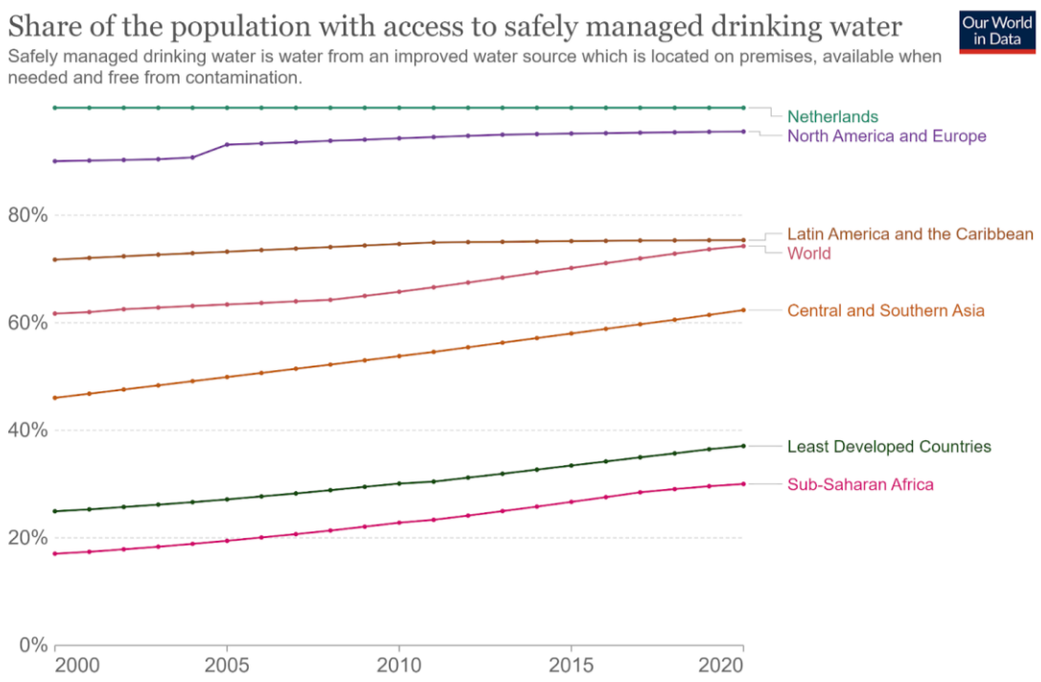

Figure 5: Share of Population with access to safely managed drinking water based on WHO/UNICEF Joint Monitoring Program (JMP) data (Our World in Data, 2023).

In fact, at the current rate of progress, the world will only reach 81% coverage by 2030.

As a result, the target will be missed, and 1.6 billion people will remain without safely managed drinking water.

In order to cover 100% of the globe's population by 2030, the pace of progress per year must increase by six times (United Nations JMP, 2023).

Thus, it is evident that the progress in mitigating this issue is far from satisfactory.

On top of that, a closer examination of the regional breakdown within the global statistics reveals a discrepancy between different regions worldwide.

On a positive note, there are examples of success where water access is available to the entire population.

However, on the other side of the spectrum, there is the alarming situation of regions such as Sub-Saharan Africa where 70% of the population, that is 847 million people, lack access to safely managed drinking water (Our World in Data, 2023).

Moreover, examining the water access crisis from a different perspective and looking at nominal total numbers in Figure 6 provides a more comprehensive understanding of the depth of the water access crisis in the most severely affected regions of the world, particularly Sub-Saharan Africa.

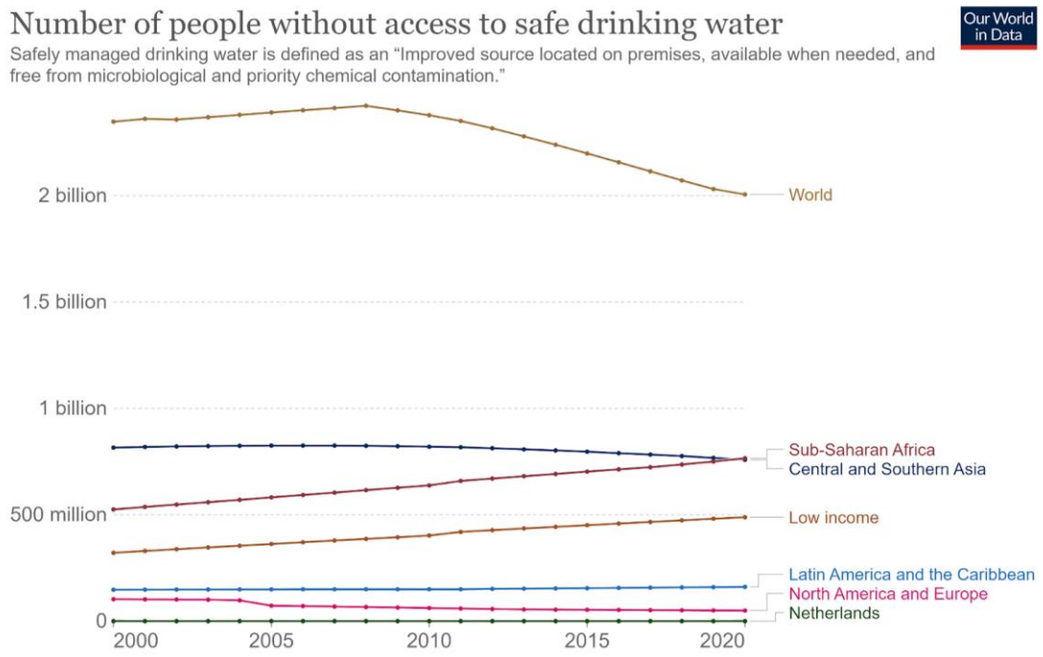

Figure 6: Number of people without access to safe drinking water based on WHO/UNICEF Joint Monitoring Program (JMP) data (Our World in Data, 2023).

In fact, despite the percentual increase in access to safely managed drinking water in Sub-Saharan Africa, the simultaneous rise in population reveals the staggering reality that the number of people affected in this region has actually increased.

As a matter of fact, the population of Sub-Saharan Africa has doubled since the beginning of the new millennium. This significant demographic shift led to a 50% increase in individuals without access to such a basic need as safe drinking water (Our World in Data, 2023).

The in-depth analysis presented in Appendix A highlights the intricate and complex nature of the global crisis addressed in this project. In fact, it is a crisis that is set to become even more challenging over this century due to the relentless growth of the population and the escalating impacts of climate change.

Thus, the call for action could not be more urgent. To meet sustainable development goal six and ensure universal access to the basic need for safe water on people's premises, an intensification of investments and efforts is needed. For, technology holds the key to making this the reality for all, rather sooner than later.

Zooming In

Contextual Disparities

As verified, breaking down the global figures by region reveals a significant discrepancy in access to safe water. In fact, it is observed that while regions such as Europe and North America report near-universal access to water, regions like Sub-Saharan Africa and Central and Southern Asia, in contrast, outline a dire reality where access is still lacking for more than a third of the population (Our World in Data, 2023).

This uneven distribution underscores a geographic disparity that demands focused attention to understand the underlying causes.

Thus, the following contextual analysis, and more in-depth analysis in Appendix B, focuses on identifying and comprehending these factors, starting with the most pertinent question raised regarding the root cause of such differences:

Do these regions lack access to water in general?

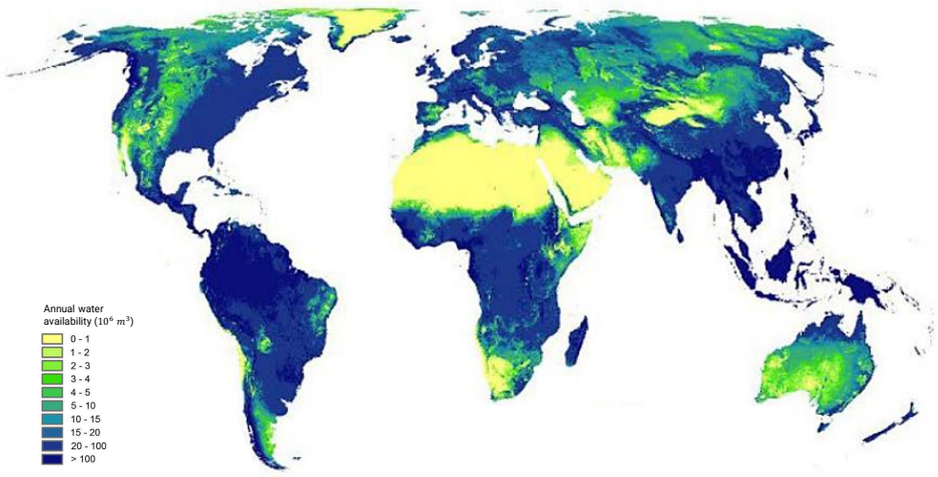

Figure 7: Global annual natural renewable water availability map with 0.1 degrees resolution (11.1km*11.1km) (Vanham et al., 2022).

As Figure 7 suggests, the answer is no. The global renewable water availability map fails to identify a direct reason for the lack of access to drinking water, as confirmed in Appendix B.

In fact, Southeast Asia is the region of the world with the most water resources and still is one with the least access to safe water.

Thus, access to safe drinking water is not directly linked to the abundance or scarcity of water resources.

Instead, as concluded in Appendix B, it results from limited infrastructure and limited water management and transportation systems.

This results from a long-present lack of monetary resources and proper investment in water-related and general infrastructure. This situation can be verified by looking at Figure 8, which showcases the undeveloped electrical grid in the African continent compared to Europe.

Figure 8: Map of the electrical grid of the EMEA Region using a predictive model for accurate electrical grid mapping (Gersherson et al., 2019)

Infrastructure's Impact on Water Availability and Communities

In fact, infrastructure development is the most direct solution to mitigate the lack of access to safely managed drinking water (WHO/UNICEF JMP, 2023).

Firstly, proper infrastructure enables effective management of water resources, ensuring a reliable supply throughout the year and guaranteeing water availability even in times of scarcity (Figure 9).

Secondly, the distribution of water from available sources to everyone's premises is only possible with distribution networks, which include proper storage, filtering or treatment facilities, piped networks and pumps.

Despite all of these being essential to ensure safe drinking water is accessible to everyone, pumps have a key role in it as pumps provide the mechanical force necessary to move water from the source to its final destination, overcoming geographical and gravitational challenges.

Without pumps and proper distribution infrastructure, there is a lack of access to safe drinking water in households, forcing people to collect water themselves (Figure 10).

This is the reality of the most affected regions of the world where the limited or non-existent infrastructure ultimately results in individuals having to spend a significant amount of time ensuring that they and their households have access to this basic need (Figure 11).

Figure 9: Water supply chaos during a drought season in Chennai, India, 2019.

Figure 10: Women in Aweil, Northern Bahr el Ghazal, collect water from a nearby water source to irrigate their fields, 2009.

1.6 BILLION PEOPLE TAKE THE STEPS TO HAVE ACCESS TO SAFE DRINKING WATER TOO LITERALLY

In Asia

One roundtrip to collect water is **21 minutes** on average **in rural areas** and **19 minutes in urban areas**

In Sub-Saharan Africa

One roundtrip to collect water takes **33 minutes** on average **in rural areas** and **25 minutes in urban areas**

For 29% of the population (37% in rural areas and 14% in urban areas), **improved drinking water sources are more than 30 minutes away**

Sub-Saharan Africans Spend **40 Billion Hours a Year Collecting Water**

Figure 11: Infographic on water collection duration in Asia and Sub-Saharan Africa (WHO/UNICEF, 2023)

Local Needs

This dire reality is even more alarming when considering that people carry 20L of water for at least half of each trip (WHO/UNICEF JMP, 2023).

In fact, the aforementioned roundtrip durations translate to an average of 6 kilometres a day, carrying 20 litres or 20 kilograms of water, as the distance between households and safely managed drinking water sources is, on average, within 2.5 to 3.5 km (van Ginneken et al., 2011).

According to a study performed in the Nampula province in Mozambique measuring route paths and distances to water sources for 1103 households (Ho J.C. et al., 2014), the walking pace when fetching water is, on average, 3.75 km/h.

In Figure 12, an illustrative sample village is mapped, identifying the water sources, route paths and distances between the water sources and the community households.

In this study, a total of 54 clusters of households were selected at random, adding that the mean number of people per household was 4.1 and that 76% of the water collection route's terrain was sandy.

In addition, the people studied use an average of 23.2 L of water per capita per day, with a median value of 19.9 L.

This means that the people responsible for the daily collection of water often have to walk the roundtrip more than once a day – in this study, an average of 13 times a week (Ho J.C. et al., 2014).

In principle, a pumping system and a water transportation network replace each of these roundtrips, bringing water from the water sources to the households' premises. Thus, a pumping system is the key solution to this critical and severe issue.

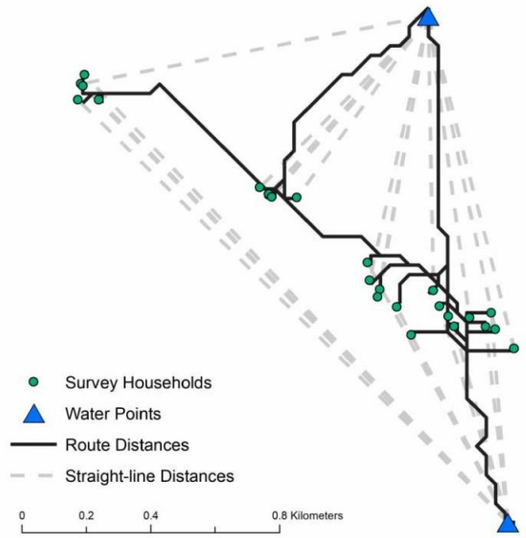

Figure 12: Mapped water sources and route paths and distances for households in a sample village in Nampula province, Mozambique (Ho J.V.et al., 2014).

A PUMPING SYSTEM REPLACING EACH OF THE WATER FETCHING ROUNDTRIPS BRINGS WATER TO HOUSEHOLDS' PREMISES, SOLVING THE PRESSING ISSUE

Infrastructure and Local Constraints

Although investing in infrastructure would help mitigate the present issue, it is vital to recognise that solutions proven successful in regions like Europe and North America may not directly apply to Sub-Saharan Africa and Central and Southern Asia since these regions lack basic surrounding infrastructure.

This means that replicating such complex infrastructure in these regions isn't feasible in the short term.

For instance, simply installing an electric pump connected to the electrical grid, which is prevalent in more developed regions, is not feasible in these regions where a reliable electric grid is non-existent.

As a matter of fact, for most of the population in Africa, the electrical grid is either absent or highly unreliable.

This gap means relying solely on electricity to pump water is not possible at the moment.

In addition, considering the economic landscape of Sub-Saharan Africa, reliance on fossil fuels for water pumping systems poses significant challenges as well. The expense of buying and transporting fuels and their volatile and inflation-dependent availability make using them an unsustainable and often unaffordable solution (Figure 13).

Therefore, looking at alternative and more tailored approaches for these dispersed and spread-out regions, decentralised and locally implemented solutions stand out to offer practical and effective means to address the issue at the local level.

Figure 13: Fuel shortages in Lagos, Nigeria, 2019. Photograph from Nairametrics.com.

Decentralised Solutions Powered by Solar Energy

However, powering decentralised systems requires harnessing locally available energy sources.

Among the various energy sources available, solar energy is the one with the most potential to contribute to the universal mitigation of the issue in the most affected regions of the world.

Firstly, this is due to the fact that the most affected regions of the world are coincidently the regions of the world with the highest solar exposition (World Bank Group, 2020).

Africa, particularly, is abundantly exposed to sunlight, ranking on top as the continent with the most solar exposure.

Secondly, the amount of energy that the earth receives from the sun is immense. In fact, the Earth gets more solar energy in one hour than the entire world uses in a year (Nussey, 2019). As seen in the daily totals of irradiance in Figure 14, significant amounts of solar energy per square meter can be harnessed for water pumping.

Hence, harnessing solar energy is a powerful, decentralised and reliable means of powering water transportation systems. This is evident in the ability to be implemented in a wide range of geographical settings since it can be harnessed anywhere the sun shines, particularly around the Equator, where it can be obtained reliably throughout the year (World Bank Group, 2020). Moreover, solar energy provides flexibility since it can be scaled to meet specific local needs by increasing or decreasing the area of collection.

Additionally, sustainability is another key benefit of solar-powered systems. By using solar energy, the dependence on grid electricity and fossil fuels is reduced, minimising the environmental impact while also reducing the operational costs.

Considering these advantages, solar energy has all the characteristics to be the energy source that powers change in the lives of people in need.

Therefore, in the following chapter, state-of-the-art water pumping systems that are powered by solar energy are identified and analysed.

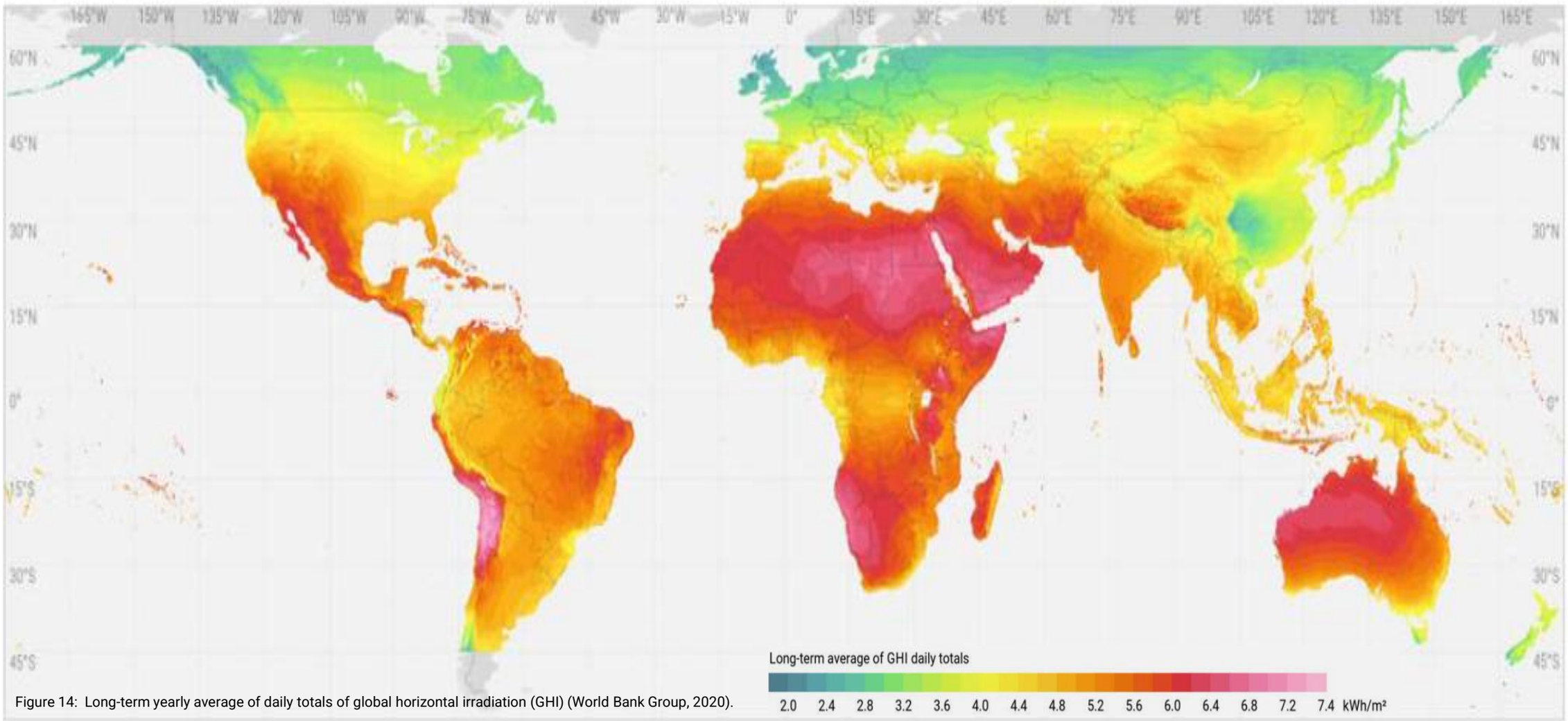

Figure 14: Long-term yearly average of daily totals of global horizontal irradiation (GHI) (World Bank Group, 2020).

State-of-the-art

Over the past century, researchers and innovators have recognised the potential of harnessing solar energy to address water challenges. Their endeavours have led to the development of solar-powered water pumping systems, where solar energy is transformed into mechanical energy and, ultimately, used to pump water.

In this chapter, the leading solutions are analysed and compared, and a breakthrough opportunity is identified.

Contents

- Solar-Powered Water Pumps Overview
- Thermodynamic Cycles
- Photovoltaic Panels
- Augmenting the State-of-the-art

Photography Credit: GOJO Organization

Solar-Powered Water Pumps Overview

The constant effort to harness solar energy has resulted in the development of innovative systems that have proven the potential of solar-powered water pumping systems.

Solar-powered water pumps, in principle, harness the incoming radiation, transforming it into usable power that is then used to pump water.

As seen in Figure 15, these systems can be characterised based on their working principles. The first distinction lies in the energy conversion principle. On the one hand, there are systems that collect solar energy as heat, using thermodynamic cycles to convert it to mechanical energy, which, ultimately, is used to pump water. On the other hand, there are systems that transform solar radiation firstly into electrical power, through the photoelectric effect, by means of photovoltaic panels, using this electrical energy to power electric water pumps.

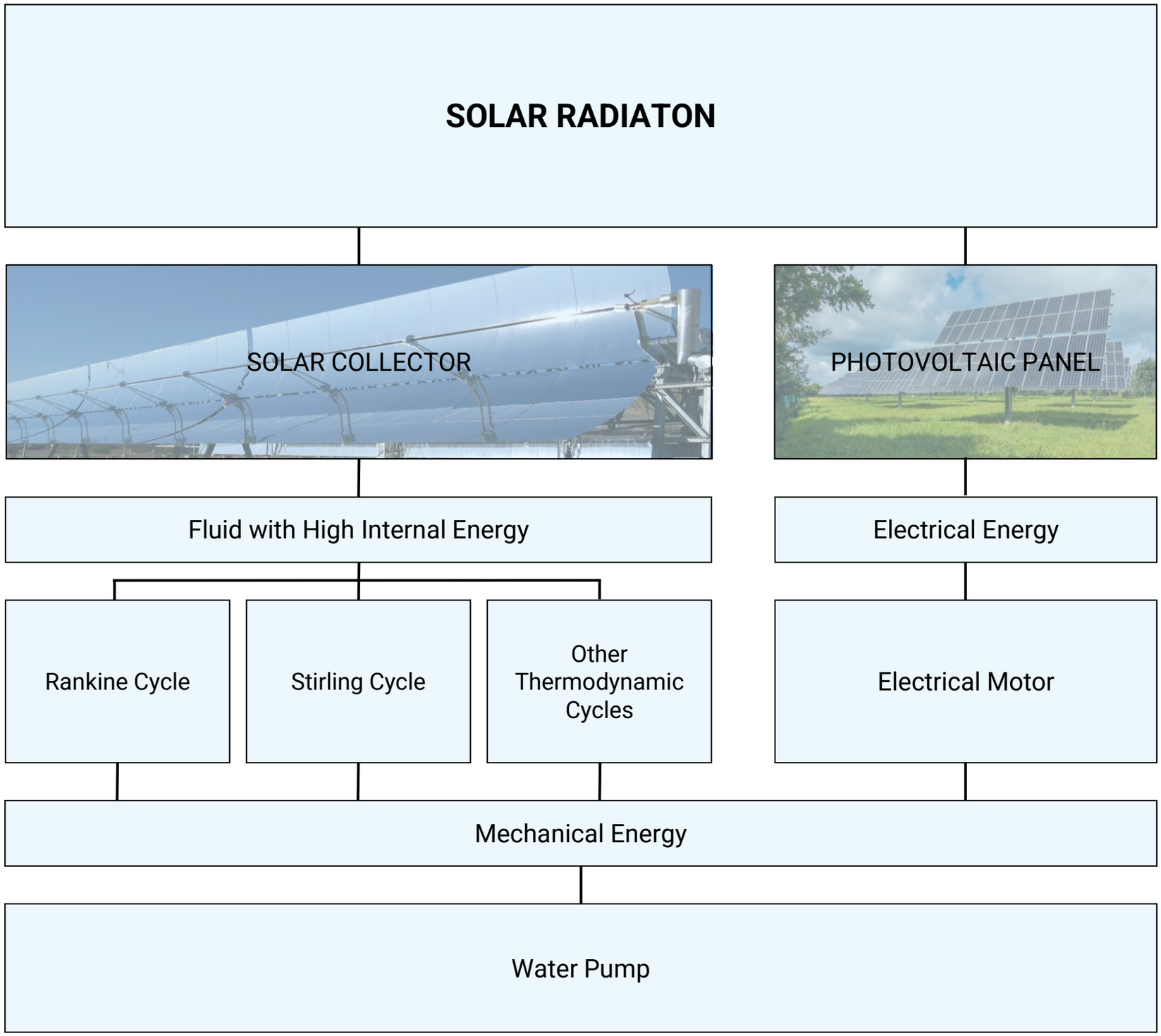

Figure 15: Diagram overviewing solar water pumping classes.

Thermodynamic Cycles

Thermodynamic cycles are processes that convert heat into usable energy, powering the modern world. These cycles are the driving force of the energy-driven society and are behind most power plants that generate electricity, combustion vehicles, heaters and coolers for industries and homes (Figure 16).

Thus, when exploring the earliest developments of solar-powered water pumps, as seen in the timeline in Appendix C, it is natural to see that the first systems are clever adaptations of these well-known thermodynamic cycles and establish working principles.

Rankine Cycle

The most common thermodynamic cycle is the Rankine cycle. This cycle is at the heart of most conventional thermoelectric power plants and is the working principle of the steam engine. It involves water heating to produce pressurised steam, which is then used to drive turbines to generate mechanical energy that is most often used to power generators and produce electricity. In most power plants, fossil fuels or nuclear reactions are used to generate the heat to produce the steam. However, solar collectors can also be used to heat the water and produce steam.

Powering a Rankine cycle with solar energy, however, can be challenging as evaporating water requires a lot of energy. Thus, parabolic solar concentrators are often required. This increases the complexity of the system, as parabolic concentrators represent adding costs and need a sun tracking system to work properly, following the sun's movement to reflect the radiation to the focal point.

This is a major setback for the Rankine cycle due to the high installation cost. To overcome this, as seen in Appendix C, simpler and cheaper flat plate collectors can be implemented by making use of other fluids with lower boiling temperatures. However, these refrigerant liquids are expensive and hazardous to health and to the environment. All these factors represent drawbacks to the implementation of the Rankine cycle in solar-powered solutions, summarised in Table 1.

Figure 16: Examples of applications of the Rankine cycle – Steam train (left); Nuclear power plant (right).

Stirling Cycle

Contrarily to the Rankine cycle, the fluid with high internal energy used in the Stirling cycle is a gas. In fact, this thermodynamic cycle operates by cyclically compressing and expanding a working gas to convert heat energy into mechanical work. It consists of four distinct phases – heating, expansion, cooling, and compression – that occur within a sealed chamber, harnessing the temperature difference to drive a piston or displacer, generating mechanical energy.

This means that it does not rely on the phase transition from liquid to gas, meaning it can work with low-grade heat. Thus, it has greater potential for solar-powered applications.

Known for its efficiency and working window versatility, the Stirling cycle is employed in engines and heat pumps, offering a sustainable alternative in various applications.

Carnot Cycle and Efficiency

Another thermodynamic cycle worth mentioning is the Carnot cycle, which represents the maximum theoretical efficiency for a heat engine operating between two temperature reservoirs. Although not practically achievable, it provides the maximum theoretical efficiency of real-world engines, given by $\eta_{Carnot} = 1 - {}^{T_C}/_{T_H}$.

Thus, all thermodynamic cycles are limited by the theoretical limit determined by the temperatures of the hot and cold sources, in ºKelvin, meaning that the higher the hot temperature, the higher the efficiency of these cycles (Shapiro, 2014).

This means that although the Stirling cycle can work with low-temperature differences, it is more efficient at higher-temperature differences. To achieve this, solar-powered Stirling cycles are implemented with parabolic collectors, again increasing the complexity of the system and its cost.

Table 1: Solar-Powered Thermodynamic Cycles for Water Pumping Overview

Cycle	Advantages	Disadvantages
Rankine	• Very mature technology • High efficiency in larger power plants	• Not so suitable to small installations • Requires parabolic concentrators/ uses environmentally hazardous refrigerant fluids • High installation and maintenance costs
Stirling	• Very mature technology • High Efficiency • Wide working window range of temperature	• The cycle is not self-starting • Is more efficient with parabolic collectors • High installation and maintenance costs

Photovoltaic Panels

Photovoltaic (PV) panels stand as the current overall best power source for solar-powered water pumps (Awan et al., 2021), with their advantages and disadvantages summarised in Table 2. PV panels are adaptable, scalable, and, in most cases, more cost-effective than thermodynamic cycles, making them suitable for various contexts.

The foundation for photovoltaic technology was laid in the 19th century when the photoelectric effect was first discovered. Yet, it was only in the 1950s that experiments with solar panels to pump water effectively began due to their low efficiency and high costs at the time (Pytlinski, 1978).

However, recent years have witnessed further advancements in efficiency and cost (Figure 17) in PV panels and all the required satellite components, such as electric pumps. This is a result of the huge interest and research in photovoltaic panels, electric systems and electric pumps that have multiple applications in modern society.

As a result, PV-powered water pumps are modular systems that can be easily dimensioned to specific needs by assembling various off-the-shelf components into one integrated system that can be upgradable as well.

In addition, due to the conversion of solar energy to electric current, these systems can be used for multiple local applications that are electrically powered, not just water pumping.

Furthermore, there is freedom to move the position of the water pump as it is not limited to the solar collecting point.

Thus, this now fairly mature technology is a versatile, effective and sustainable solution to power decentralised water pumps.

However, PV-powered water pumping installations need several components, including photovoltaic panels, electric inverters, control units, and the pump itself. All these components add significantly to the resulting high overall cost and lead to an increased system complexity. As a result, dimensioning, installing and maintaining such a system requires specialised personnel.

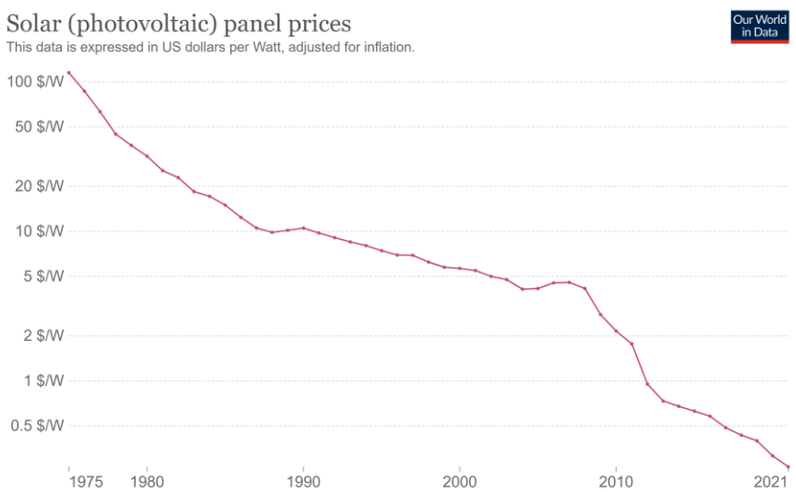

Figure 17: Solar photovoltaic panel prices based on International Renewable Energy Agency (IRENA) data (Our World in Data, 2023).

Additionally, PV panels are fragile and sensitive to dust and debris. This is a drawback to their implementation in such regions where robustness is essential, as illustrated in Figure 18.

Adding to their fragility, the panels are hard to repair. In fact, due to the brittle nature of the semiconductor materials and the sealed structure and architecture of the cells, faulty panels are often replaced rather than repaired.

Lastly, although PV panels effectively harness renewable energy representing a great and more sustainable solution, their lifespan is limited to 30 years (Bošnjaković et al., 2023), and their end-of-life is a sustainable burden as the panels are hard to recycle and end up being electronic waste.

In fact, 96000 tons of PV module waste are expected to be generated by 2030 worldwide and 86 million tons by 2050 (Bošnjaković et al., 2023).

Table 2: Solar-Powered Water Pumping with Photovoltaic Panels Overview

Advantages	Disadvantages
• Adaptability and scalability • High efficiency • Mature Technology • Low operating costs • Multi-purpose installations • Energy storage is possible	• High installation costs • Fragile • Hard to repair • Needs cleaning maintenance • Complex system • Limited life-span of around 30 years • Environmental burden at end of life

Figure 18: Photovoltaic panels installation for solar-powered pump in Faya, Chad 2021, Nigeria, 2019. Photograph from Peacebuilding Fund.

Augmenting the State-of-the-art

In this project, the opportunity to integrate Shape Memory Alloys to convert low-grade heat into mechanical energy was identified as a promising potential breakthrough in harnessing solar energy for water pumping (Figures 19-21).

Due to the crystalline phase transformation that occurs at a solid state upon an increase in temperature, SMAs can effectively convert a difference in their internal energy into mechanical labour (Rao et al., 2015).

This supports this project hypothesis that SMAs can be the element that transforms the heat collected with a solar collector into usable energy that powers a water pump.

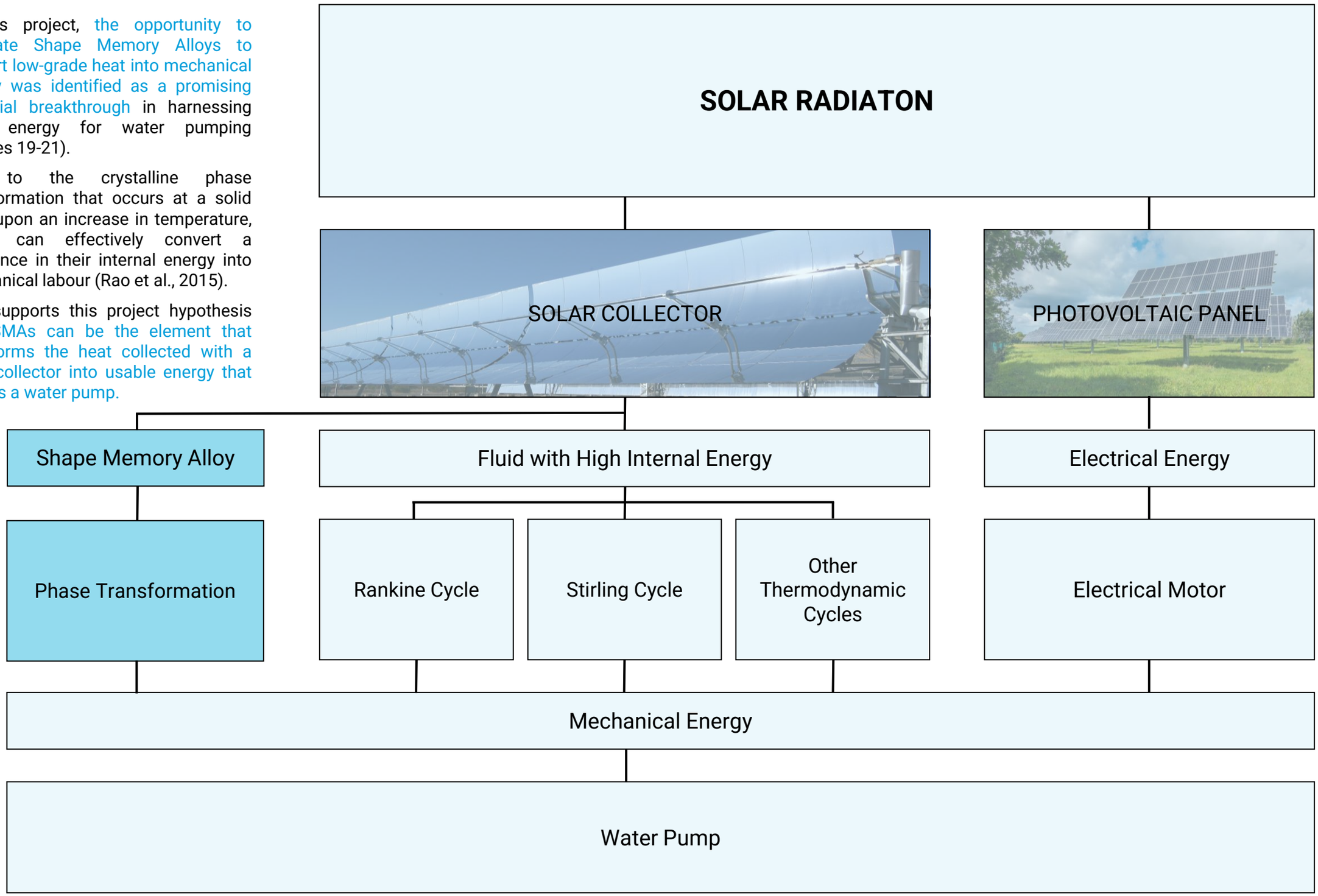

Figure 19: Diagram overviewing solar water pumping classes, including the new proposed system.

Opportunity – Shape Memory Alloys

Strengths

- Direct energy conversion into usable mechanical labour
- SMAs allow for a more straightforward working principle with fewer moving parts and more affordable materials
- Less fragile components and moving parts enable durability and robustness
- The straightforward working principle requires less specialised maintenance. In addition, a flat plate collector needs less cleaning and is less sensible to dust
- More sustainable end-of-life as SMAs can be corrosion-resistant and are reusable or recyclable at the end-of-life

S

Weaknesses

- Shape Memory Alloys present phase transformation fatigue which impacts the long-term performance.
- Technology readiness is lower when compared to other state-of-the-art technologies

W

Opportunities

- Cost-Effective and Accessible Alternative - Integrating SMAs into a solar water pump presents an opportunity for a more affordable and accessible solution compared to existing technologies.
- With a practical application the SMA technology may mature into a reliable and scalable technology for solar energy harnessing.

O

T

Threats

- If improvements make photovoltaic panels more affordable and accessible, it could If photovoltaic panels' fragility and end of life are considerably improved
- Considerable improvements in photovoltaic panels' affordability and accessibility can pose a competitive challenge to SMA-driven pumps.

Figure 20: SWOT analysis of the integration of Shape Memory Alloys for water pumping according to the author's assessment.

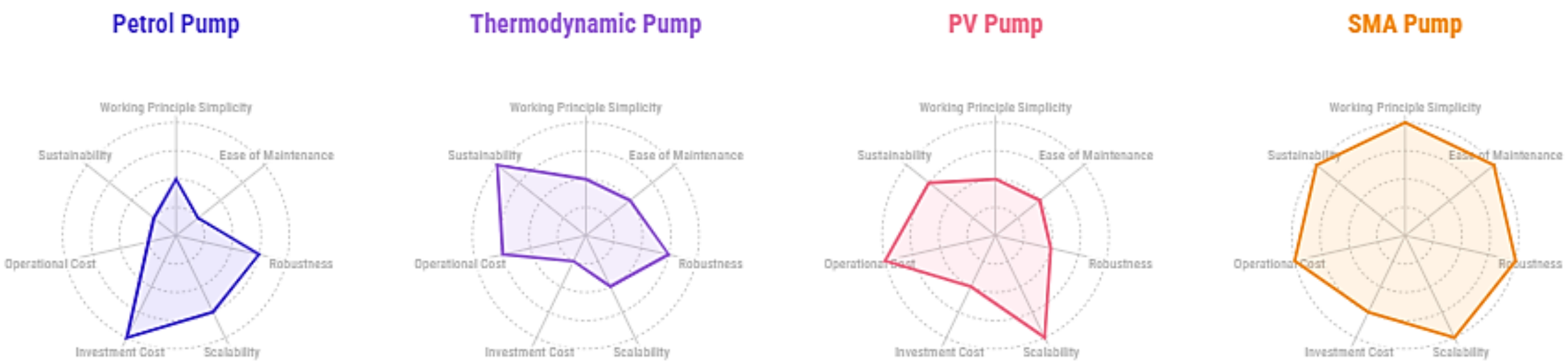

Figure 21: Comparative analysis between the state-of-the-art alternatives according to the author's assessment.

Design Direction

Built upon the identified opportunity, this chapter defines the design challenge and the direction in which the solution will be developed while breaking down the challenge and identifying the requirements.

In addition, this chapter describes the process of materialising findings into an envisioned concept (Figure 22).

Contents

- Design Challenge
- Requirements
- Design Direction – Approach
- Conversion of Heat into Mechanical Energy
- Shape Memory Alloy-Driven Pumping Element
- Heating and Cooling of the Shape Memory Alloy
- Integration of the Subsystems

Figure 22: Exploded view of positive displacement water pump.

Design Challenge

Having identified the problem and understood its context, analysed the existing solutions and identified a potentially disruptive hypothesis (Figure 23), the goal and solution scope of this project is framed as:

Design an affordable, robust, and scalable SMA-driven solar-heated water displacement pump that can be implemented in the identified regions lacking access to safe drinking water, supplying water to people who have access to an improved water source, but that is not accessible on their premises.

To achieve this, the design challenge can be broken down into the sub-challenges of designing a system that:

1. Harnesses solar energy – maximising the effectiveness-to-cost ratio;
2. Converts the harnessed heat into usable mechanical energy by means of Shape Memory Alloy;
3. Uses this mechanical energy to power a water pump that meets the pumping needs of the implementation sites.
4. Integrates all these subsystems in a standalone solution that is desirable, feasible and viable.

For, it should meet the following requirements:

Requirements

- Power the Local Water Transportation Needs
- Standalone Solution
- Self-starting
- Affordable Installation and Operation
- Robust and Reliable
- Adaptable, Scalable and Versatile
- Wide Operating Working Window
- Sustainable and Environmentally Friendly (non-hazardous, non-toxic).
- Easy to Install
- Easy Maintenance
- Long Life – Minimal thermal fatigue or deterioration.

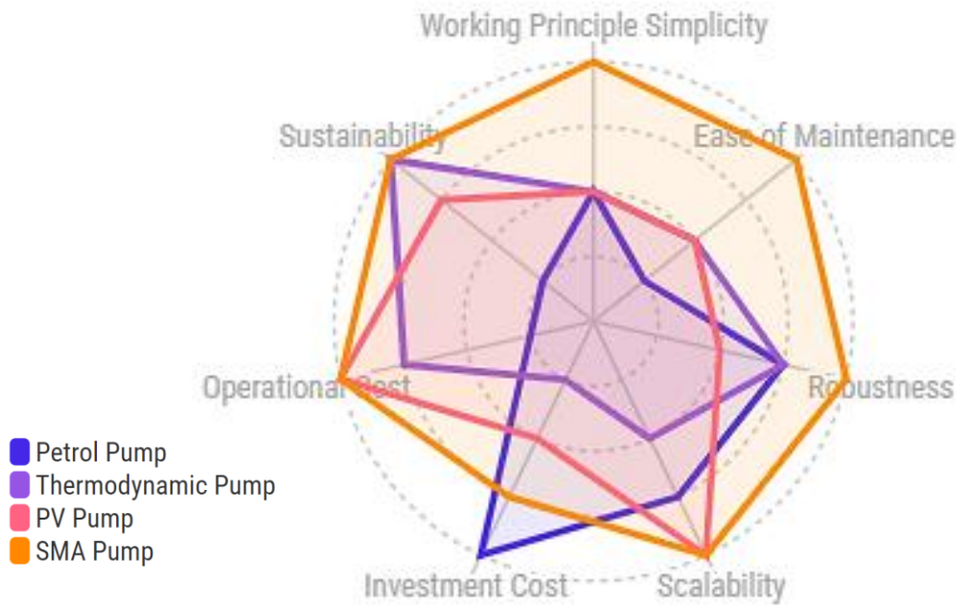

Figure 23: Comparative analysis between the state-of-the-art according to the author's assessment.

Design Direction – Approach

In order to meet the specific needs of the implementation sites, the pumping system must fulfil multiple requirements.

Meeting all of them is, of course, important for developing a solution that is desirable, feasible and viable. However, prioritising within the scope of this project, the focus is on developing a standalone working principle that is self-starting, adaptable and simplistic while keeping the potential to meet the other criteria.

In fact, if the pump can work in a basic and straightforward setup in the laboratory context, a solid foundation is established to potentially meet the other requirements, such as affordability and efficiency.

Thus, the strategy of addressing each of the pump's subsystems in a segregated way is ideal for the long-term goals of the project and for conducting experimental iterations. With this approach, each variable of the system can be dimensioned and optimised separately while ensuring that every component is under its optimal working window. Moreover, this aligns with other requirements, such as the adaptability to different implementation sites, as each will have its own needs and characteristics.

One key takeaway from the exploration of the context and state of the art is the recognition of the complexity of the assignment at hand. It is acknowledged that the design phase may require various iterations and consideration of new insights until a valuable and standalone solution is ready to be implemented on-site.

To break down this complexity, in this chapter, the various elements of the proposed concept of the pumping system are morphologically addressed, and the decisions for the design direction are explained.

Conversion of Heat into Mechanical Energy

At the heart of the working principle is the element that transforms the heat energy harnessed from the sun into mechanical energy. This element must be able to convert variations in its temperature into usable mechanical labour. For this, Shape Memory Alloy was selected as it is able to produce mechanical labour with relatively small changes in temperature and work within an easily reachable range of temperatures, making it a good fit for this application.

More specifically, the alloy selected for this application was the nickel-titanium alloy Nitinol. As Appendix D reveals, Nitinol is the Shape Memory Alloy that best balances the characteristics needed for this application, namely high working stresses and strains, great resistance to corrosion and resistance to overheating temperature (Rao et al., 2015). In addition, it has been extensively studied and is accessible. These help ensure both high performance and durability.

Regarding the phase transformation, this alloy can undergo both the martensitic and austenitic phase transformation-ending temperatures between atmospheric and 100ºC. This property eliminates the need for solar concentrators and matches the liquid temperatures of water, which is crucial for its integration to convert low-grade heat into mechanical energy.

To perform this effectively and reach optimal efficiency, the SMA must work under its optimal working window.

This means using the SMA in the straight wire configuration, under normal tension and fully stretched.

The straight wire configuration ensures optimal performance, durability and cost-effectiveness (Mohd Jani et al., 2017). In fact, strains under 5% and normal tensions under 200MPa and maximum are reported as the optimal performance working window that ensures the most efficient heat to mechanical labour conversion and best phase transformation fatigue resistance (Jani J.M., 2016), which means more phase transformation cycles and longer working life.

In addition, the wire configuration is the most basic, available, most studied, most cost-effective and cheapest SMA geometry (Jani J.M., 2016).

Moreover, as the wire is cooled down in the straight configuration when manufactured, the austenitic crystalline structure is already set straight by default (Jani J.M., 2016). This means that there is no need for additional heat treatments, making this choice the most cost-effective, which is crucial to this project.

Given these characteristics, the decision to integrate the SMA into the pumping system in a straight wire configuration is a straightforward choice.

Furthermore, having the wire working under optimal conditions means maximising the outputted mechanical labour without compromising the longevity of the wire. This labour is given by $W = F*\Delta x$, where the labour per cycle is determined by the force done by the wire multiplied by its elongation.

For the ultimate goal of the system, it is necessary to define how the SMA will be integrated to pump water using this elongation and paired force.

Shape Memory Alloy-Driven Pumping Element

Having the SMA wires work under normal tension means they work as a linear actuator, characterised by a high force-to-displacement ratio. As there are various types of pumps, the pump selection should be tailored to these characteristics.

In general, pumps can be divided into two main groups, which are rotary pumps and linear positive displacement pumps.

Rotary pumps

Rotary pumps operate through a rotating mechanism to move water. As it rotates, it creates a void that draws water into the pump. The rotation then forces the water through the pump and out downstream. Due to their characteristics, these pumps work at considerable angular velocities and need a minimum speed to be able to pump water. They are typically used in high-flow or steady-flow scenarios.

Positive Displacement Pumps

Positive displacement pumps, as the name suggests, displace water by trapping a specific volume and forcing it through the pump's outlet. Some examples include piston pumps, diaphragm pumps, and gear pumps. These pumps are characterised by being able to pump a consistent flow rate per cycle, regardless of the pressure conditions. Displacement pumps are more suitable for applications requiring precise volumetric flow or high pressure and can be used in both low-frequency and high-frequency applications.

With this overview in mind, the positive displacement pumps are the best option for a solar-powered SMA-driven application.

In fact, solar-powered applications have a unique challenge due to the variable power input harnessed, which results in variable pumped water flow. This poses a problem for rotary pumps, which require an optimal rotation speed and a minimum rotation speed to work that, if not met, the pump does not overcome the head, and the pump does not work. In contrast, displacement pumps can overcome this issue as they can adjust to the variable energy input while maintaining the same pumping parameters per cycle, such as pumping head and volume displaced. Different power inputs result in a change in the cycle's frequency, allowing the pump to work in a wide range of energy inputs.

In addition, positive displacement pumps can be easily integrated with the described SMA actuator since they are both linear. Simply coupling the pump's piston with the SMA allows for water to be pumped. Moreover, these pumps integrate non-return valves, making them ideal for low-frequency cycles, which will likely be the case.

Lastly, positive displacement pumps are affordable and easy to dimension for different pump heads and volumes being displaced by adjusting the area and travel of the piston.

These characteristics make positive displacement pumps ideal for the proposed system since they can pump water over a fixed pumping head and work for a wide range of energy inputs.

Heating and Cooling of the Shape Memory Alloy

One of the most important contributors to the efficiency of the proposed system is the effective heating and cooling of the SMA that ultimately powers the pumping of water.

At first glance, without any clever system, the pump can have a period of one day, heating up during the day and cooling during the night. However, this approach would require enormous energy storage and, thus, a large mass of SMA material, which is the critical element regarding cost. Thus, the daily period is not a feasible option. In contrast, the approach of having multiple heating and cooling cycles of the SMA is much more desirable.

This, however, requires an additional system that alternatively heats and cools the SMA wires.

Several options for the task were ideated and considered, and some of them are listed in Appendix E, which presents the concept selection.

As explained in Appendix E, the requirements for the pumping system, such as self-starting, affordability, and ease of manufacturing, led to the focus on the most valuable concept proposition, which is the hypothesis that integrating the SMA wires into the collector in a way that they are heated by default and cooled at the end of the cycle. If this hypothesis is proven feasible, the pumping system will be self-starting, which is, of course, desirable.

Explaining this principle further, the concept proposes an integration of the SMA wires within the flat-plate collector, and as seen in Figure 24, the SMA wires are inside pipes that are integrated into a buffer medium within the flat-plate solar collector. This buffer medium is suggested to be water, and it stores the collected energy in internal energy, increasing its temperature. This hot water medium is characterised by a high specific heat, buffering the variable incident energy inputs from the sun. The fact that it is liquid helps heat transfer from the collector to the water and to the SMAs through convection.

With this setup, the SMA wires are heated by default through conduction by the heated surroundings. This increase in temperature in the SMA wires makes them change phase and contract, which powers the displacement pump and pumps water. However, at the end of the cycle, the SMA wires need to be cooled down so they return to the initial state, ready to contract and power the pump again. Thus, the cooling is crucial for the reversibility of the cycle so the system can pump multiple times a day.

This cooling is proposed to be done with water directly at the wire premises by running water in a cooling tube covering the SMA wires in the collector.

This means that the water surrounding the SMA wire also has to be heated up for its contraction. This is, of course, energy being lost per cycle. However, this is the cost required for the reversibility to the starting position and to have the self-starting working principle, which is of greater importance for the desirability of this system. This energy loss can be minimised by reducing the amount of water in the cooling pipes by making these thinner and optimising the cooling flow.

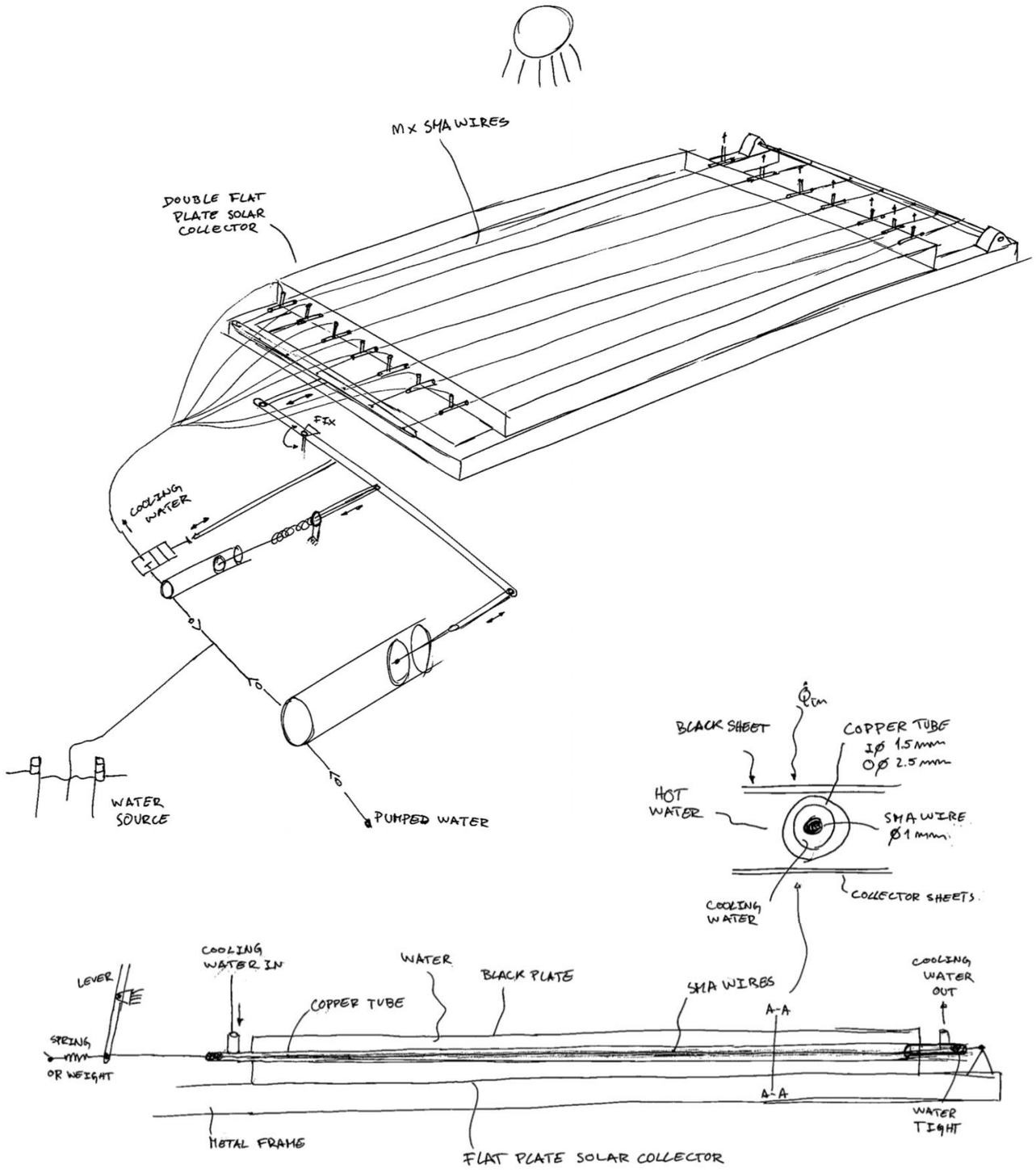

Figure 24: Schematic of the conceptualised solar-heated water displacement pump..

Integration of the Subsystems

With the three most important elements of the system explained, the challenge lies in the synchronisation of these various phases in a harmonic sequence of cycles.

Starting with the labour-outputting element, the one-way SMA is able to contract and output mechanical labour when heated up, and it relaxes when it is cooled down. This means the SMA contraction and the respective labour are coupled with the heating phase of the cycle (Figure 25).

This mechanical labour must then be used to pump water. This can be done by directly coupling the SMA wire with the pump's piston. However, at the end of the cycle, when the wire is cooled down, the piston of the pump must be brought back to its original position. Since the one-way straight SMA wire is not able to do force in that reverse direction, energy has to be stored during the contraction phase. This can be done in various ways, including the lifting of a weight or through the compression of biased springs.

In this concept, the energy-storing mechanism is proposed to be done during the contraction phase. In this phase, the piston is brought back to its original position, ready to pump water, and the energy produced in the contraction is stored. Thus, when cooling down, this energy is used to pump water.

Additionally, as the cooling phase will likely be faster, steadier and more consistent when compared to the heating phase, having the pump synchronised with the cooling phase makes the pumping easier to control and more reliable.

Thus, it was decided to associate the heating phase with energy storage and bringing the piston back and to associate the cooling phase with water pumping.

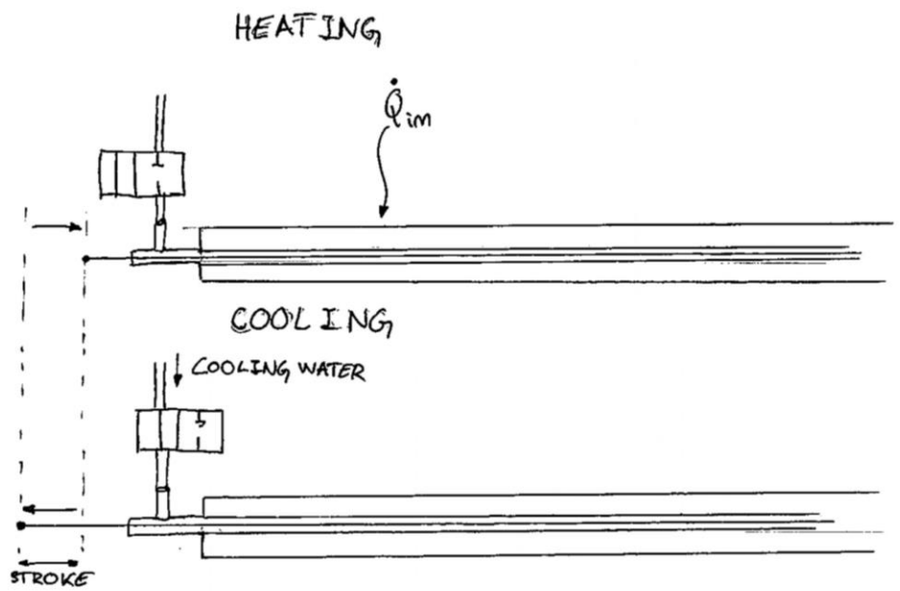

Figure 25: Schematic of the heating and cooling phases.

To complete the working principle, the change between stages has to be controlled. As the system is heated up by default, the control is done by running or stopping the cooling water through the SMAs. Ideally, this should be controlled by the displacement of the wire, meaning that the cooling water is run when the wire is fully contracted and stopped when fully relaxed. This ensures that the system is able to sense its stage and provides a robust control system, ensuring the system keeps running. Other solutions explored in Appendix E include externally powered control systems, for instance, making use of an independent solar panel that powers the cold water system. Such an option, although effective, increases complexity and costs, and thus, it does not meet the requirements of this pump.

Since the cooling water can only be pumped at the end of the contraction and stopped only at the end of relaxation, the cooling water system must also have its own energy storage.

This can be done in two ways. In a simpler way, water can be stored at a set height to provide the required head to run it through the cooling lines and have a valve that is displacement controlled, stopping and opening the cooling circuit when desired.

In a less simple but more compact way, this energy can be stored by means of an additional pump coupled with a biased spring and trigger. Again, the energy would be stored in the compression of the spring during the contraction and used at the end of the cycle to cool down the wire (Figure 26). The flow of water can then be controlled by means of a simple switch valve controlled by the displacement of the wire.

Now that the individual elements of the proposed concept and their integration into the overall working principle have been explained, the subsequent chapter delves into the laboratory experiments conducted to validate and iterate it.

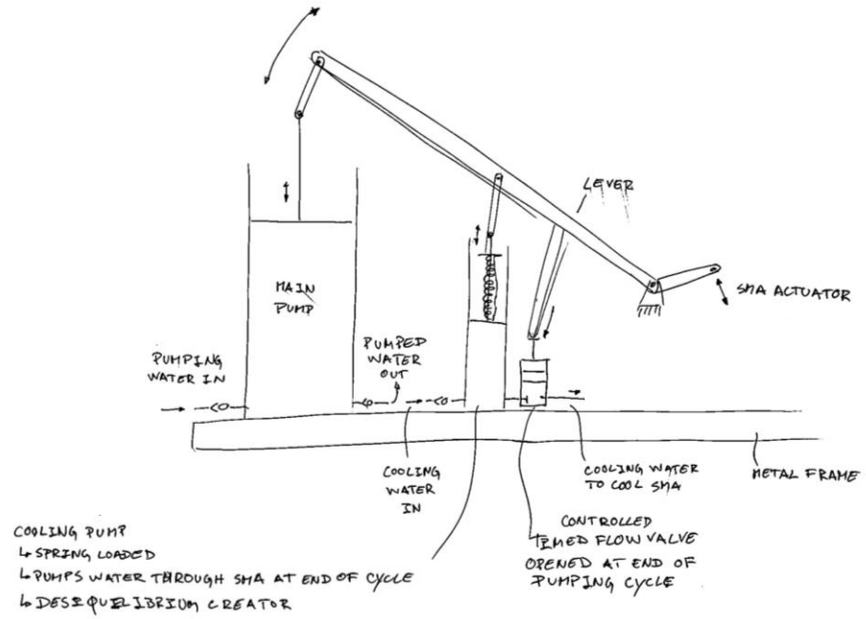

Figure 26: Schematic of pumped option for the cooling.

Experimental Design

With the geometry of the system and the working principle conceptualised (Figure 27), the focus shifts to validating and developing through what is in this report referred to as Experimental Design.

This is an iterative phase where each experiment's results lead to valuable insights that feed the next iteration loop.

After each milestone, and following the previously described approach, new subsystems will be progressively added, each building upon the prior towards a functional pumping prototype.

Contents

- Validation of the Shape Memory Alloy potential
- Design Iteration
- Design Iteration Validation

Figure 27: Preview of Shape Memory Alloy wire in experimental setup.

Approach

In the Experimental Design phase, the focus is on materialising the findings, the ideas, and the conceptualised working principle. This is a result-oriented approach where development and prototyping come together in a blended process.

This approach is very valuable in this project as feasibility, performance, and simplicity are of the utmost importance. By going through the prototyping and manufacturing of the whole system, the system's pain points and the critical elements can be identified. This hands-on approach ensures a feasible development and contributes to keeping the pumping system as simple and as cheap as possible.

With the main goal of developing a proof of concept, this chapter is structured in three sequential phases, as seen in Figure 28.

In the sequential phases, the design challenges and research questions are addressed in structured experiments that follow logical reasoning for the evolution direction.

Thus, the system developments are based on the analysis of practical experiments and findings, and the logic can be acknowledged by the reader to understand the decisions, allowing for a complete transfer of knowledge and the reproduction of the results.

Experimental Design – Chapter Structure

- Validation of the SMA and Concept Potential
  - Experiment 1 – Confirming SMA Working Window
    - Results
    - Analysis and Takeaways
  - Experiment 2 – Water Heating and Cooling
    - Results
    - Analysis and Takeaways
    - Additional Takeaways and Iteration Direction
- Design Iteration
  - Overview of New Concept
  - Design Iteration – Manufacturing In Focus
  - Design Iteration – Performance In Focus
  - Design Iteration – Proof of Concept Prototype
- Design Iteration Validation
  - Experiment 3 – Testing Proposed Design
    - Results
    - Takeaways
  - Experiment 4 – Pump Integration
    - Results
    - Analysis and Takeaways
  - Experiment 5 – Final Prototype
    - Results
    - Analysis
    - Takeaways

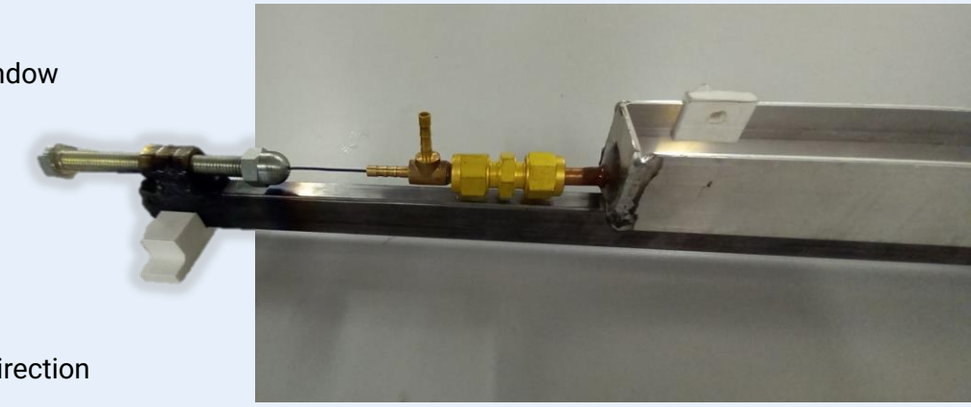

Figure 28: Diagram overviewing the Experimental Design chapter Structure with a preview of experimental setups.

Validation of Shape Memory Alloy and Concept Potential

Experiment 1 – Confirming SMA Working Window

This phase started with a basic mechanism capable of producing labour, even without actively pumping water.

Research goals:

- **Understand the strength of SMA's**
- **Check the working window** – confirm phase transformation temperatures and load conditions for maximised stress-strain pair.

Setup Description

The setup is shown in Figure 29, and it consists of a simple but upgradable work frame where experiments can be made with a meter of an SMA wire.

As seen, it has a steel frame dimensioned to support the loads of the SMA wire, so the displacements measured are solely from the wire itself.

On one end, the frame has a screw attachment for the SMA wire, so it can be pre-tensioned if required. On the other end, it allows for multiple configurations of loads, such as a biased spring or a pulley configuration.

For the simplicity of the first experiments, the pulley and constant load configuration was preferred. This aligns with the identified optimal loading condition in Appendix - D, which will be sought during the system design. This way, the wire works under constant normal stress, and the load can be easily changed with the weights.

The heating of the SMA wire was done with an electrical current through the Joule effect, and the cooling was air-cooled through convection to the surroundings.

The experiment was done with a 1m long and 1mm diameter NiTi SMA wire with an activation temperature of Af = 80ºC +/- 10ºC.

(a)


(b)


(c)

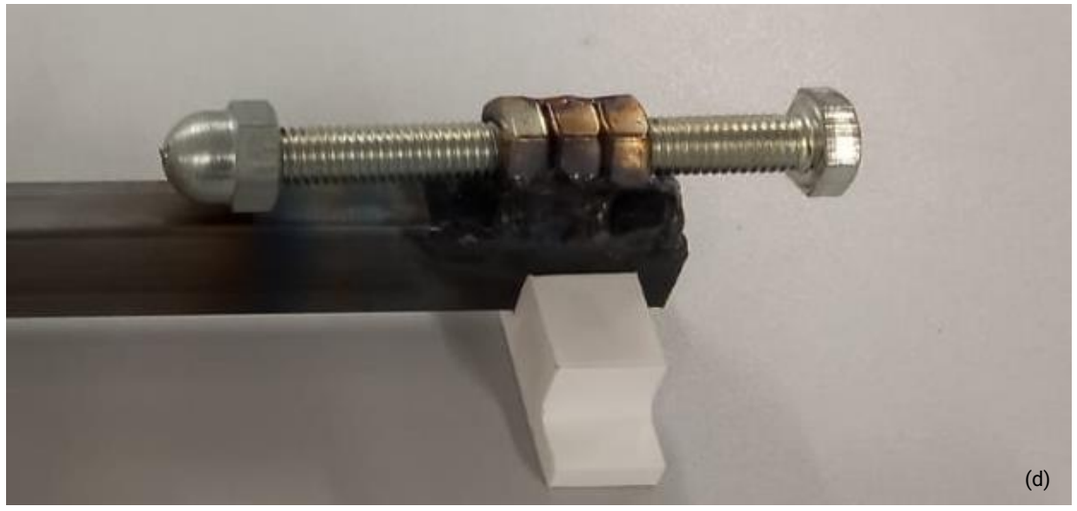
(d)

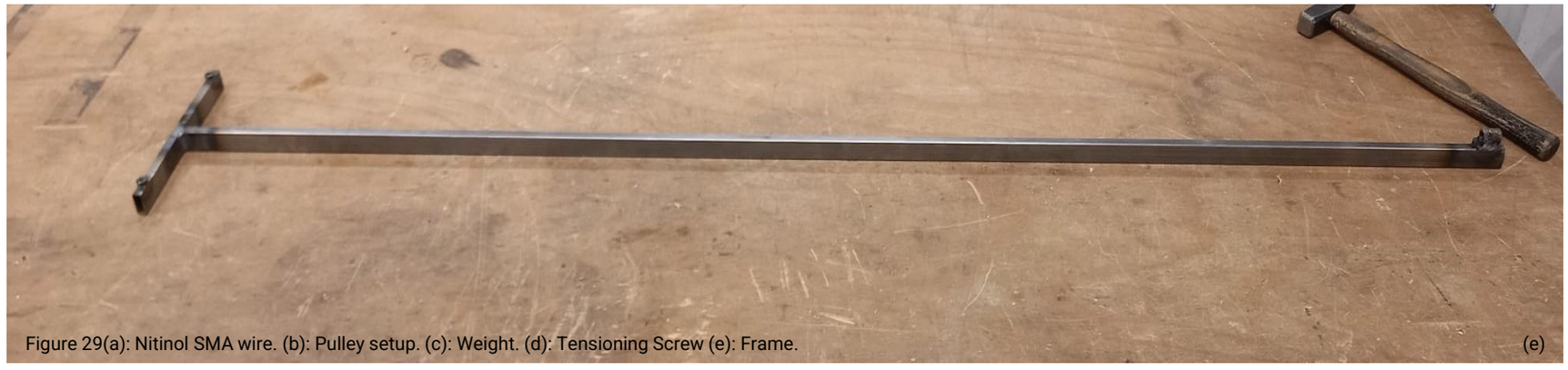
(e)

Figure 29(a): Nitinol SMA wire. (b): Pulley setup. (c): Weight. (d): Tensioning Screw (e): Frame.

Experiment 1 – Results

The research goals were addressed by measuring and mapping in Table 3 the response of the SMA wire to different loads:

Table 3: Average Measured Displacements on the Wire per Load

Load [Kg]	1	2	3	4	6	8	10	12	14	16
x Mf [mm]	162	159	155	153	148	143	140	135	131	127
x Af [mm]	183	182	182	182	180	177	174	170	167	163

Succeedingly, the collected data was normalized in Table 4 to follow the standard force-displacement graphs:

Table 4: Normalised Displacements on the Wire per Load

Load [Kg]	1	2	3	4	6	8	10	12	14	16
x Af [mm]	0	1	1	1	3	6	9	13	16	20
x Mf [mm]	21	24	28	30	35	40	43	48	52	56

Finally, the collected data was visualised in force-displacement (Figure 30) and stress-strain curves (Figure 31):

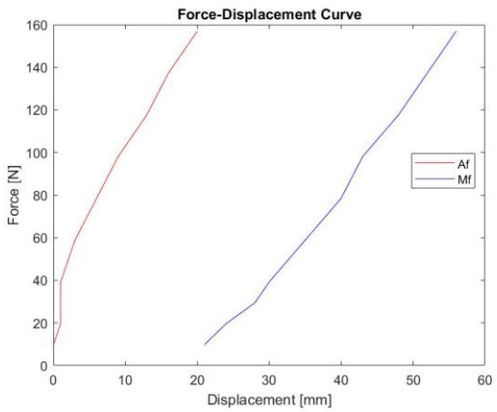

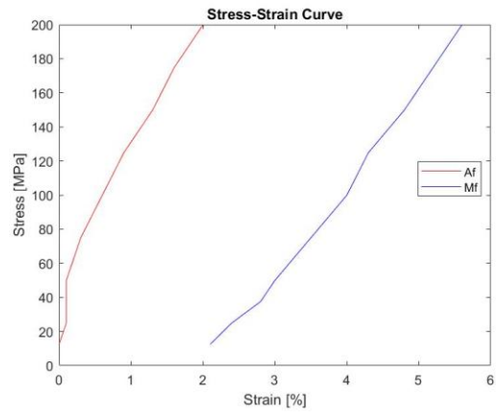

Figure 30: Experimental engineer force-displacement curve. Figure 31: Experimental engineer stress-strain curves.

Experiment 1 – Analysis and Takeaways

From these experiments, a few insights were confirmed and gathered that influence the future design direction:

Firstly, the nitinol Shape Memory Alloy is, in fact, able to lift considerable loads under normal tension without required pretraining (Figure 32). This is, of course, promising to the scope of this project as it confirms the geometry choice as well as the resulting simplicity in manufacturing and reduced costs since no heat treatments are required other than the simple cool down during the wire manufacturing.

In addition, the contraction and relaxation of the SMA wire can be done within the desired window between ambient temperature and 90ºC.

Lastly, within the theoretical limits for less phase transformation fatigue of 200MPa and 5% strains, the material is still in the initial phase where the plateau of the interval with increased strains was not reached. As compared to other literature experiments (Figure 33), the stress required to reach the strain plateau at ambient temperature is three times higher than achieved in the experiment. Achieving this plateau would provide more mechanical labour per cycle, achieving higher strains and stresses than the maximum verified of 3%. However, it could compromise the longevity of the wire. Thus, the optimal working window must be a compromise.

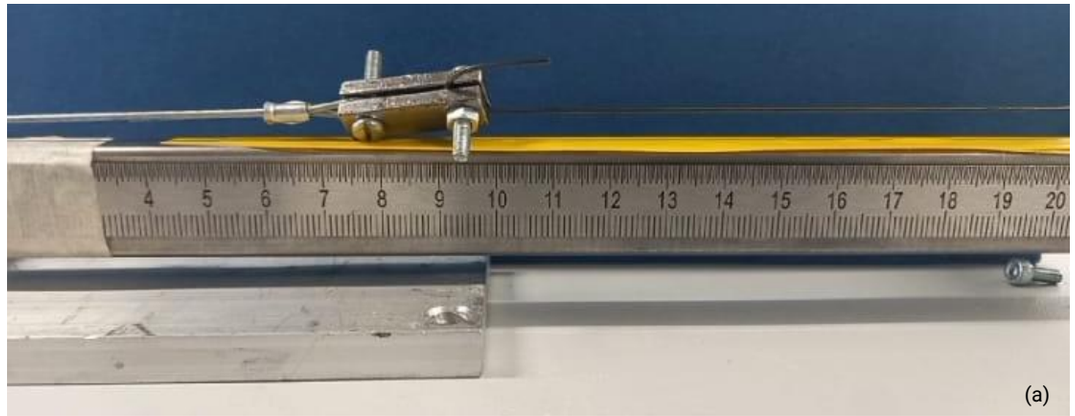

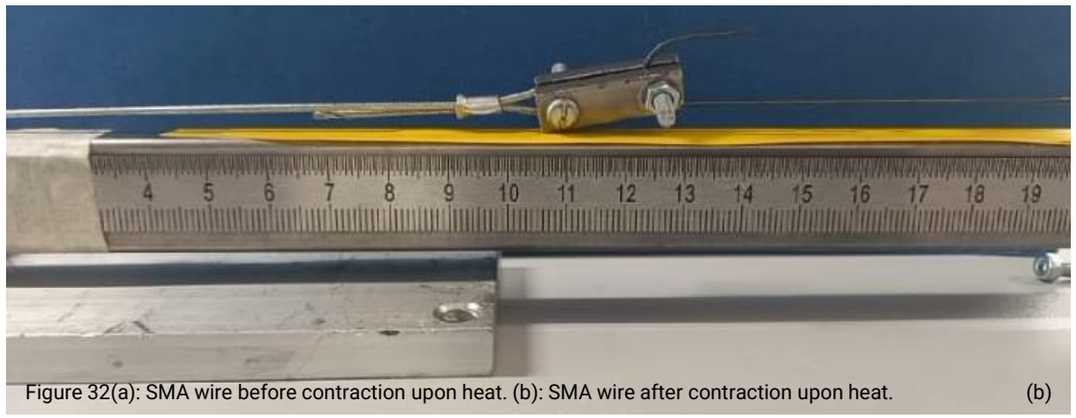

Figure 32(a): SMA wire before contraction upon heat. (b): SMA wire after contraction upon heat.

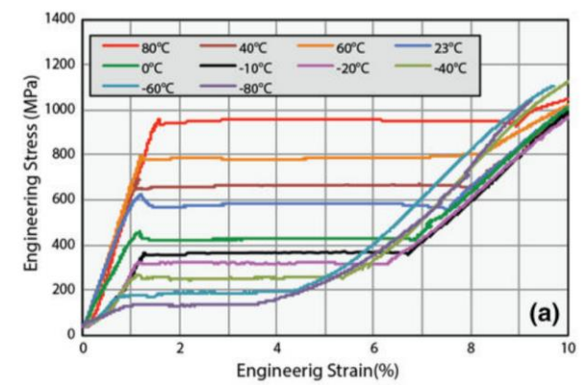

Figure 33: Engineer stress-strain curve for nitinol wire described in the literature (Duerig et al., 2017)

Experiment 2 – Water Heating and Cooling

After the first promising confirmations, the goal of this experiment was to start integrating the SMA wire in working conditions that are more representative and relevant to the ones proposed in the concept.

Research goals:

- **Confirm if cooling and heating with water is feasible** by heating the SMA wire in a hot water bath and cooling the wire with a cold water flow in a pipe where the SMA is in.

- **Understand if a self-starting condition is feasible.**

- **Gather insights on its efficiency and effectiveness** – What's the projected frequency for each cycle?

Setup Description

To answer the second research goal and to find out what a plausible cooling time for the SMA wire could be, an attempt was made to heat the SMA wire with electrical current and cool it with cold water (Figure 34).

However, this was unsuccessful as the cooling line involving the SMA wire is made of copper, and there was contact between the wire and the copper tube, so the current was passing through the copper tube instead of the SMA, and the wire was not being heated up.

This means that to test the cooling time with water, the full setup with hot water for the heating up had to be implemented.

The fundamentals of the setup were the same as in the first experiment. The same 1 meter and 1mm diameter SMA wire with an Af temperature of 80ºC +/-10ºC was used. The load is still a constant load now of 10Kgf. So, the modifications to the setup were the additions of the bathtub and the hot and cold-water subsystems.

The bathtub makes use of a 1m-long aluminium U profile closed at both ends where hot water sits around a copper pipe, where the SMA wire goes. This way, the wire is naturally heated through convection and conduction.

To cool the wire, cold water is flowed through the copper pipe. In this experiment, the inner diameter of the copper pipe is 4mm, and the outer diameter is 6mm, which means there is 6.28 mL of water that has to be heated to heat the wire. This can, of course, be optimised with a smaller inner diameter.

For the water cooling lines, at each end of the bathtub, there is a T connection where the SMA wire goes through. For water tightness, a rubber closes each end. To the upward T end, the cold water cooling line is connected. Thus, water flows from one end of the copper pipe to the other, cooling the whole SMA wire.

The cooling is now done with a 12mL syringe that has double the volume of the copper pipe. It is connected to two check valves closing the system, meaning the cold water pumping is manual and done at will.

The hot water was heated up with a tea boiler, flowed to the bathtub through the syphon principle on the one end, and pumped back to the boiler on the other end.

Figure 34(a): Prototype overview. (b): Heating setup. (c): Cooling pump. (d): Hot water entry. (e): Cooling water entry. (f): Hot and cooling water exit. (g): Tensioning screw and SMA wire.

Experiment 2 – Results

In this experiment, the temperature of the hot water bath and the elongation of the SMA wire were measured to analyse the heating phase of the system.

Table 5 and Figures 35 and 36 include the measured values and the subsequential graphs with the relation between the temperature and the behaviour of the wire.

Table 5: Experiment 2 Collected Data

t [min:s]	T [°C]	Δx [mm]
00:00	20.2	0
00:20	20.2	0
00:40	23.7	0
01:00	29.6	0
01:20	36.1	0
01:40	41.5	0
02:00	46.6	0
02:20	52.0	0
02:40	56.3	0
03:00	58.5	0
03:20	61.8	0
03:40	64.0	0
04:00	67.6	1
04:20	72.0	1
04:40	74.8	1
05:00	75.6	4
05:20	77.5	4
05:40	79.2	5
06:00	80.1	6
06:20	80.6	7
06:40	81.6	8
07:00	82.6	9
07:20	83.2	9
07:40	83.9	9
08:00	84.6	10
08:20	85.2	10
08:40	85.0	11
09:00	86.1	12
09:20	86.2	13
09:40	88.0	15
10:00	87.5	16
10:20	87.7	16
10:40	88.0	16
11:00	87.8	16

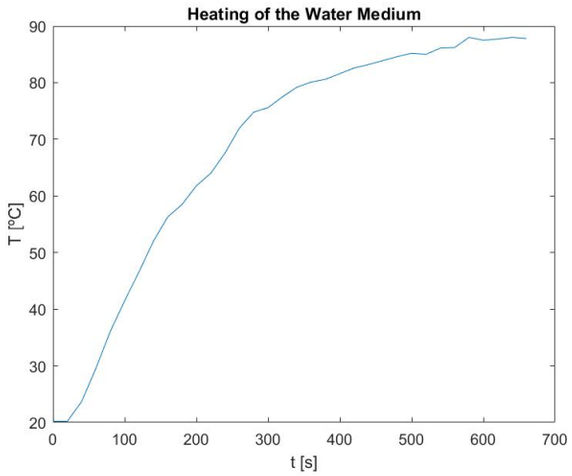

Figure 35: Temperature during the heating of the water medium

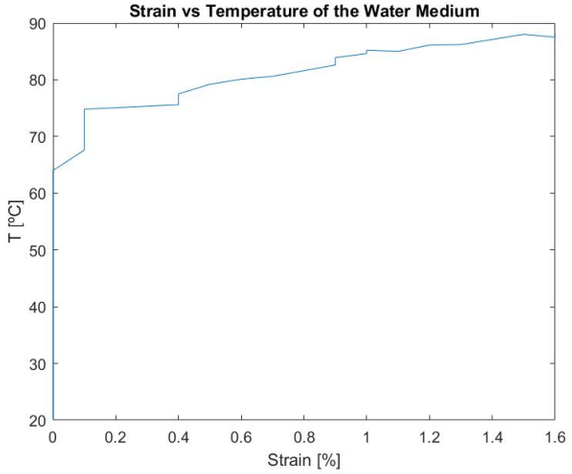

Figure 36: Relation between the temperature of the water medium and the strain of the SMA wire

Experiment 2 – Analysis and Takeaways

Heating

The heating of the hot tub had the purpose of heating and thus contracting the SMA wire. As seen in Figures 35 and 36, this process only began around the fourth minute when the copper pipe's outer surface temperature reached 67.6°C. This is an undesirable outcome of the buffer effect of the significant water mass around the copper pipe.

Phase Transformation

At the maximum bath temperature of 87.5°C, the displacement was only 16mm, indicating a strain of 1.6%. Comparing this value with the 26mm when heated with electricity in the previous experiment, it can be understood that the phase transformation was not fully reached.

Thus, the bath temperature did not reach the necessary level for total Austenite formation in the wire. This reflects the inefficiency of the setup and its limitations in increasing the bath temperature, which was mainly due to the high heat losses. The open design of the system and the conduction of heat through the aluminium tub and steel frame caused significant heat loss.

Another reason for the limited hot temperature was that the tea boiler's heating system reaches over 100°C, causing steam generation. This steam is collected in the heating tubes, stopping the syphon effect and breaking the flow of hot water into the bath. For this, a snorkel was added to the tea boiler tube to collect water from the sides instead of underneath, reducing steam intake and maintaining a steady flow of hot water.

Cooling

Lastly, regarding the cooling process, the use of the syringe to cool down the wire and recover displacement proved to be insufficient. Initially, 8mm of displacement were recovered, but additional pumping had minimal impact on the reversibility of the displacement. Thus, the cooling was insufficient, and the cooling pipe would stay hot from the heat received from the surrounding hot tub, which also caused the cold water reservoir to warm quickly.

Improvements

To achieve the desired transformation temperatures, changes to the setup were necessary. This included the introduction of a snorkel to avoid steam and the integration of a DC pump and ice in the cold water flow.

Despite these changes, the maximum contraction displacement achieved remained smaller compared to the 26mm achieved with the Joule effect. Additionally, the cold water flow proved insufficient to cool the entire meter of wire when the bath temperature was maintained between 80°C and 90°C. However, it was sufficient for the reversible displacement when the bath temperature was at lower temperatures around 65°C

As the blame could be on the fatigued deterioration of the SMA wire, experiment 1 was repeated using the Joule effect to heat the wire. As it turns out, the results were still consistent. Therefore, it became evident that the issue did not lie with the SMA wire but rather with the setup itself, which means that further changes had to be done so the system would work.

Experiment 2 – Additional Takeaways and Iteration Direction

This experiment concludes the need for an iteration of the prototype. Several potential modifications to the setup have emerged as possibilities to explore:

• Minimizing Heat Losses – One possible improvement lies in addressing the heat losses in the system, which is crucial for better efficiency. This could be done by adding proper isolation.

• SMA Wire with a narrower phase transformation window – One other improvement can be using an SMA wire with a narrower phase transformation window, characterised by higher Mf temperature and lower Af temperature.

• Higher Bath Temperature – Rising the hot bath temperature as close as possible to the boiling point of water would help reach full austenitic phase transformation and increase the measured displacements.

• Thinner SMA Wire – Using a thinner SMA wire leads to faster heat transfer.

• Lower System's Specific Heat – A reduction in the system's specific heat could result in less heat buffer, which, in turn, might lead to reduced heat loss. In the extreme scenario of significantly lowering the system's specific heat, the system also cools down during the cooling phase, resulting in a smaller temperature difference at the interface between the copper pipe and the cold water flow. This, of course, increases the sensibility to the heat input but also speeds up the transient phases. Which would improve the overall system performance.

• Shorter Cooling Pipe – Shortening the cooling pipe and increasing the number of entrances for a cold flow could lead to a lower increase in the temperature of the cooling water when running through the cooling pipe. However, this adjustment comes with drawbacks as it means either reducing the length of each SMA wire, further constraining the range of displacements, or increasing the complexity of the system by incorporating more entrances and exits for cold water.

In light of these potential improvements, it is evident that further iterations and optimisations are necessary to enhance the effectiveness and efficiency of the system. And, so, further improvements were implemented.

Design Iteration

As the first presented concept's heating and cooling system failed to work, a design iteration was performed.

In this section, the details of the iteration are presented. This includes an overview of the updated proposed system, the manufacturing details and the key elements for optimisation.

From the previously highlighted possibilities to increase the performance of the system, the focus stayed on redesigning the integration of the SMA wire in the solar collector and the way heat is exchanged from the collecting surface to the wire (Figure 37).

Figure 37: Preview of the solar collector prototype of the iterated design.

Overview of new Concept

The design iteration presented in Figure 38 focuses on the issues of the previously conceptualised collector, namely, on reducing the collector's specific heat so temperatures can be varied quicker and on improving the concept's simplicity.

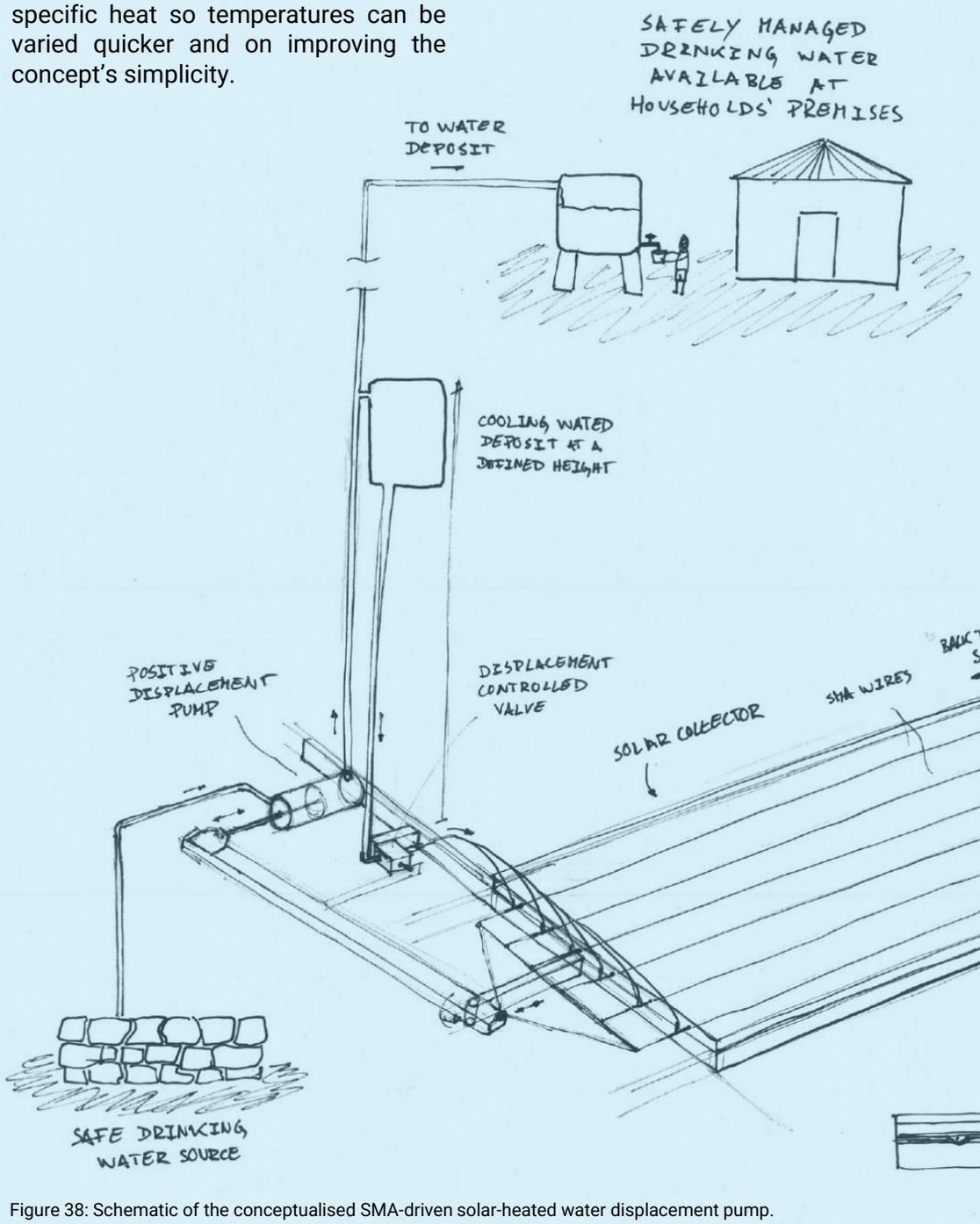

Figure 38: Schematic of the conceptualised SMA-driven solar-heated water displacement pump.

This effort led to the elegant and integrated design of a solar collector that comprises two distinct metal sheets, as seen in Figure 39.

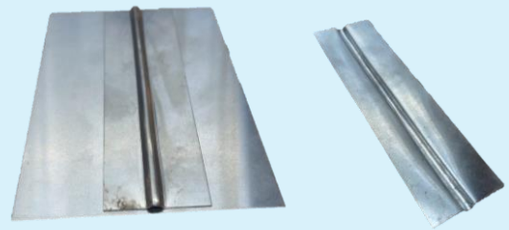

Figure 39: Solar collector sheets.

The top sheet works as a flat collector plate, with its upward-facing side coated in black paint to optimise solar absorption.

The lower metal sheet features a series of round longitudinal indentations that serve as cooling tubes for the SMA wire and the cooling water flow. These indentations can be done in various geometries and sizes and are efficiently manufactured using a roller machine and a pair of dies.

These two sheets are assembled together with an isolation layer under and a glass layer over, which play an important role in the collector's efficiency. Both these components are readily available and already optimised for such a purpose due to the developments in water-heating solar collectors.

With the proposed setup, the heating and cooling of the SMA wires can be more effective, and the resulting output power will be used to move the positive displacement pump and pump water downstream, as conceptualised.

Design Iteration – Manufacturing In Focus

Manufacturing this innovative design can be efficiently accomplished through a series of streamlined steps that can be done in series (Figure 40).

Firstly, the lower flat sheet goes through the roll-forming process for the required indentations for the SMA wires and cooling water. Through a series of dies, the roll-forming machine will crave longitudinal indentations to the required depth and size (Figure 41). This step is simple, fast and cheap, especially for thin sheets.

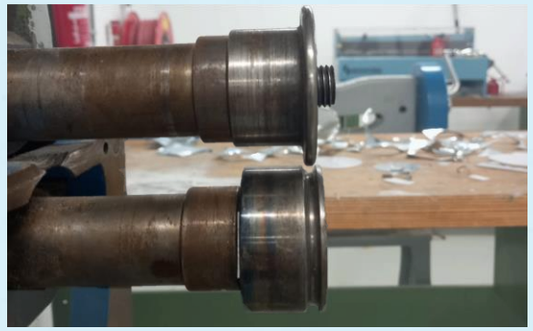

Figure 41: Roll forming machine.

Secondly, the upper flat sheet is aligned with the lower and indented one, and they are assembled together. This connection is made with a seam welder (Figure 42).

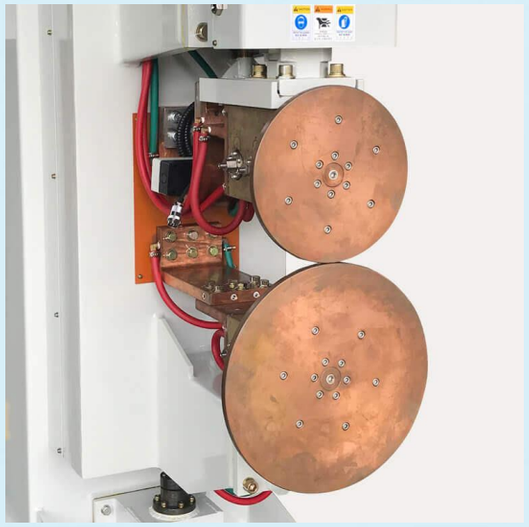

Figure 42: Seam welding machine

A seam welder is a machine that makes a continuous longitudinal and water-tight seam between indentations. It works like a spot welder; however, in this case, the electrodes are circular. As they rotate with pressure along the sheet, pulses of electricity make multiple welded spots over each other, making a strong and water-tight connection in a reliable and straightforward way.

Subsequently, the isolation foam can be applied to the collector, and the top sheet can be coated with dedicated absorbing black paint to optimise solar absorption.

From this point onwards, the collectors are moved to a drying station, and afterwards, they are fully assembled on a structural frame with a special glass closing the collector.

In addition, it is valuable to note that the painting is the only manufacturing step that uses external consumables besides electricity. Consequently, the collector's design enables simple and scalable manufacturing, resulting in a cost-effective process that is suitable for mass production, which is essential for the viability of this technology.

Figure 40: Schematic of the conceptualised manufacturing process of the solar collector of the SMA-driven solar-heated water displacement pump.

Design Iteration – Performance In Focus

To maximise the potential of the iterated water pump design, an essential focus lies on optimising heat transfer among the collector and actuator elements. This involves a comprehensive analysis of various factors, including material and thickness of sheets, wire spacing, wire thickness and indentation size.

Material Selection

When considering material selection for the water pump, key factors include low specific heat, high thermal conductivity, corrosion resistance, and low cost.

Four materials, steel, stainless steel, copper, and aluminium, stand out as possibilities for the material of the sheets. The four of them have their advantages and disadvantages in Table 6, and the relevant properties are presented in Table 7.

Of all the options, copper stands out as the material with superior performance due to its high thermal conductivity and low specific heat. Adding to this, copper is corrosion-resistant and very easy to work with, as it can be easily shaped. These characteristics make copper the most common choice for heat exchangers. However, it comes at a higher cost.

Aluminium still has fairly good thermal conductivity. However, it has by far the highest specific heat. This means that it requires twice as much energy to vary its temperature compared to the other materials. Due to this, aluminium sheets are also harder to connect through welding. Thus, despite being corrosion-resistant and a more affordable option, aluminium is not a good material choice.

Lastly, steel has good specific heat compared to copper, meaning that the transient phases are not much compromised. However, steel has lower thermal conductivity and can be harder to get an appropriate anti-corrosion treatment or solution. Nonetheless, it is more affordable and widely available, thus emerging as a compelling and cost-effective option that balances performance and affordability for this application.

Table 6: Material Selection Overview

Material	Advantages	Disadvantages
Steel	• Low cost • Easy to weld • Low specific heat • Easy to shape	• Oxidation • Low thermal conductivity
Stainless Steel	• Resistance to oxidation • Low specific heat	• Hard to bend • Very low thermal conductivity
Aluminium	• High thermal conductivity • Resistance to oxidation • Faily low cost	• High specific heat • Hard to weld
Copper	• Very high thermal conductivity • Very low specific heat • Resistance to corrosion	• High cost

Table 7: Comparison of Relevant Material Properties

Property	Steel	Stainless Steel	Copper	Aluminum
Density [kg/m³]	7.7 - 8.1	7.7 - 8.0	8.92	2.70
Melting Point [°C]	1370 - 1538	1400 - 1450	1084	660
Thermal Conductivity [W/(m·K)]	50 - 80	14 - 45	398	205
Tensile Strength [MPa]	250 - 700	500 - 1000	210 - 220	80 - 700
Young's Modulus [GPa]	200 - 210	190 - 220	117	69
Specific Heat [J/(kg·K)]	460 - 510	480 - 520	385	900

Sheets Thickness

Regarding the thickness of the sheets, having the sheets as thin as possible reduces the specific heat of the system, which increases its efficiency in the transient phases. However, thinner sheets have less material and, consequently, less conduction to the wires. In addition, if made extremely thin, the manufacturing also comes at higher costs. Thus, it is important to simulate the optimal sheet thickness that balances low specific heat, high conduction, and low cost.

Wire Thickness and Spacing Density

Similarly, the spacing between wires and their thickness must be optimised for this application. Having more and thinner wires makes the conduction of heat more uniform along the solar collector. In addition, thinner wires have higher surface area to volume ratio, which is important for faster heat transfer. However, the collection area per wire will be smaller and thinner wires are more expensive when it comes to cost per volume of SMA.

Indentation Size

Lastly, the indentation size is also a parameter to be looked at for optimal performance. Thinner indentations decrease the volume of water to be heated up in each cycle, directly minimising energy losses and enhancing the overall efficiency. However, if these indentations are made too thin, the effectiveness of the cooling may be compromised as the pressure loss is higher.

Thus, it is evident that the optimisation of the proposed collector is a multivariable problem that requires special attention and advanced simulations to achieve optimisation.

Other Modifications to the Concept

Regarding the energy storage for the water cooling phase, although both options have their advantages and disadvantages, it was decided to go with the water deposit instead of the spring pump as it is the simplest, most reliable, and cheapest. With this solution, it is necessary to ensure that the water in the deposit does not get too warm, as this would compromise the cooling of the wires. To ensure this water does not get too warm, the deposit can be isolated and the water used for the cooling circuit can be run through a heat exchanger that cools this water with the water that will be pumped, for instance.

Design Iteration – Proof of Concept Prototype

As previously mentioned, the manufacturing processes involved in this project include press cutting for the metal sheets, the rolling forming of tube indentations, and seam welding to join the sheets and create watertight indentations. However, a seam welder, although a common and straightforward machine, was not readily available at the university facilities (IO, 3mE, TNO). Alternatively, the metal sheets were spot welded in place, and soldering was applied along the edges to ensure watertight seals (Figure 43). This way, the solar collector was prototyped, and its functioning will be as if it was seam welded, although seam welding would have offered a more straightforward and robust connection, simplifying the process of achieving watertight seals.

Thus, although not the ideal manufacturing process for this application, soldering was the alternative solution to meet the immediate needs of the project. Due to its time-consuming nature and to the difficulties in creating a long and watertight, it was advised to scale the collector down as much as possible. Not to compromise too many results, it was decided to scale down by two-thirds, which means 0.66 metres of SMA wire can be heated and cooled in this prototype.

To securely assemble the prototype within the current frame, a specially designed frame for the sheet was created (Figure 44). This frame includes silicone isolation strips for house windows, minimising heat losses due to conduction. The sheet is fixed to the frame using bolts, which are also isolated with rubber washers.

In this way, the prototype was ready for experiments. However, it is important to recognise that there is still room for further improvements in the system's performance, such as:

• Reducing the sheet thickness to improve thermal efficiency and overall system performance.

• Incorporating insulation on the lower face of the sheets to help minimise heat losses and improve the system's efficiency.

• Reducing the indentation tube size enables more efficient heat transfer and increased cycle frequency, minimising the amount of water needed to cool down the system, leading to less energy being required to pump this cooling water, contributing to better overall performance.

These enhancements represent exciting opportunities for future refinements, promising to push the system's performance further and contribute to the ongoing development of this innovative pump.

Figure 43: Soldering process.

(a)

(b)

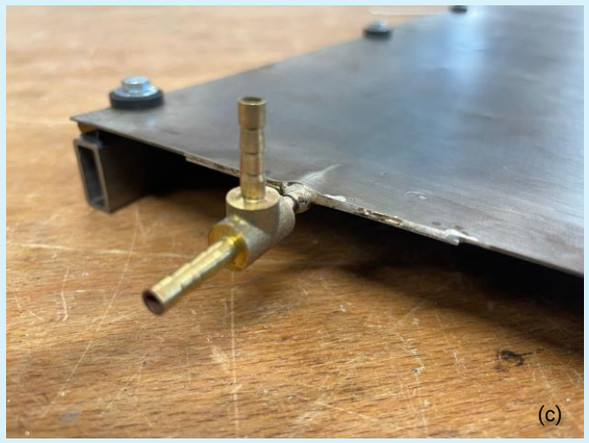

(c)

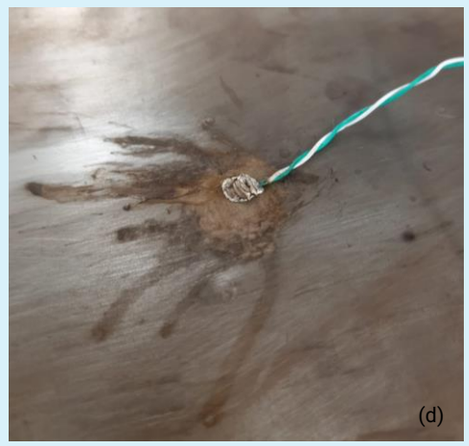

(d)

Figure 44(a): Soldered collector sheets. (b): Support frame. (c): Water and SMA connectors. (d): Thermocouple connection. (e): Assembled solar collector.

(e)

Design Iteration Validation

Experiment 3 – Testing Proposed Design

To test the previously presented proposed design and working principle of the solar collector, a hi-fi prototype was manufactured. This is one part of the whole system that, in the end, integrates multiple of these.

Research goals:

- **Validate the proposed design** – in other words, if the heating and cooling are more effective
- **Validate working principle** – confirm the self-starting hypothesis

Setup Description

The setup fundamentals are the same as in Experiment 2. The frame is the same, the SMA wire and the load are the same, but the heating system is different.

In this case, the prototyped solar collector is used to heat and cool the SMA wire. The heating is now done with a heat gun, simulating the increase in temperature on the top surface of the collector when the sun shines on it.

The cooling is done with the same DC motor and power supply as in Experiment 2. The experiment was done with the same 1mm NiTi SMA wire with an activation temperature of Af = 80ºC +/- 10ºC. However, this time, 0.66m were heated and cooled instead of the previous 1 meter.

The temperatures were measured with thermocouples (Figure 45) at three points of the collector (Figure 46). These were soldered to the steel sheet and were evenly spread out and centred with the indentation where the SMA is.

Figure 45: RS 1319A K-Type Thermometer

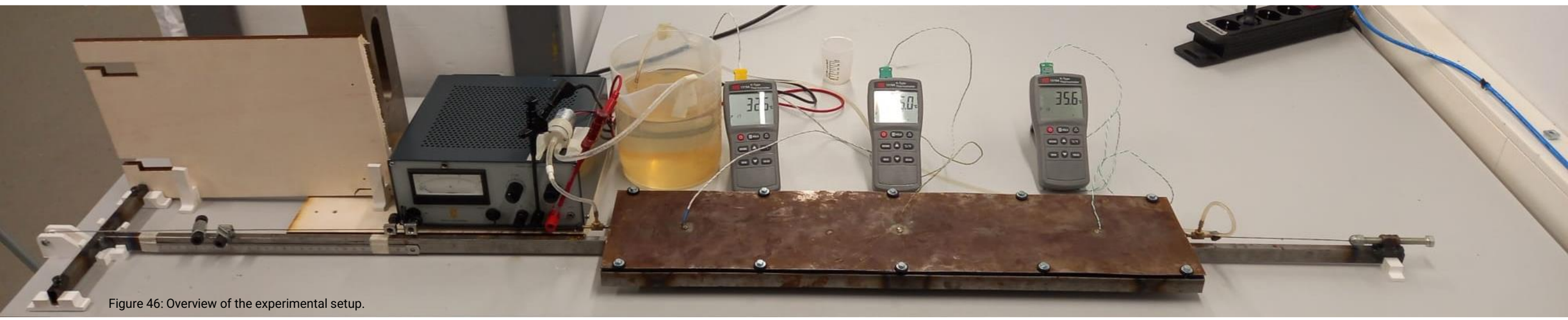

Figure 46: Overview of the experimental setup.

Experiment 3 – Results

The implemented solar collector resulted in fully executed phase transformations as the temperature measured was above Af. As a result, the system was able to lift the 10kg weight repeatedly.

The frequency at which it was able to do this was once every 20 seconds, with 2 seconds dedicated to the cooling process. The cooling required 25ml of cold water to achieve the desired temperature reduction and relax the SMA wire to a reversible position for the cycle to restart.

Additionally, the system showcased a displacement of around 15mm per 0.66m of wire, which is equivalent to strains of 2.3%.

Furthermore, the cooling was, for the first time, displacement-controlled. In fact, and as desired for the proposed design, at the end of the contraction of the SMA, the cooling was activated by moving the switch of the cooling pump. Moreover, at the end of the relaxation, this switch was shut off, allowing the wire to heat up again.

Experiment 3 – Takeaways

The results of this experiment were not only significant, but they also marked a major milestone in the development of the project. The heating and cooling working principle was fully validated, and the system's performance was vastly improved.

Additionally, the self-starting hypothesis was also confirmed, as the system was able to start on its own upon incident heat, seamlessly controlling the cooling with the displacement of the wire and repeating the cycle autonomously.

This remarkable achievement was a significant boost to the project's research goals, and it sets a solid foundation for future improvements, especially given that a lot can be improved to increase the system's performance.

This allows the addition of the next step of integrating the displacement pump and pump water, which is the ultimate goal of this project.

Experiment 4 – Pump Integration

As the SMA actuator working principle was validated, the sequential step is to make use of the produced mechanical labour to pump water by means of a displacement pump.

Since the SMA wire can only do force in one direction, the way of outputting the mechanical labour is by storing the energy laboured by the wire when it is heated up and contracted and using this energy to actuate the displacement and bring the system to its initial position when the wire is cooled down.

In addition, as the system outputs considerable forces but low displacements, a breakdown of the force has to be included. This was done by means of a lever, which is a very important element as its breakdown ratio is what ultimately controls the volume of water being displaced in the trade of the pumping head.

The ability to play with parameters such as the volume of water displaced per cycle and the relative pump head is relevant to this system. Thus, adjustability and room for tuning was a focus in the following setup

Research goals:

- **Gather insights on the integration of a pump to the system** – Identify the requirements for the lever to successfully integrate a positive displacement pump in the system with the desired volume displaced and pump head.
- **Prove the concept and pump water**

Setup Description

The majority of the setup was as described in the previous experiment. Thus, only the changes are mentioned in this section.

As mentioned, a lever has to be integrated into the system, meaning that the frame has to be upgraded.

As seen in Figure 47, the frame now includes a lever pivot point that is adjustable in position so the small arm of the lever can have multiple discrete lengths.

Regarding the lever, it was built for adaptability, meaning that the length of the smaller arm of the lever can be adjusted by means of a screw; the angle of the lever can be adjusted to create the right room for the displacement pump; there are multiple attaching points to the mount displacement pump in the lever, allowing again for adjustability in the lever breakdown ratio.

In addition, a longitudinal rack was welded to the frame to mount the other end of the displacement pump, as seen in Figure 48. By making use of the manufactured attaching components, the displacement pump can be secured in a wide window.

The wire tensioning screw was also made longer to allow for a greater adjusting window, as the SMA must now displacement exactly in a specified window.

The energy storage was done using springs.

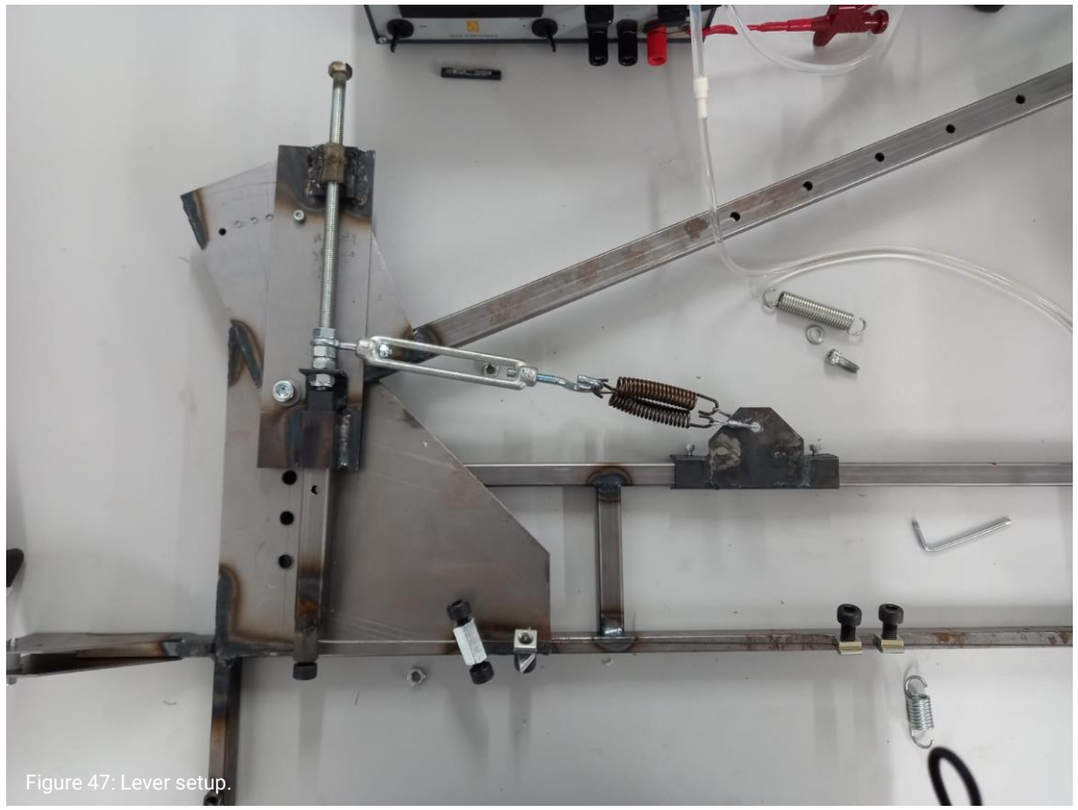

Figure 47: Lever setup.

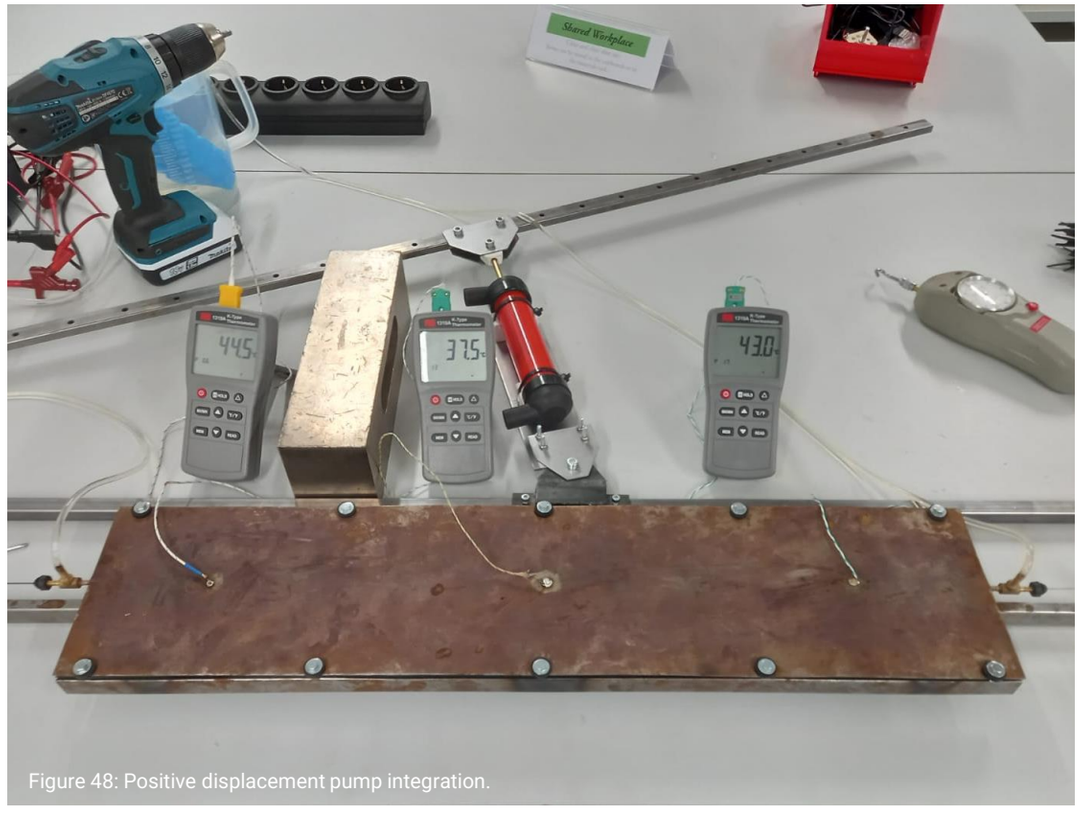

Figure 48: Positive displacement pump integration.

Experiment 4 – Results

The system did not work as the actuator was able to contract the SMA wire and move the pump's piston, but it was never able to return to the initial position when cooled down and thus pump water.

It was also verified that the wire was, in fact, relaxing, as could be visually seen in the lack of tension. However, the lever and, consequently, the pump were stuck, not returning to its initial position

Experiment 4 – Analysis and Takeaways

During the efforts to make the described setup work and pump water, a combination of the adjustable parameters was never found.

In fact, much playing with the length of the lever arms, the position of the pump, and the position and strength of the springs was done (Figure 49). However, these efforts were never enough to make the system work.

During the experiment, multiple insights were gathered regarding the reasons for the lack of pumping:

• The system had too much static friction – The main reason for the irreversible movement of the lever was the friction associated with the returning phase. Multiple factors contributed to this, including the fact that the vectors of the forces of the wire and the pump were not on the same plane of action. This induces momentum on the pivot point, leading to additional friction.

• The lever had flexibility – There was flexibility present in the lever, not on the steel beams themselves, but rather on the adjustable smaller arm of the lever. This meant that the wire could be displaced without displacing the pump, which, of course, is not desired.

Figure 49: Springs.

• The pump had too much friction – This meant that the pump required considerable output labour to overcome its friction and move to pump water.

With these gathered insights, a few directions can be taken to improve the system's performance and reach the ultimate goal of pumping water.

The main one included going back to using the weight as the energy-storing medium. The shift to the springs was motivated by the more compact solution. Which can in itself represent simplicity and cost reduction. However, springs can be less reliable and less optimal for this application, as their force changes with displacement, which, as it is well known by now, is not optimal for the SMA working window. This effect can be minimised by decreasing the arm of the mounting position, which reduces the displacement, but this comes with the cost of increased force on the pivot point, increasing friction. Another solution could be using gas springs, as they can have a closer to constant working window. However, they are a more complex solution which can be associated with higher costs. With this overview, storing the contracting energy on the potential energy of the weight may be the optimal solution, as it is extremely reliable and consistent, quite simple, and easily adjustable (Figure 50). These advantages, for now, overcome the disadvantage of being a less compact solution.

In addition to this, a new lever can be built. This lever should be simpler and stiffer.

Finally, an improved pivot point can be integrated to reduce the system's friction and, consequently, improve the performance.


Figure 50: Weights.

Experiment 5 – Final Prototype

As time comes to an end, this experiment is also the last of this graduation project. This final prototype is a refined iteration of the previously presented SMA-driven displacement pump, with the ultimate goal of pumping water.

Research goals:

- **Prove the concept and pump water**

Setup Description

The setup fundamentals are the same as in experiment 4. This means that 0.66m of a 1mm diameter Nitinol Shape Memory Alloy wire with an activation temperature of 80ºC +-10ºC is being heated up and cooled down with a prototype of the proposed solar collector that is being heated up with a heat gun and cooled down with cold water that is pumped with an external power supply.

Nevertheless, building upon the previous setup, the identified issues were addressed so that the system's friction could be marginally reduced. The return to the weight, the new lever and the improved pivot point (Figure 51) shift the eventual inefficiencies of the system to the displacement pump.

Thus, maybe not so surprisingly, the pump turned out to be the new critical point (Figure 52). In fact, the pump, as it came from its manufacturing, had too much static friction, and the system was not overcoming it, meaning that water was not being pumped.

As it turned out, the original piston had too much friction. As a result, a new piston had to be designed (Figure 53). However, the required balance between good sealing and low friction was quite hard to meet. In fact, due to the low speed and low force applied to the piston, it is necessary to have a proper seal so water does not return and low friction so that the SMA can overcome the friction force and pump water.

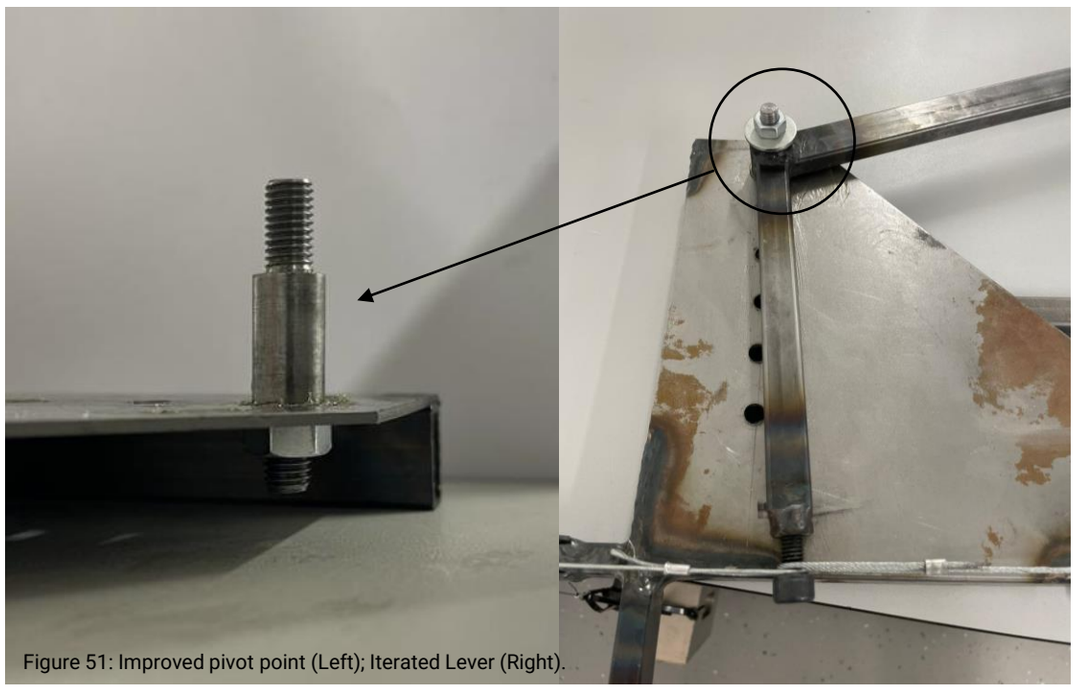

Figure 51: Improved pivot point (Left); Iterated Lever (Right).

To overcome this issue, a new piston and check valve were designed and integrated into the displacement pump, and the issue was mitigated, although not perfected.

Furthermore, regarding the description of the setup at hand, the lever breakdown ratio was 0.206, or 4.85, with the smaller arm measuring 180mm and the longer arm 875mm. The weight used was 10kg, applied in the same application point as the wire, adding a normal tension of 127.3MPa to the wire when contracting.

The full final setup can be overviewed on the following page in Figure 54.

Figure 52: Assembled displacement pump

Figure 53: Redesigning the pump's piston and check valve.

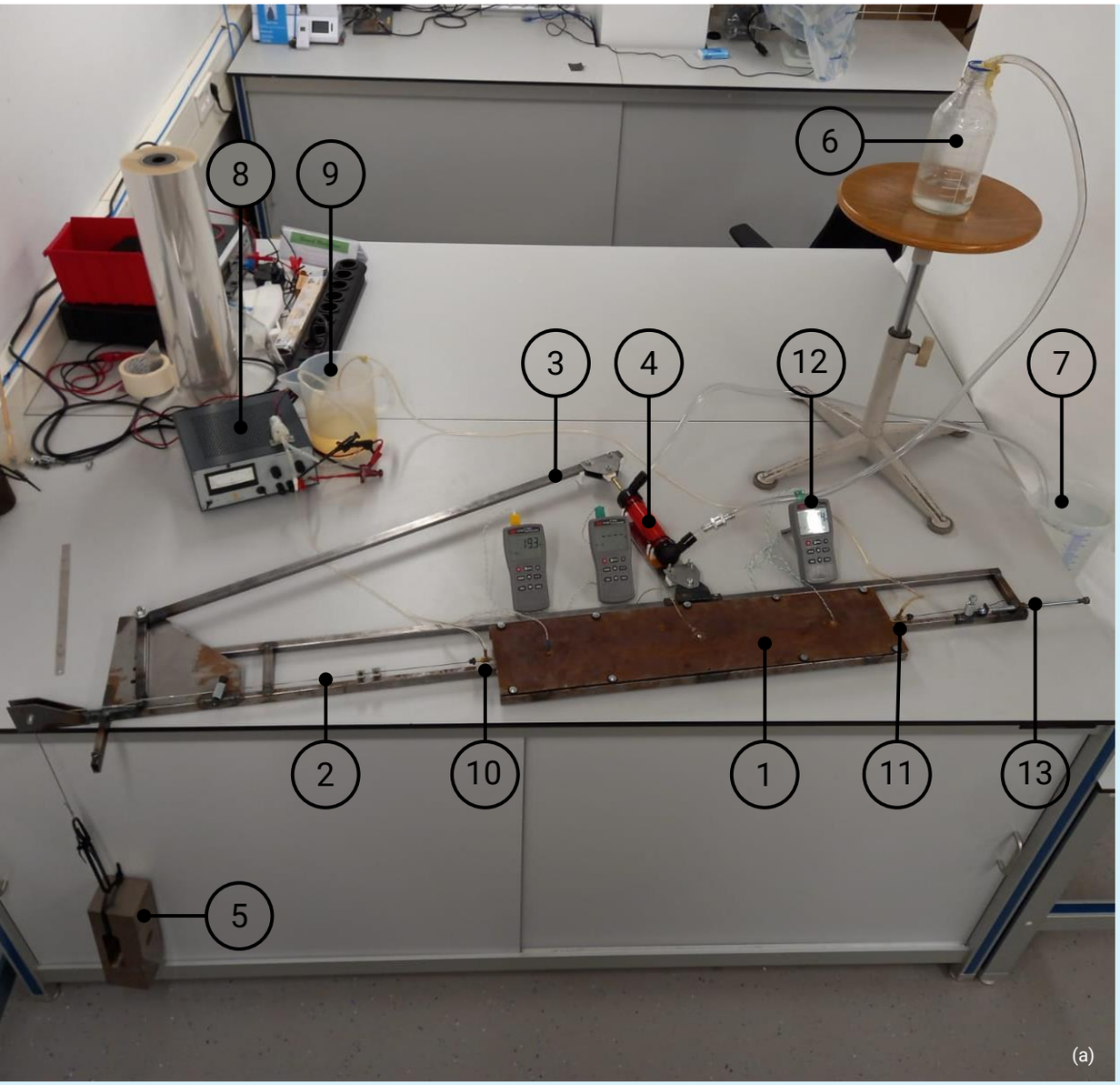

(a)

Legend:

1. Flat plate solar collector
2. Shape Memory Alloy nitinol 1mm-diameter-wire
3. Lever
4. Displacement pump
5. Weight
6. Downstream reservoir
7. Upstream reservoir
8. Power source and DC cooling pump
9. Cooling water reservoir
10. Cooling water entrance
11. Cooling water exit
12. Thermometers
13. Wire screw tensioner

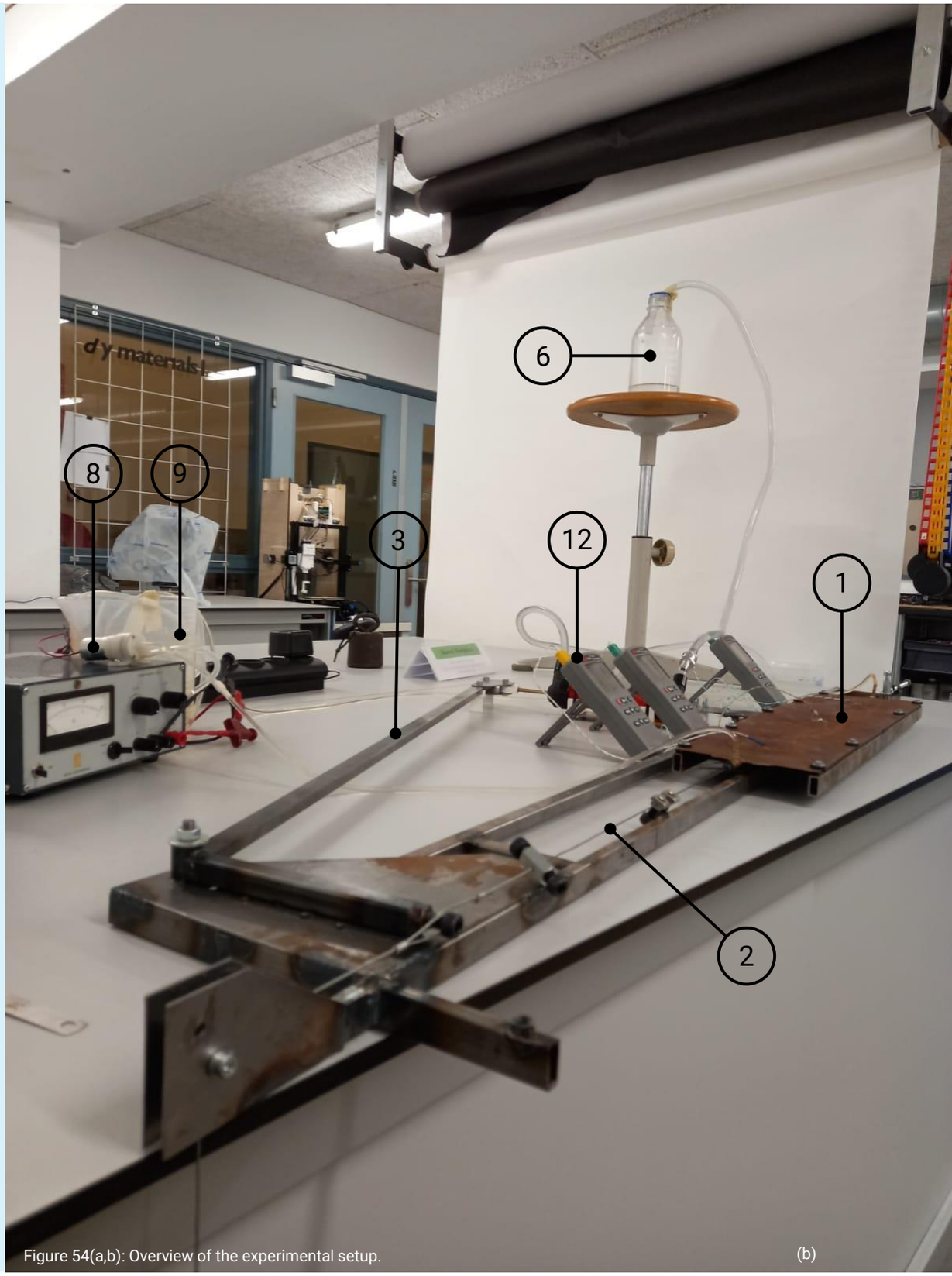

Figure 54(a,b): Overview of the experimental setup.

(b)

Experiment 5 – Results

Static Measurements

Before the input of heat to the system, the required forces to move the lever and, thus, the pump were measured with the dynamometer seen in Figure 55:

The force necessary at the wire application point without weight load is 52N. This is the force associated with the heating phase of the wire and represents the lever's friction and the force necessary to the opening of the piston's check valve and move the pump's piston. When the weight was added to the system, this force was measured at 156N. Similarly, these forces were measured at the pump's application point, measuring 6N without the weight load and 17N with it.

Likewise, the forces were also measured for the phase of relaxation of the wire. At the pump's application point, the force required to pump the water downstream is 18N, at the lever, this force was measured to be 86N. This is the force required to pump water over the 0.8m with the implemented displacement pump.

Dynamic Measurements

Regarding the results with heat input, the main one is that the system works as it pumps water, more specifically, 22mL at a head of 0.8m (Figure 56).

This was associated with the measured displacements of 28mm at the pump piston and around 6mm at the lever. This translates to a displacement of 6mm at the SMA wire, which corresponds to a strain of 0.9%.

The cooling water flow, currently being pumped using electricity, was measured with a pressure sensor. The system requires a total flow of 25 mL for approximately 2 seconds at a pressure of 0.116MPa to cool effectively, which is equivalent to 1.6m of head.

Lastly, regarding the pumping frequency, the heating and cooling took around 35 seconds per cycle.

Figure 55: Dynamometer


Figure 56: Pumped water deposit.

Experiment 5 – Analysis

These results reveal the upside of having a system that pumps water. This was the desired outcome for this project, and so there are reasons to call it a successful experiment.

However, the system is quite unoptimised, and as the results revealed, the volume of water that is being pumped per cycle is just smaller than the volume needed to cool the SMA wire at the end of the cycle. In addition, the cooling water is being pumped at 0.116MPa, which is equivalent to having a water deposit at 1.6m in height. Since the system's displacement pump was pumping water at only 0.8m, the system was not producing enough power to be a standalone solution.

This lack of performance is a consequence of a still unoptimised system. This statement can be reasoned by the low values of strains that the SMA is showcasing and the high values of forces required to open the piston's check valve and move the piston when contracting the wire.

In fact, the SMA wire was only showcasing strains of 0.9%, which is a significant decrease compared to the 2.6% verified in Experiment 3, without the pumping system, which was already a relatively low value compared to the set goal of staying within the fatigue cared working window of 5%. This is extremely relevant to the performance of the pump as if strains of 5% were reached, the system would be pumping 5 times more water, pumping 125mL per cycle.

Overviewing the experiment, the main reason for these low strains, when compared to the previous Experiment 3, is likely to be the significant static friction present in the system, especially in the pump. This static friction means that to start moving the pump's piston, more force has to be applied. This, combined with the fact that the heating and contraction of the wire is rather slow, causes the piston to move in discreet motions, being static for a while and then suddenly being displaced. This means that at the end of the contraction and relaxation, the wire is still applying force to the pump, but it does not move anymore. This represents, of course, a loss of displacement and, consequently, a loss in the output power.

Moreover, moving the piston and opening its check valve requires a very considerable amount of force – 52N at the wire's application point. This means that at the contraction phase of the wire, 52N out of the 156N are used to move the piston. In other words, a third of the force is lost to friction and non-labour-outputting tasks during the contraction phase, as this is not stored and is also not used to move any water. Thus, the efficient reverse piston movement and opening of its check valve were revealed to be a critical contributor to the performance of the system.

Furthermore, improving just the static friction would contribute marginally to the improvement of the system's performance and more impressive volumes of water would be pumped.

Experiment 5 – Takeaways

The milestone of successfully pumping water was achieved. It can be affirmed that the system is operational and meets the desired degree of simplicity and accessibility, as the demonstrated experiments have been executed with a low budget, making use of basic tools and readily available material.

Overcoming this challenge required iterative design and problem-solving. Initially, the spring and gas spring mechanisms did not provide the optimal load curves, leading to ultimately reverting to a weight-based system. This method of leveraging the contraction of the wire to lift a weight and then harnessing that stored energy to pump water upon wire relaxation has proven to be simple, reproducible, reliable, and easy to fine-tune.

Adding to that, reducing the friction within the system was crucial. A redesign involving a simplified and stiffer lever, coupled with a new machined pin with reduced friction, has enhanced the system's performance.

Additionally, the original piston of the pump was reengineered to strike the delicate balance between low friction and effective sealing, which was not reachable with the original pump's piston or with simple modifications. In the process of designing the new piston, the design of a bike pump's cylinder, piston and check valves was seen as a great example of the characteristics that the displacement pump of a future system should have.

This process revealed one of the main takeaways from this experiment, which is that every element of the system is critical and that all of them have important contributions to the system's performance. It is a system that works as a whole where the subsystems' performance depends on the other subsystems. To be optimised, all of its parts must work together harmoniously (Figure 57).

Thus, efficiency remains a primary area for improvement, and the current system has not yet reached an optimised state. For increased performance and more impressive results, there are several aspects of the prototype that require further enhancement:

• The collector's specific heat capacity can be decreased by using thinner sheets (Figure 58), which would speed up heating and cooling, thereby increasing performance and reducing the water volume needed for cooling.

• Similarly, a thinner indentation within the collector would facilitate faster thermal cycling and further reduce the water required for cooling.

• The piston of the pump still has excessive friction, resulting in non-continuous movements due to high static friction. A more refined pump design could reduce this friction and allow for better efficiency and more water to be displaced.

Furthermore, the cooling is still being controlled by an external source. The cooling with the high deposit could have been done, but it is not a component that requires further testing, as it is straightforward that it would work with the suggested design and valve (Figure 59). In addition, it would restrict the flexibility of the laboratory experience, as it is easier to fine-tune the DC pump.

Figure 57 Close-up of the experimental setup.


Figure 58 Steel sheets with various thicknesses.


Figure 59: Switch valve.

Conclusion

As the project comes to an end with the working principle validated through a proof-of-concept prototype (Figure 60), this final chapter sums up the project conclusions and highlights recommendations for future work.

Contents

- Conclusions
- Future Recommendations

Figure 60: Close-up of the proof-of-concept prototype of the SMA-driven solar-powered water displacement pump.

Conclusions

The project has been successfully completed with a proof of concept that aligns with the established objectives of simplicity and accessibility. In fact, the water pump prototype was created on a minimal budget, utilising simple tools and materials that are widely available, highlighting its potential for scalable application as the elegant integration of the SMAs into the collector's design is a notable achievement, showcasing the feasibility of manufacturing these panels in series through cost-effective processes.

In addition, the hands-on experience with the working principle concluded that efficiency is a crucial aspect of a solar-heated water displacement pump. Characteristics such as the material working window and its performance, the collector geometry and the efficiency of the heat transfer in the solar collector combined with the minimisation of energy losses and friction are critical aspects essential to achieve significant performance.

Moreover, this preliminary success has laid a solid foundation, revealing that while the current system is functional, the untapped potential of the technology is still vast. The experiments suggest that the system has not yet showcased its peak performance, suggesting that with further research and development, marginal advancements in efficiency and power output are within reach. Thus, the presented work paves the way for further research to build upon these initial findings, ultimately leading to a more mature technology that can contribute to the mitigation of the dire reality of the two billion people lacking access to safely managed drinking water today.

Future Recommendations

As the project transitions beyond the scope of the current academic work, several recommendations are proposed to further the development and potential impact of the presented pumping system:

Firstly, a systematic thermodynamic study should be conducted to enhance the efficiency of the heat transfer in the solar collector. This means evaluating different materials and geometrical dimensions for the sheets and performing simulations to maximise performance and efficiency.

An in-depth investigation into the Shape Memory Alloy (SMA) composition and optimal working window is critical. This should include a reevaluation of the different alloy options to strike the optimal balance between power output, number of cycles and cost.

The life limit of the SMA wire under the designed conditions should also be studied. This is a critical point to ensure the pump meets the required durability and the system's viability.

In addition, the current manufacturing techniques should be reviewed for the seamless integration of all the elements with an eye on scalability and cost reduction.

An in-depth study of the potential implementation sites and their demographic and geographic characteristics should be done. This should include a precise mapping of the pumping needs of illustrative target communities as well as an idea of the elevation and distance to cover to transport the water. This gives insights into the range of necessary output power of the system and allows dimensioning.

After these, and to measure the system's efficiency for a fair comparison with benchmark pumps, a minimum-value solar collector should be prototyped and tested with representative incident radiation. Improving the current prototype's performance would help showcase the potential of the technology and attract more attention to the project.

Moreover, from a more culture-sensitive perspective, future research should include a comprehensive analysis of the sociocultural impact of the implementation of this technology in the affected regions of the world, as it is important to understand the impact of such a change in people's lives, namely for women.

Furthermore, a more detailed plan that includes justified development steps and targets, a funding plan and potential partners is essential for the success of the progress. This plan should also include a business plan, ensuring that the project is feasible, scalable, and viable.

By pursuing these recommendations, the project can evolve from the prototypical design proposition to a technically optimised solution with the desired, feasible and viable potential for real-world applications. This will ultimately help the ongoing global effort to meet the Sustainable Development Goal 6, providing access to the basic need for safely managed drinking water for everyone (Figure 61).

Figure 61: Child drinking safely managed drinking water. Photography from UNICEF, 2019.

References

A/RES/70/1. (2015). Transforming our world: The 2030 Agenda for Sustainable Development. https://www.un.org/en/development/desa/population/migration/generalassembly/dccs/globalcompact/A_RES_70_1_E.pdf, Retrieved December 2023

Awan, A. B., Zubair, M., Memon, Z. A., Ghalleb, N., & Tlili, I. (2021). Comparative analysis of dish Stirling engine and photovoltaic technologies: Energy and economic perspective. *Sustainable Energy Technologies and Assessments*, 44, 101028. https://doi.org/10.1016/j.seta.2021.101028

Boretti, A. (2020). Cost of dispatchable electricity from concentrated solar power, solar tower plants, with 10 hours' molten salt thermal energy storage. *E3S Web of Conferences* 173, 02003. https://doi.org/10.1051/e3sconf/202017302003

Bošnjaković, M., Galović, M., Kuprešak, J., & Bošnjaković, T. (2023). The End of Life of PV Systems: Is Europe Ready for It? *Sustainability*, 15(23), Article 23. https://doi.org/10.3390/su152316466

Caille, F. (2017). L'énergie solaire thermodynamique en Afrique. *Afrique Contemporaine 2017/1* Nº 261-262, pages 65 à 84. DOI 10.3917/afco.261.0065

Coventry, J., Andraka, C. (2017). Dish Systems for CSP. *Solar Energy*, Volume 152, pp 140-170. https://doi.org/10.1016/j.solener.2017.02.056

Deshpande, A., Miller-Petrie, M. K., Lindstedt, … Reiner, R. C. (2020). Mapping geographical inequalities in access to drinking water and sanitation facilities in low-income and middle-income countries, 2000–17. *The Lancet Global Health*, 8(9), e1162–e1185. https://doi.org/10.1016/S2214-109X(20)30278-3

Gersherson, D., Rohrer, B., Lerner, A. (2019). A new predictive model for more accurate electrical grid mapping. https://engineering.fb.com/2019/01/25/connectivity/electrical-grid-mapping/, Retrieved December 2023

Ho, J. C., Russel, K. C., & Davis, J. (2014). The challenge of global water access monitoring: Evaluating straight-line distance versus self-reported travel time among rural households in Mozambique. *Journal of Water and Health*, 12(1), 173–183. https://doi.org/10.2166/wh.2013.042

Jani, J.M. (2016). Design Optimisation of Shape Memory Alloy Linear Actuator Applications. PhD Thesis, RMIT University

Jani, J.M., Leary, M., & Subic, A. (2017). Designing shape memory alloy linear actuators: A review. *Journal of Intelligent Material Systems and Structures*, 28(13), 1699–1718. https://doi.org/10.1177/1045389X16679296

Mancini, T. et al. (2003). Dish-Stirling Systems: An Overview of Development and Status. *Journal of Solar Energy Engineering*, Vol. 125 pp 135-151. DOI: 10.1115/1.1562634

Molden, D. (2007). Water for food Water for life: A Comprehensive Assessment of Water Management in Agriculture. International Water Management Institute. Earthscan. https://www.iwmi.cgiar.org/assessment/files_new/synthesis/Summary_SynthesisBook.pdf, Retrieved December 2023

Moran, M.J., Shapiro, H. N., Boettner, D.D., Bailey, M.B. (2014) Fundamentals of Engineering Thermodynamics, 8th Edition, Wiley. ISBN 1118832302, 9781118832301

Muhammad Z.M. et al. (2022). A review on design parameters and specifications of parabolic solar dish Stirling systems and their applications. *Energy Reports* 8, pp 4128-4154. https://doi.org/10.1016/j.egyr.2022.03.031

NASA. (2017). Map of the electrical grid of the world. https://www.nasa.gov/feature/goddard/2017/new-night-lights-maps-open-up-possible-real-time-applications, Retrieved June 2023

Nussey, B. (2019). The earth gets more solar energy in one hour than the entire world uses in a year. Freeing Energy. https://www.freeingenergy.com/the-earth-gets-more-solar-energy-in-one-hour-than-the-entire-world-uses-in-a-year/, Retrieved December 2023

Our World in Data. (2023). Research and data to make progress against the world's largest problems. https://ourworldindata.org/, Retrieved December 2023

Pytlinski, J. T. (1978). SOLAR ENERGY INSTALLATIONS FOR PUMPING IRRIGATION WATER. *Solar Energy*, Vol.21, pp. 255-262.

Rao, A., Srinivasa, A. R., & Reddy, J. N. (2015). *Design of Shape Memory Alloy (SMA) Actuators*. Springer International Publishing. https://doi.org/10.1007/978-3-319-03188-0

Tamera. https://www.tamera.org/solar-research/ Retrieved December 2023

The World Bank. (2019). Global Solar Atlas. https://globalsolaratlas.info/download/world, Retrieved December 2023

Tortajada, C. (2014). Water infrastructure as an essential element for human development. *International Journal of Water Resources Development*, 30(1), 8–19. https://doi.org/10.1080/07900627.2014.888636

United Nations. (2023). Extended Report Goal 6. https://unstats.un.org/sdgs/report/2023/extended-report/Extended-Report_Goal-6.pdf, Retrieved December 2023

United Nations Department of Economic and Social Affairs. (2023). The Sustainable Development Goals Report 2023: Special Edition. https://doi.org/10.18356/9789210024914

van Ginneken, M., Netterstrom, U., & Bennett, A. (2011). More, Better, or Different Spending? *Water Papers* 67321-AFR https://www.ircwash.org/sites/default/files/Ginneken-2011-More.pdf, Retrieved December 2023

Vanham, D., Alfieri, L., & Feyen, L. (2022). National water shortage for low to high environmental flow protection. *Scientific Reports,* 12(1), 3037. https://doi.org/10.1038/s41598-022-06978-y

WHO/UNICEF Joint Monitoring Program. (2023). Progress on household drinking water, sanitation and hygiene 2000–2022: special focus on gender. https://washdata.org/reports/jmp-2023-wash-households, Retrieved December 31, 2023

World Bank Group Energy Sector Management Assistance Program. (2020). Global Solar Atlas 2.0: Technical Report (English). http://documents.worldbank.org/curated/en/529431592893043403/Global-Solar-Atlas-2-0-Technical-Report, Retrieved December, 2023

World in Maps, (2023). World population density. https://worldinmaps.com/world/population-and-settlement/population-density/, Retrieved December 2023

Wong, Y. W., Sumathy, K. (1999). Solar thermal water pumping systems: A review. *Renewable and Sustainable Energy Reviews*, 3(2–3), 185–217. https://doi.org/10.1016/S1364-0321(98)00018-5

Appendix A – Problem and its Evolution – Call for Action

The global overview quantifies the severity of the water problem our society is facing, highlighting that there has been a considerably significant global effort aimed at making the Sustainable Development Goals a worldwide reality.

Remarkably, since the settlement of the SDGs in 2015, an average of ten billion dollars have been disbursed annually to assist the development of the water sector (WHO/UNICEF JMP, 2023).

However, despite these substantial efforts, the pace of progress and the evolution of the global situation, as seen in Figure A1, remain insufficient to meet the ultimately settled goal.

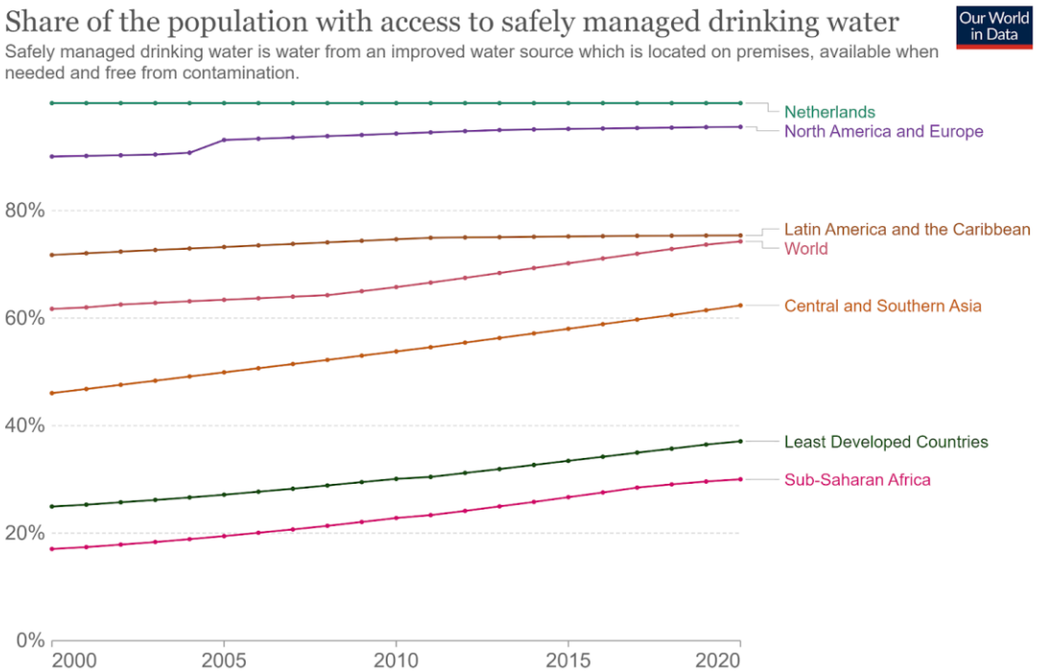

Figure A1: Share of Population with access to safely managed drinking water based on WHO/UNICEF Joint Monitoring Program (JMP) data (Our World in Data, 2023).

In fact, at the current rate of progress, the world will only reach 81% coverage by 2030.

As a result, the target is missed, and 1.6 billion people will remain without safely managed drinking water.

For a favourable extrapolation that reaches 100% by 2030, the progress pace must increase by six times per year (United Nations JMP, 2023).

Thus, it is evident that the progress in mitigating this issue is far from satisfactory.

On top of that, a closer examination of the regional breakdown within the global statistics reveals a striking discrepancy between different regions around the world.

On a positive note, it is heartening to observe that there are examples of success where water access is available to the entire population.

However, on the other side of the spectrum, it is very alarming to look at the situation of regions such as Sub-Saharan Africa – that englobes 847 million habitants – where 70% of the population lack access to safely managed drinking water (Our World in Data, 2023).

Moreover, examining the water access crisis from a different perspective and looking at nominal total numbers (Figure A2) provides a more comprehensive understanding of the depth of the water access crisis in the most severely affected regions of the world, particularly Sub-Saharan Africa.

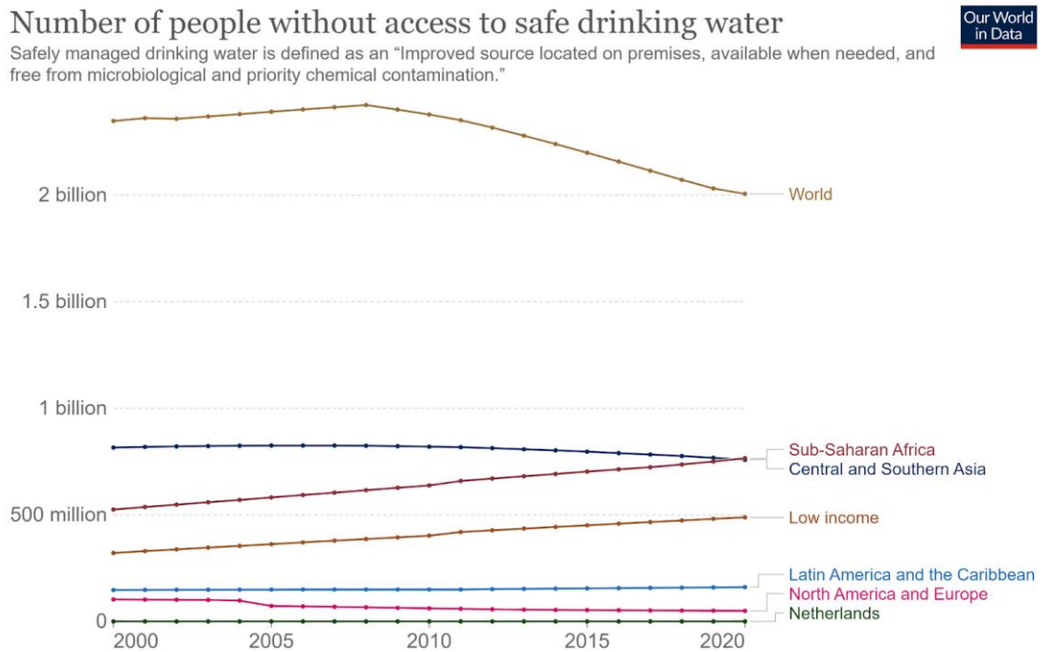

Figure A2: Number of people without access to safe drinking water based on WHO/UNICEF Joint Monitoring Program (JMP) data (Our World in Data, 2023).

In fact, despite the percentual increase in access to safely managed drinking water in Sub-Saharan Africa, the simultaneous rise in population reveals the staggering reality that the number of people affected in this region has actually increased.

As a matter of fact, the population of Sub-Saharan Africa has doubled since the beginning of the new millennium (Our World in Data, 2023).. This significant demographic shift led to a frightening 50% increase in individuals without access to such a basic need as safe drinking water.

This newly unveiled factor, population growth, significantly influences the challenges and constraints already identified.

Moreover, it is crucial to acknowledge that the population growth trend is not solely present in Sub-Saharan Africa but, in fact, a global trend, as it is addressed and analysed in the following section.

Figure A3: Skyline of Shanghai from 1990, with 8.6 million inhabitants, compared to 2010, with 20.3 million. In 2023, Shanghai has 29.2 million inhabitants. Photography from population.un.org.

Population Growth

As seen altogether, the present water crisis is intensified by the exponential growth of the world's population, which has doubled over the past half-century (Figures A3 and A4).

On top of that, looking at the locations where the population is growing at the fastest rate identifies an additional obstacle – the places where water access problems are most extreme are also where the population is growing at the fastest rate.

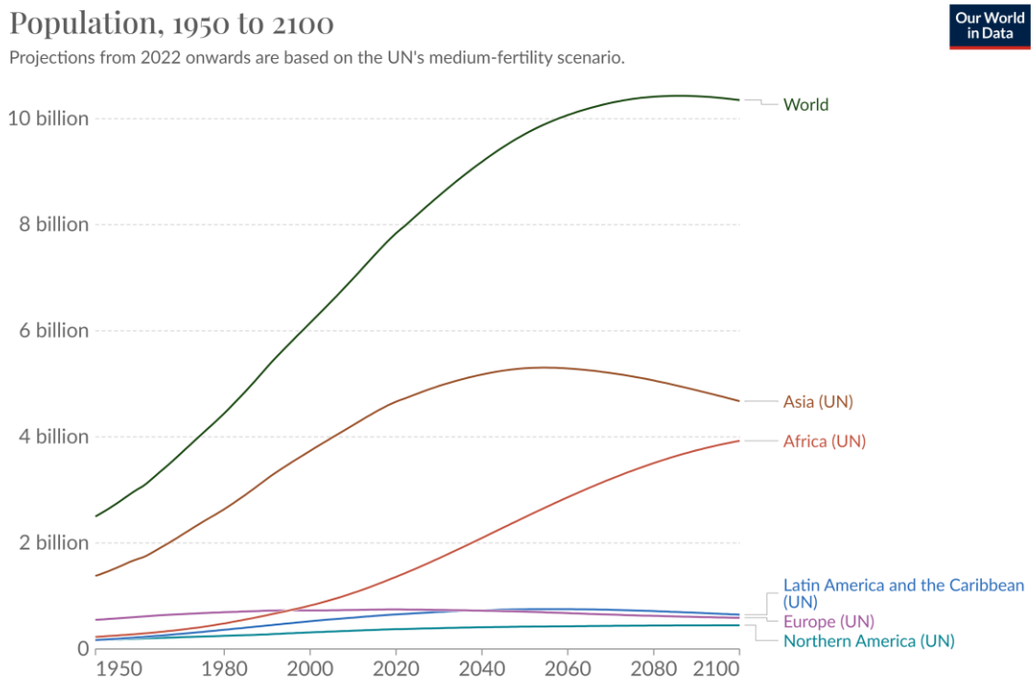

Figure A4: Projected population growth from 1950 till 2100 based on United Nations World Populations Prospects from 2022 (Our World in Data, 2023).

In fact, Africa's population is projected to double by the end of the century.

This prediction underscores that achieving the Sustainable Development Goal 6 by 2030 is not a guarantee of a permanent solution to the issue.

On the contrary, ensuring safely managed drinking water for the entire global population is a challenge that will demand ongoing investment and effort, even beyond 2030, until the global population settles at over ten billion people by 2080.

Hence, given the extra obstacle, providing everyone with safely managed drinking water becomes exceedingly challenging.

Nonetheless, these are not the sole additional challenges acting against the current. In fact, climate change and its related consequences further compound the complexity of the situation.

Climate Change

In addition to the rise in the populace on our planet, climate change and its consequences are also intricately connected with water access.

One of the most critical manifestations of climate change on this matter is altered precipitation patterns, which lead to more frequent and severe droughts in some regions and increased rainfall in others. These changes disrupt the steadiness of the availability and distribution of freshwater resources, posing a serious challenge to effective water resource management (Figures A5-7).

On top of that, rising temperatures escalate evaporation rates from critical water bodies, especially in the regions already struggling with droughts and limited water supplies.

Compounding these impacts are the more frequent and severe weather events like intense storms and hurricanes, which can flood or contaminate water supplies.

Altogether, global warming and its consequences are projected to intensify in the coming decades.

Therefore, the call for action could not be more urgent, especially given the impact the lack of access to safely managed drinking water has on human life.

Figure A5: Melting glaciers in Pakistan led to record monsoon season and deadly flooding in the province of Balochistan in August 2022. Photographed by Fida Hussain.

Figure A6: A shepherd drinks water on the dry bed of Manjara Dam, which supplies water to Latur and nearby villages in the Indian state of Maharashtra. Photographed by Manish Swarup.

Figure A7: Flooding in the Northern District of Karonga, Malawi, 2015.

Impact on Human Life

Water is the most vital element for human life. It plays a fundamental role in all facets, from health and sanitation to agricultural, economic and societal activities.

Thus, the deprivation of access to safe drinking water, the essence of life, has profound consequences on human life, as without it, people cannot live (Figure A8).

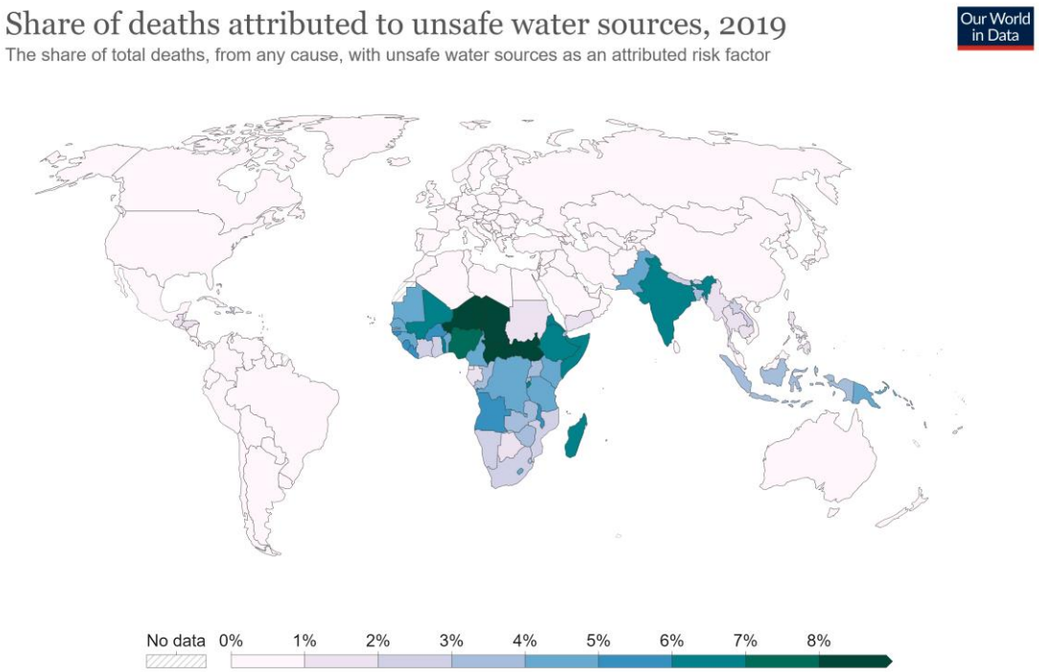

Figure A8: Share of deaths attributed to unsafe water sources based on IHME Global Burden of Disease data from 2019 (Our World in Data, 2023).

An estimated 1.2 million people died because of unsafe water sources in 2017. This represents 2.2% of global deaths.

In the year 2017, the share of annual deaths attributed to unsafe water ranged from a maximum of 14% in Chad – around one in every seven deaths – to less than 0.01% across most of Europe.

In low-income countries, unsafe water sources account for 6% of deaths on average (Our World in Data, 2023).

These statistics are extremely alarming and warning. Although even if the lack of access to safely managed drinking water does not lead to the irreversible life-ending outcome, it still has major implications that affect various aspects of the way people live, including health, well-being, proper nutrition, societal organisation, as well as economic development.

Health and Sanitation

The lack of access to clean and safe drinking water makes communities vulnerable to waterborne diseases. Without clean water for drinking, cooking, or washing, maintaining minimum hygiene becomes a challenge, leading to diseases such as cholera, dysentery, or typhoid.

In addition, insufficient clean water supply impedes proper sanitation, which is crucial to public health by preventing the spread of infections.

Daily Impact

The lack of safe drinking water at the premises of households forces people to carve out significant time of their routines to collect water every day, at the expense of other tasks. This collecting water task, on top of being a very time-consuming task, is extremely physically demanding. Carrying heavy loads of water on a daily basis can lead to injuries and physiognomy repercussions, among other long-term health problems.

Gender Equality and Education

Traditionally, women and girls are often the most affected by the consequences of water scarcity, as they are typically responsible for water collection for their communities (Figure A9). During that task, they can spend hours daily walking back and forth, which could otherwise be spent on education or income-generating activities. This not only perpetuates the present cycle of poverty and gender inequality but also limits personal growth and development.

Figure A9: Women carrying water in India. Photographed by Andre Fanthome.

Food Security

Water scarcity and climate change also impact food security since agriculture heavily relies on consistent water availability. When water access is scarce, crop yields are decreased, and thus, less food is available. Over time, this can lead to malnutrition and, once again, diseases and infections, which is especially detrimental to children as it can cause stunted growth and long-term health issues (Figure A10).

In addition, by undermining food production, water scarcity financially strains economies. Low harvests lead to a direct loss of income, preventing reinvestment in their agricultural practices. This can trap farming communities in a cycle of poverty, stifling economic growth.

Migration and Displacement

Water scarcity also has profound social implications, often serving as a catalyst for migration, displacement and conflicts. In fact, it can force communities to leave their homes in search of more stable water resources. Thus, internal and cross-border movements become more common.

This migration can stress existing tensions or create new conflicts over water rights and resources, leading to increased instability. In fact, 153 countries share water bodies with neighbouring nations.

Figure A10: Children in Rwanda. Photography from UNICEF.

Appendix B – Contextual Disparities

Access to safely managed drinking water varies significantly across different regions. As Appendix A concludes, certain regions of the world, such as Sub-Saharan Africa and Central and Southern Asia, are more affected than others. However, the global renewable water availability map, as seen in Figure B1, fails to capture this.

In fact, the abundance or lack of access to water does not correlate proportionally to the abundance or scarcity of water resources.

As a matter of fact, Southeast Asia is the region of the world with the most water resources and still reports alarming numbers regarding access to safely managed drinking water (Vanham et al., 2022).

Thus, the challenge of water scarcity and its accessibility extends beyond the mere presence of water resources. This prompts a more in-depth exploration of the factors contributing to the difficulties in securing safe drinking water in specific regions.

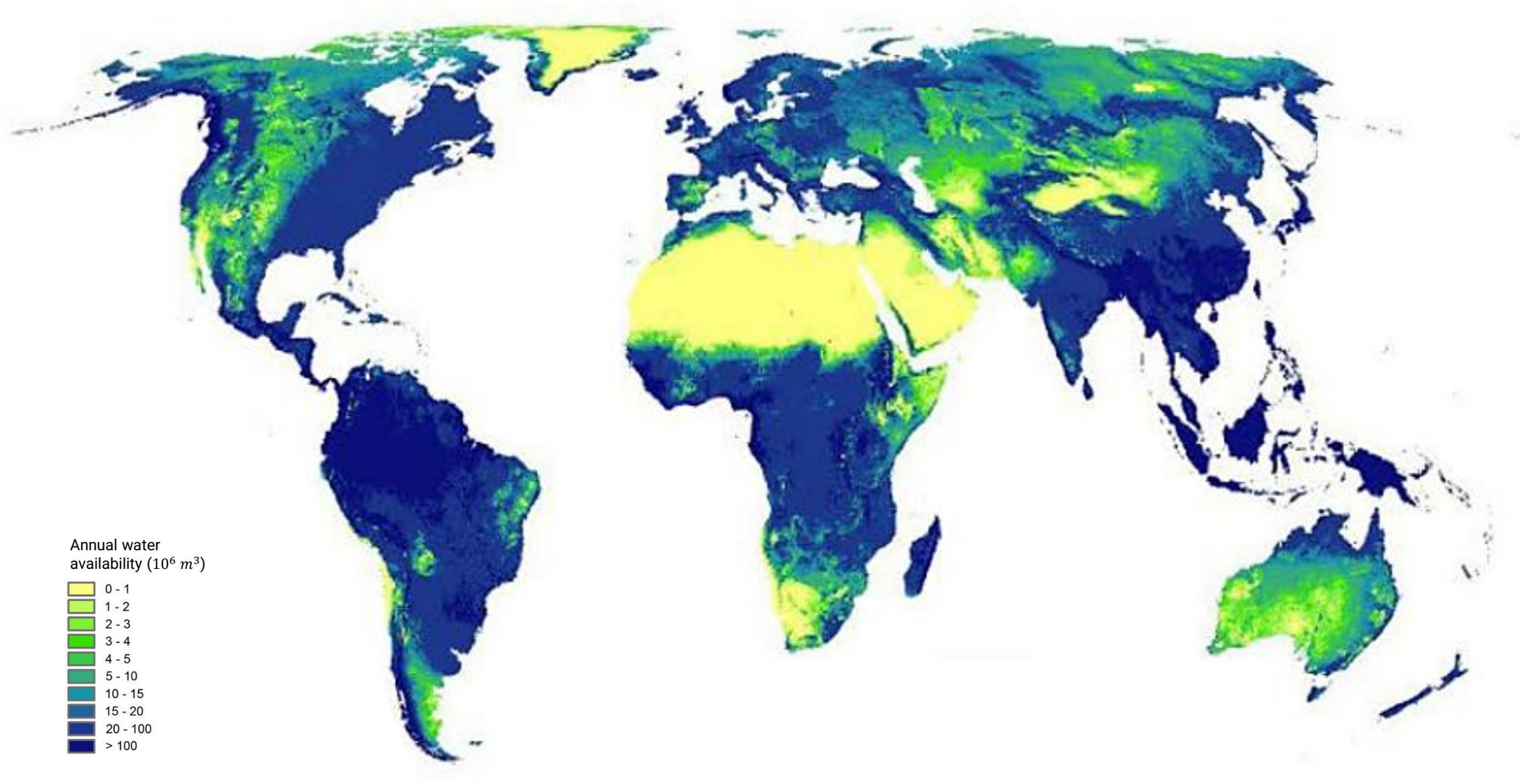

Figure B1: Global annual natural renewable water availability map with 0.1 degrees resolution (11.1km*11.1km) (Vanham et al., 2022).

Water and Population Distribution

When considering the availability of natural water resources, it's insightful to compare this data with the global demographic distribution seen in Figure B2 (World in Maps, 2023).

This is relevant because a common perception might suggest that arid regions, such as deserts, significantly contribute to the global water stress narrative due to their inherent lack of water. Yet, it is crucial to note that these desert areas have minimal impact on the global water stress picture since they are home to very few people.

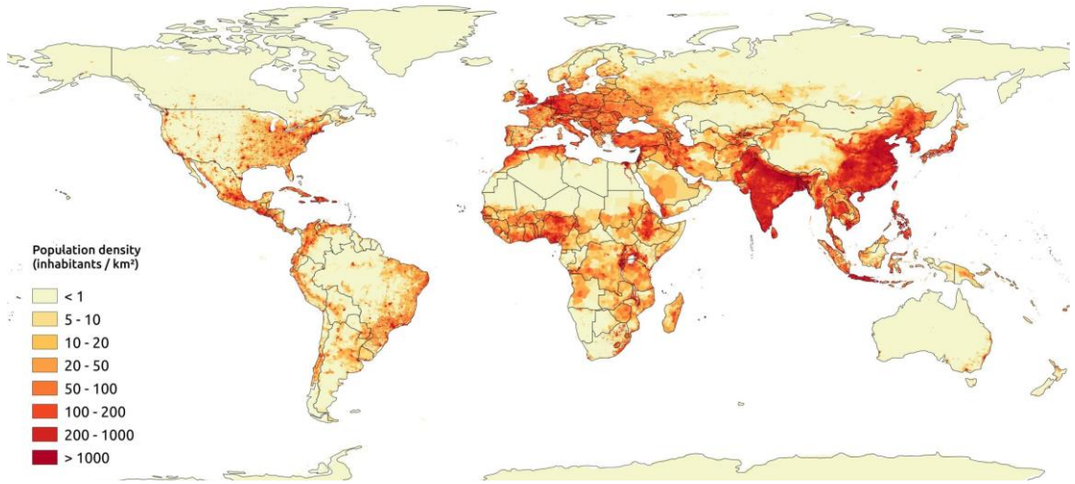

Figure B2: Global population distribution (World in Maps, 2023).

Infrastructure and Water Scarcity

Upon research to identify the key factor contributing to water scarcity in the most affected regions of the world, it became evident that it results mainly from inadequate infrastructure, water management and water transportation systems.

As reported in the literature (Molden D., 2007), this is a result of the overall lack of economic development (Figure B3).

In this literature, economic water scarcity is declared if human, institutional, and financial capital limit access to water even though water in nature is available locally to meet human demands. In practice, economic water scarcity is declared when water resources are abundant relative to water use, i.e., when less than 25% of the water from available water bodies is withdrawn for human purposes, but malnutrition exists.

Similarly, little or no water scarcity means abundant water resources relative to use, with less than 25% of water available being withdrawn for human purposes.

Lastly, physical water scarcity means water resources are approaching or have exceeded sustainable limits. In practice, more than 75% of water bodies are withdrawn for agriculture, industry, and domestic purposes.

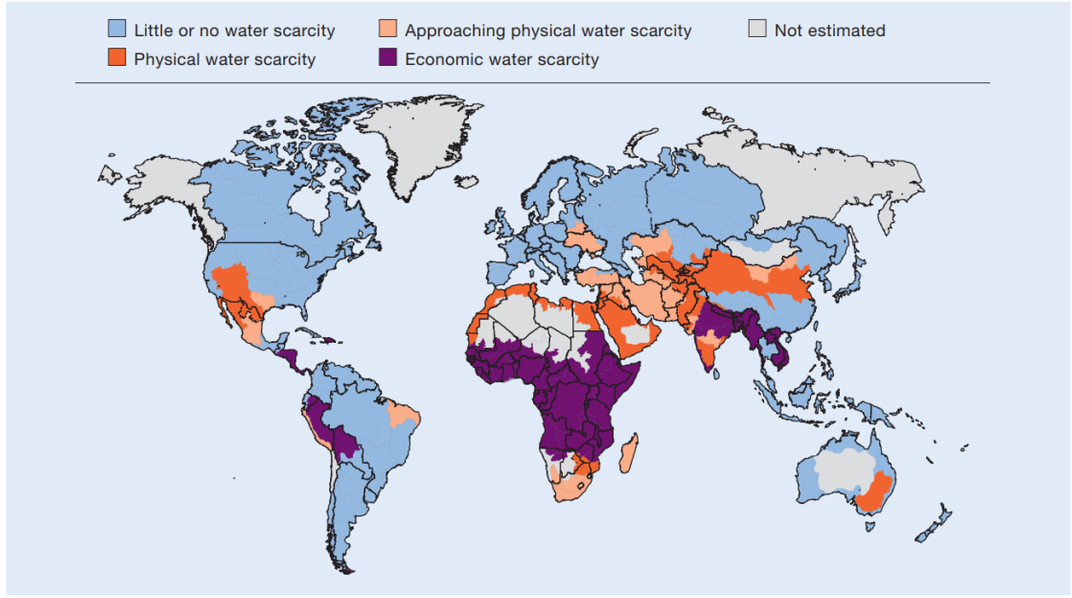

Figure B3: Global distribution of areas of physical and economic water scarcity (Molden D., 2007)

Much of Sub-Saharan Africa is characterized by economic scarcity, so further water development could do much to reduce poverty (Molden D., 2007). Economic water scarcity results in difficulties accessing enough water for agriculture or drinking. In addition, even where infrastructure exists, the distribution of water may not be fair.

Thus, communities in regions characterised by economic scarcity lack access to safe water at their premises and have to rely on other means to have access to water (Figure B4).

Figure B4: Water deposit being filled with tanker truck, Kenya, 2011. Photographed by Jo Harrison/Oxfam

Infrastrucutre and Water Scarcity – In Focus

Thus, the primary reason for the lack of water supply and water management infrastructure lies in the broader context of underdevelopment, as these regions also lack access to other critical infrastructures, such as electricity.

This can be easily visualised by looking at the electrical grid map of the world in Figure B5. In fact, the regions of the world with the least access to safely managed drinking water, which are Sub-Saharan Africa and South-East Asia, can be clearly identified by contrasting with regions such as Europe and North America, where access to safe water reached 95.5% of the population by 2020.

This deeply rooted infrastructural problem is reflected in every aspect related to water supply, availability and access.

Inadequate storage systems result in water scarcity during peak demand periods or in periods of water stress. The lack of access to well-established supply networks leads to difficulties in securing reliable and clean water sources, especially on a daily basis. In addition, treatment facilities are less prevalent and often don't meet international water quality standards, posing health risks to the population.

In contrast, Europe has water supply networks that efficiently distribute water to households and communities, ensuring reliable access. Treatment facilities ensure that water quality complies with rigorous standards, minimising health risks associated with waterborne diseases. Additionally, Europe's advanced storage systems guarantee a steady and secure water supply throughout the whole year, even during unexpected situations or disruptions.

Thus, it is clear that the main reason behind the lack of access to safely managed drinking water in the most affected regions of the world is economic and lies in the severely undeveloped water infrastructure.

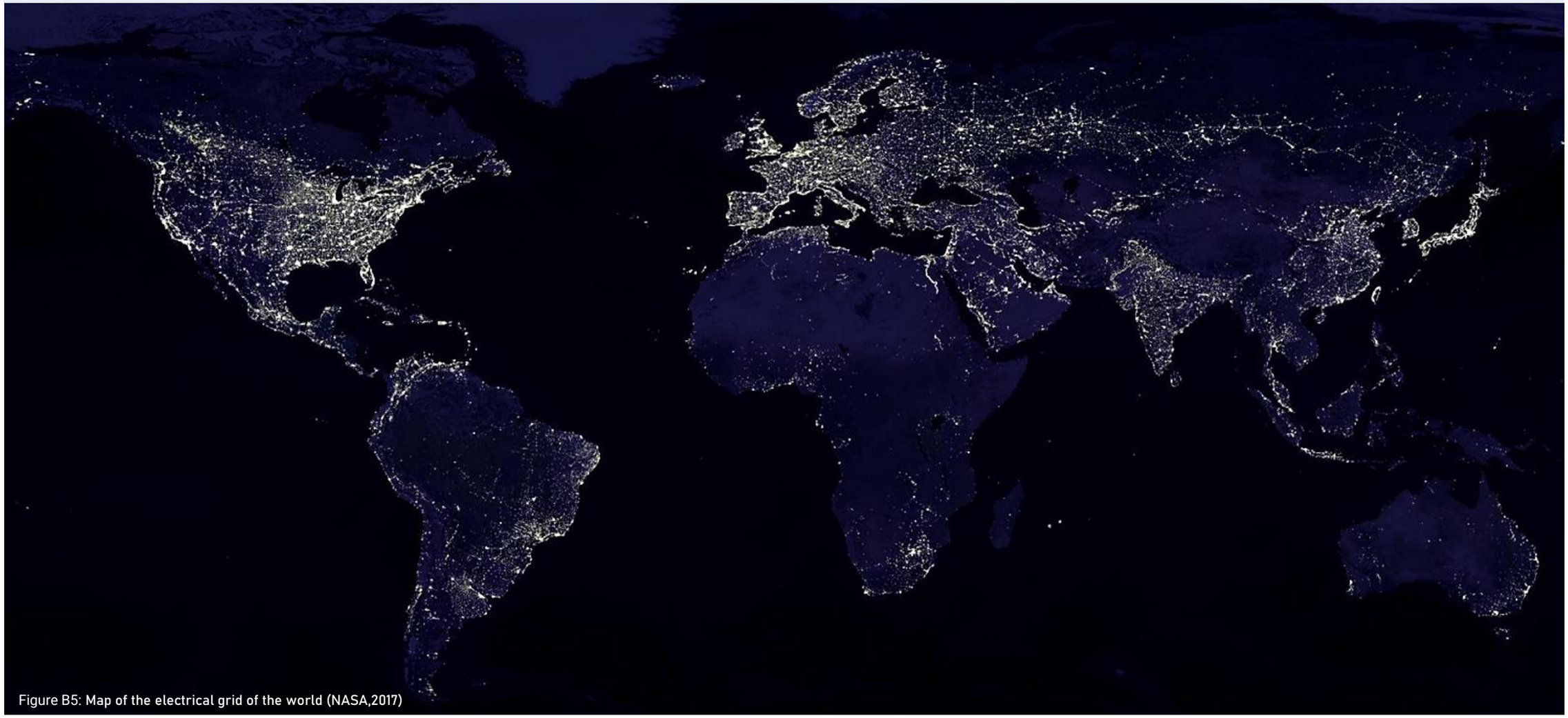

Figure B5: Map of the electrical grid of the world (NASA,2017)

Appendix C – Timeline of Thermodynamic Solar Pumps

The timeline starts with the dawn of solar-powered water pumping experiments. During the pioneering stage, the focus was on putting together functional stand-alone systems, making use of well-established thermodynamic cycles. In this nascent phase, efficiency and cost-effectiveness were no great concern.

1900-1950	1950-2000	2000-FUTURE

A. Eneas, 1901

California, United States of America

During the early decades of the twentieth century, there were a series of significant experiments. Among the pioneering solar pumps was the installation led by A. Eneas in California in 1901, Figure C1.

Figure C1: Eneas' solar-powered irrigation installation. Photography from South Pasadena Public Library

The pump consisted of a 10.2-meter diameter with a central opening of 4.6m truncated cone reflector with 1788 flat mirrors (Figure C2). The system was mounted on a clock-driven equatorial axis to track the sun (Pytlinski, 1978).

The design redirected radiation onto a central 4-meter-long tube boiler with a volume of 0.38m^3 of water and 0.20m^3 for steam generation. At a pressure of 1.03 MPa, the steam-propelled condensing engine coupled to a centrifugal pump.

The system was able to pump water at a rate of 5.3m^3 per minute, overcoming a 3.6m head. The peak power was around 10 horsepower or 7.35 kW.

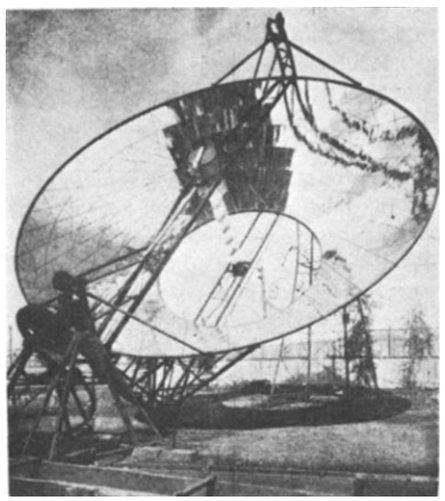

Figure C2: Eneas' solar-powered irrigation installation (Pytlinski, 1978).

Shuman, 1911

Pennsylvania, United States of America

In 1910, Shuman introduced a lamellar boiler comprising two copper sheets with a 5-centimeter gap and a black top plate. The goal was to generate saturated steam. However, steam was not experimentally achieved (Pytlinski, 1978).

In 1911, Shuman acted on this insight by adding a series of flat reflecting wings. These focused the radiation onto the boilers. In total, twenty-six linked arrays, with a total area of 956.5 m^2, were assembled (Figure C3). The setup was east-west aligned, eliminating the need for solar tracking (Pytlinski, 1978).

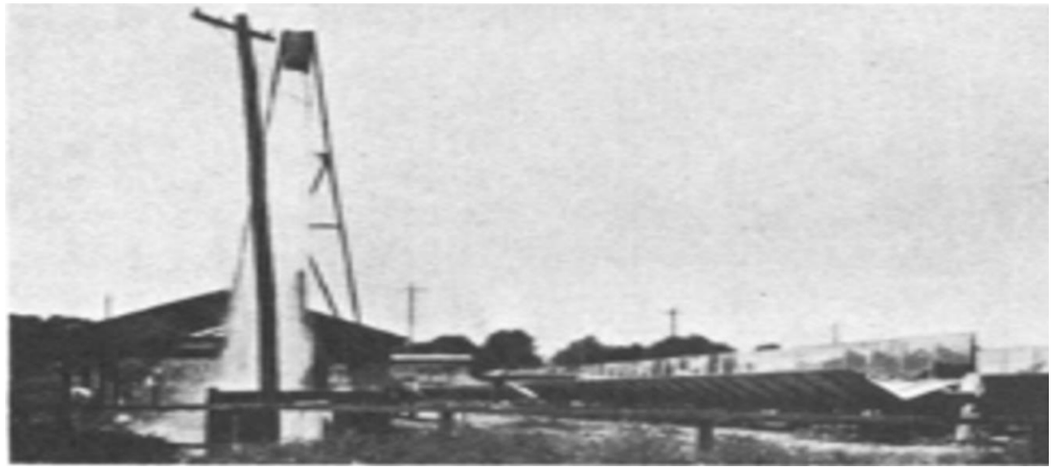

Figure C3: Shuman's solar-powered irrigation installation. (Pytlinski, 1978)

This pumping plant showcased improved numbers, pumping 11.3m^3 of water per minute to a height of 10m. This translated to a peak power output of 24 hp (17.9kW) being generated by the steam engine (Figure C4), while the daily average stood closer to 16 hp (11.9kW).

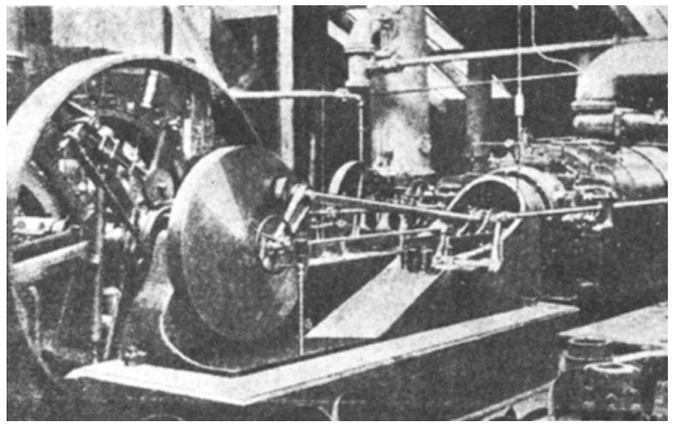

Figure C4: Shuman's low-pressure steam engine (Pytlinski, 1978).

Thermodynamic Solar Water Pumps – Timeline

Shuman and C. Boys, 1913

Meadi, Egypt

Following the successful plant from 1911, Shuman and C. Boys established a substantially improved irrigation plant in Meadi, Egypt, in 1913, where the potential for such a pump was greater (Pytlinski, 1978).

The main changes were to the flat reflectors, which were now parabolic mirrors, channelling the radiation to glass-covered boiler tubes aligned along the focal axis, as seen in Figures C5 and C6.

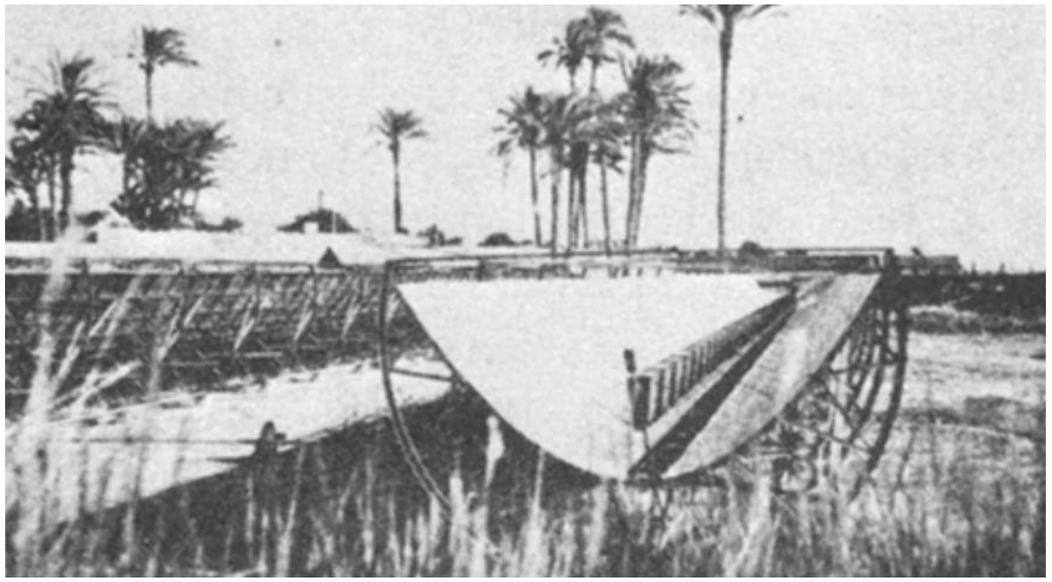

Figure C5: Shuman and Boys' solar-powered irrigation installation (Pytlinski, 1978).

With an optimised parabolic concentrator that yielded a total area of 1280.8 m^2, the power plant generated up to 73 hp, equivalent to 54.4 kW.

Shuman and Boys recognised that such an improvement in output power was justified not only by the refined design but mainly by the greater solar harnessing potential of such a region.

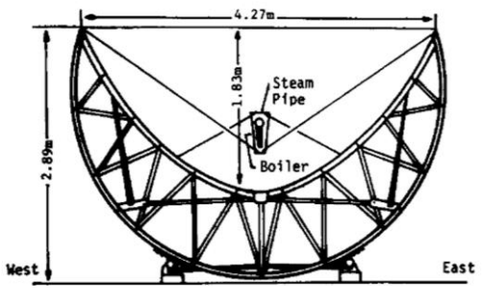

Figure C6: Shuman and Boys' parabolic collector (Pytlinski, 1978).

Insights

- Since the very beginning of the 20th century, researchers and innovators recognised the potential of harnessing solar energy to address water challenges. Their endeavours have led to the development of solar-powered water pumping systems, where solar energy is transformed into mechanical energy and, ultimately, used to pump water.
- As thermodynamic cycles and heat engines were the available and leading power-generating technology at the time, the earliest developments of solar-powered water pumps were clever adaptations of these well-known working principles.
- Most of the first solar-powered water pumps were based on the Rankine cycle and were characterised by their inefficiency and large collecting areas, some reaching over 1000 m^2.
- Running a solar-powered Rankine cycle with water as the working fluid was not feasible with just flat plate collectors, as water would be hard to boil. Thus, the first solar-powered cycles were implemented with parabolic collectors. This increased the complexity of the system and its cost.

Thermodynamic Solar Water Pumps – Timeline

1900-1950	1950-2000	2000-FUTURE

After decades of development, efforts shifted towards more efficient or simpler thermodynamic cycles. In the search for efficiency, refrigerant liquids with lower boiling points were introduced. In addition, other technologies were developed, and the Stirling engine gained popularity.

SOFRETES, 1969

Bossey Bongou, Nigeria

In 1969, the French Society for Thermal Studies and Solar Energy (SOFRETES) installed a solar pump for a small village in Bossey Bangou, Nigeria (Figure C7).

Figure C7: SOFRETES water pump installation in a small village in Bossey Bangou, Nigeria (Caille F., 2017).

The pump consisted of 27 flat plate collectors featuring 66m^2. This relatively small installation had, as core components, a two-cylinder expansion engine, a hydraulic press, and a diaphragm pump (Figure C8). It relied on water as the primary heat transfer fluid, with heat transferred from water to the working fluid R100.

The pump had a pumping capacity of 30 cubic meters per day and could operate within a pumping head range of 12m to 20m. Seven similar pumping plants were installed in multiple places in Africa.

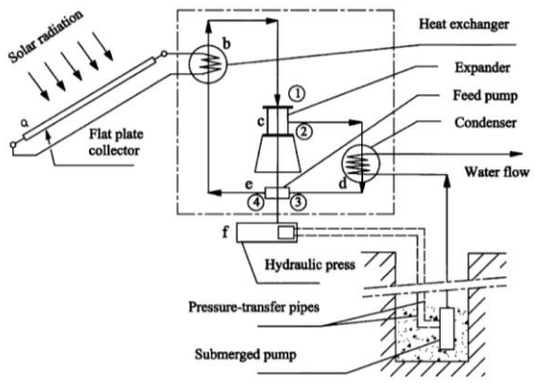

Figure C8: Schematic of SOFRETES solar water pump. (Wong and Sumathy, 1999)

SOFRETES, 1976

Guanajuato, Mexico

In 1976, the same company, SOFRETES, installed a larger solar water pumping station in Guanajuato, Mexico (Pytlinski, 1978). This remarkable installation covered an impressive area of 2499m^2 using flat-plate collectors to collect solar energy (Figure C9).

Figure C9: SOFRETES solar-powered water pumping plant in Guanajuato, Mexico (Pytlinski, 1978).

The station's operation was quite sophisticated (Wong and Sumathy, 1999). The running hot water heat in the collectors was brought to a central heat exchanger, transferring its heat to the working fluid, Refrigerant 11. The condensation of the working fluid powered the vapour turbine, which was coupled to an electric generator to generate 30kW of electrical power.

This power drove two pumps, enabling the station to supply approximately 1000m^3 of potable water each day to the nearby community of San Luis de la Paz.

Until its closing in 1983, the company SOFRETES built more than 90 thermodynamic solar installations in Africa, Mexico and the Middle East. Most of them have now disappeared due to a lack of maintenance or competition from generators. However, considering their ingenious solar-powered operation, they can still offer relevant solutions for the environmental and climatic challenges faced today.

Thermodynamic Solar Water Pumps – Timeline

1900-1950 | **1950-2000** | 2000-FUTURE

ADDS, 1998

Arizona, United States of America

The Advanced Dish Development System (ADDS) project focused on extending the application of Dish-Stirling systems to water pumping by improving its reliability and incorporating advanced components (Figure C10).

Figure C10: ADDS Dish-Stirling system (Mancini et al., 2003).

The system starts after detecting that solar irradiation is within specifications by tracking the sun, starting the heat engine, and supplying electrical power (Mancini et al., 2003). The system produces up to 11 kW at optimum conditions and can be deployed in large-scale applications.

This energy is then used to drive a conventional submersible water pump, a 3-phase 480-V with 10hp, which translates to 7.5kW.

The ADDS system has demonstrated a peak efficiency of 24.5%. The estimated annual performance for the system operating in Huachuca, Arizona, is energy production of 17353 kWhrs and an annual efficiency of 18.9%.

Insights

- Parabolic solar concentrators represent a significant increase in the costs of the water pumping installation. This is due to the need to track and follow the sun's orientation to ensure that the radiation is being concentrated at the desired focal point. Thus, solar concentrators require movable structures that are expensive. In addition, parabolic geometries are also more expensive, harder to manufacture, and more costly to maintain. As a result, installations in the desired African communities opted for flat-plate collectors that were easier to maintain.
- As the efforts shifted towards more efficient or more cost-effective thermodynamic cycles, there were various Rankine-based installations making use of flat plate collectors. However, these had to use other working fluids with lower boiling temperatures. These fluids, usually referred to as refrigerants, represent a significant increase in the cost of the system. In addition, there is a risk of water contamination as the fluids are environmentally hazardous.
- At the end of the century, innovative power plants making use of the Stirling Cycle gained popularity as the technology proved more efficient and more cost-effective (Muhammad Z.M., 2022).
- Thermodynamic cycles are more efficient and work more effectively if higher temperatures are achieved, $\eta_{Carnot} = 1 - {}^{T_C}/_{T_H}$ (Shapiro, 2014). This means that although the Stirling cycle can work with low-temperature differences, it is more efficient at higher-temperature differences. To achieve this improved performance, solar-powered Stirling cycles are implemented with parabolic collectors, again increasing the complexity of the system and its cost.

Thermodynamic Solar Water Pumps – Timeline

In the 21st century, thermodynamic solar-powered pumping plants have shifted towards low-heat-grade cycles or larger power plants with new functionalities. This was caused by the advancements in PV technology that made solar energy harnessing more versatile and accessible than ever.

EuroDish, 2001

Almería, Spain

In 2001, two 10 kW EuroDish units, shown in Figure C11, were installed at the Plataforma Solar de Almeria in Spain (Mancini et al., 2003).

Figure C11: Two 10-kW SBP Eurodish prototypes at Plataforma Solar de Almería, Spain (Mancini et al., 2003).

The 8.5m diameter concentrator consists of a thin shell and a glass-fibre-reinforced resin sandwich with mirrors applied to its surface. The concentrator is supported by a space frame ring truss that is rotatable. To simplify shipping, the shell is divided into 12 identical segments that fit into a standard container for assembly at the site.

The Stirling engine used in this system is the SOLO 161, (Figure C12). The first measurements of peak system efficiency resulted in 20%. The annual performance of a EuroDish system estimation is the production of 20252kWh of electric energy and an annual efficiency of 15.7%.

Figure C12: The 10-kW SOLO 161 V160cc engine and receiver (Mancini et al., 2003).

The production costs were high at about $ 100,000 US per dish system.

Ripasso Energy, 2012

Upington, South Africa

Ripasso Energy was founded in 2008 in Sweden with the aim of developing and commercialising Stirling engine technology (Coventry and Andraka, 2017). One of their plants, seen in Figure C13, is installed near Upington, South Africa, where the solar irradiation levels are among the highest in the world.

Figure C13: Ripasso test site at Upington, South Africa (Coventry and Andraka, 2017).

The system consists of a dual-reflector dish that uses a Stirling engine from Kockums and a tracking system provided by Titan Tracker, a Spanish company (Coventry and Andraka, 2017).

The two times 30 kW three-phase AC dishes feature carousel-style movement in azimuth rotation and a cradle-like structure for elevation rotation. The reflector consists of a lightweight truss support and mirrors made of glass mirrors that are bonded to reinforced plastic composite.

In 2012, this Ripasso Energy electrical power plant set the current solar-to-electric efficiency record of 32% on a 28°C day.

Thermodynamic Solar Water Pumps – Timeline

In the 21st century, thermodynamic solar-powered pumping plants have shifted towards low-heat-grade cycles or larger power plants with new functionalities. This was caused by the advancements in PV technology that made solar energy harnessing more versatile and accessible than ever.

SunPulse, 2001

Tamera, Portugal

The SunPulse Water seen in Figure C14 is a solar water pump with a low-temperature Stirling Engine, running on sunlight and using air as its working fluid (Tamera).

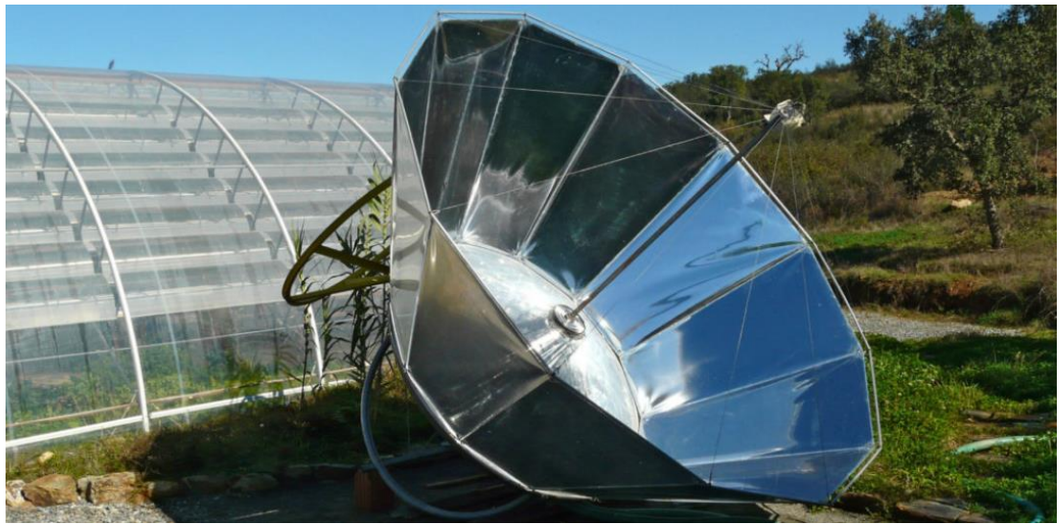

Figure C14: Tamera SunPulse Water Stirling solar water pump (Tamera).

The stand-alone pump is started by manually rotating the flywheel, starting the engine. The prototype uses a reflective mirror made of 0.1mm thick reflective polymer films inflated with air pressure over a lightweight aluminium frame (Figure C15). This innovative collector concentrates the solar radiation that is used to power a Stirling engine coupled with a hydraulic press. With an output hydraulic power of 300W, it is ideal for decentralised water provisioning without any additional infrastructure.

Figure C15: Tamera SunPulse Water pumping water (Tamera).

Crescent Dunes Solar Energy Project, 2015

Tonopah, United States of America

The Crescent Dunes Solar Energy Project, situated approximately 300 kilometres northwest of Las Vegas, is a solar thermal power facility with an output power of up to 110 MW and 1.1 GWh of energy storage (Boretti A., 2020). Its innovative technology consists of a central receiver tower, where 32000 tons of molten salt stores heat energy. As it can store heat, this power plant presents a great advantage as it also supplies solar energy during the nighttime (Figure C16).

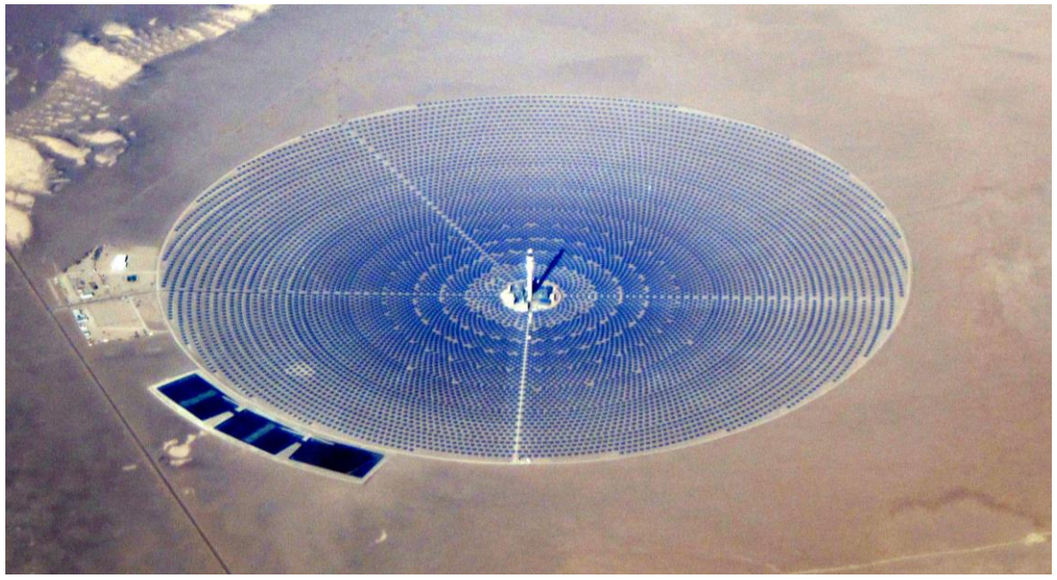

Figure C16: Crescent Dunes Solar Energy Project plant (Boretti A., 2020).

The plant consists of 10347 heliostat mirrors, which reflect and concentrate the radiation onto a central 200-meter-height tower. Each heliostat comprises 35 mirror facets. The combined solar field has a gigantic 120 hectares of collecting area.

The heat stored at the tower is used to generate steam and produce electricity through a Rankine cycle.

However, the electricity generated by the Crescent Dunes project comes at a higher cost compared to surrounding photovoltaic solar plants, mainly due to the investment cost of around 1 Billion dollars. The operating costs are around $135 per MWh, compared to the more cost-effective rate of under $30 per MWh available from the relatively close photovoltaic solar farm in Nevada.

Thermodynamic Solar Water Pumps – Timeline

1900-1950	1950-2000	2000-FUTURE

Insights

- The Stirling cycle is now the most applicable thermodynamic working principle with the most potential. The technical feasibility of Stirling solar dishes has been successfully demonstrated in multiple regions of the world, offering high levels of performance. However, the working principle still has some disadvantages, such as the manufacturing and operating costs, and it does not self-start, needing an extra system for that.
- As a result, the primary application of solar-powered Stirling cycle systems is geared towards electricity generation connected to electrical grids, given the reliance on external energy for starting.
- Advancements in photovoltaic technology pose a growing challenge to traditional thermodynamic solar-powered plants. Photovoltaic solar panels continue to become more accessible, emphasising their cost-effectiveness. This competition with photovoltaic panels, coupled with the maturity of the Stirling cycle, points towards a confirmation of this trend. Thus, only a significant breakthrough innovation will impact the future of solar-powered water pumping systems.

Appendix D – Shape Memory Alloys

Shape Memory Alloys represent a promising breakthrough in harnessing solar energy for water pumping. This chapter introduces these materials and their properties, providing the background knowledge required.

SMAs are a class of smart materials characterised by their ability to change between two distinct solid phases: martensite and austenite. This phase transformation can be started by heating or cooling beyond specific transformation temperatures, resulting in substantial and fully reversible strains (Figure D1). These strains and the stresses associated with them can be used in various applications, particularly in actuator mechanisms.

In addition, the main characteristic that brought significant attention towards these materials is their exceptional ability to "remember" and revert to a different shape upon being heated above certain temperatures. This phenomenon, referred to as the Shape Memory Effect (SME), is a consequence of the material's structural reorganisation into a predefined or pretrained austenitic structure during the phase transformation triggered by heating.

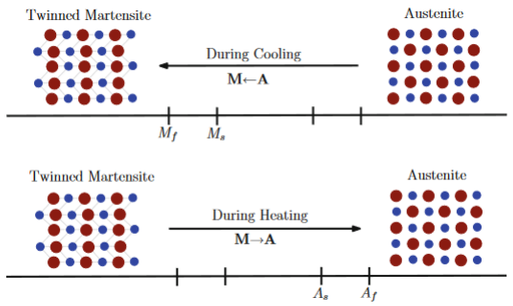

Figure D1: SMA phase transformation (Rao et al., 2015).

While various materials, ranging from metallic alloys to plastics, have the Shape Memory Effect, the primary objective in this application is to maximise mechanical output while minimising costs. Among all the Shape Memory Materials available, NiTi alloys stand out as the most promising choice (Table D1). These alloys are renowned for their strength, fairly widespread availability, and corrosion resistance, making them the most suitable for this project's purpose.

Table D1: Comparison of some important properties of three commercially available SMA's (Rao et al., 2015)

Properties	NiTi	CuZnAl	CuAlNi
Specific heat (J/Kg°C)	450–620	390–400	373–574
Thermal conductivity (20°C) $\left(\frac{W}{mK}\right)$	8.6–18	84–120	30–75
Density $\left(\frac{g}{m^3}\right)$	6.4–6.5	7.54–8	7.1–7.2
Latent heat (kJ/Kg)	19–32	7–9	70–9
Electrical resistivity (10^{-6} Ωm)	0.5–1.1	0.07–0.12	0.1–0.14
Thermal expansion coefficient $\left(\frac{10^{-6}}{K}\right)$	6.6–11	17	17
Maximum recovery stress (MPa)	500–900	400–700	300–600
Normal working stress (MPa)	100–130	40	70
Maximum transformation strain (%)	6–8	4–6	5–6
Young's Modulus (GPa) (M and A)	28–83	70–100	80–100
Transformation temperature range (°C)	(–200) to 200	(–200) to 150	(–200) to 200
Maximum overheating temperature (°C)	400	150	300
Melting, casting and composition control	Difficult	Fair	Fair
Forming (rolling, extrusion)	Difficult	Easy	Difficult
Cold-working	Fair	Restricted	Difficult
Machinability	Difficult	Very good	Good

The output of mechanical labour is the result of the loading condition at the Shape Memory Alloy. This loading can be done in multiple ways, including working conditions of normal tension, compression, bending and torsion (Figure D2).

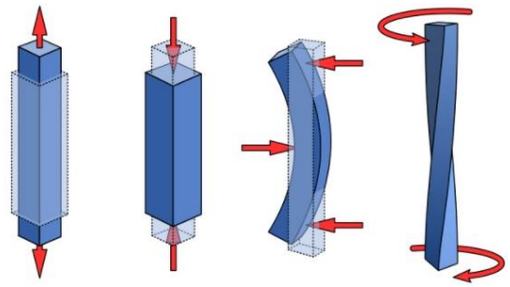

Figure D2: Deformation modes (adapted from Wikipedia, 2023).

From which, the normal tension configuration is the one that provides the highest conversion efficiency and longevity of the SMA, being able to achieve up to 1 million cycles compared to 10000 cycles for bending and torsion configurations. (Jani J.M. et al., 2017).

Regarding the geometry of the SMA working under normal tension, wire configurations prove to be the most effective choice, as evaluated in Table D2 (Jani J.M., 2016). In fact, wires excel in traction conditions due to their geometry, offering strong mechanical properties. Wires are also easy to manufacture and cost-effective, making them a feasible and viable option.

In addition, wires have a good surface-area-to-volume ratio, which makes them more responsive to heating and cooling through convection or conduction.

Moreover, the SMA wire's austenitic crystalline structure can be set during the cooling down phase after extrusion when manufactured. This means that there is no need for additional heat treatments, making the manufacturing process simpler and more cost-effective.

Table D2: SMA linear actuator form and shape comparison (Jani J.M., 2016)

Actuator form	Properties	Remarks
Wire	▪ Actuation stroke up to ca. 5% strain. ▪ Actuation force up to 200 MPa (full stroke) or 350 MPa (reduced stroke) for trained NiTi actuators. ▪ Very moderate dynamic requirements (less than 1 Hz). ▪ On-Off actuation. ▪ Translational movement or rotation angles less than 90. ▪ Fatigue cycles up to 10^6.	▪ Optimal usage of material where minimal use of material for amount of work generated. ▪ Tension loading: produces highest efficiency compared to other load types.
Spring	▪ Recommended to apply external heat source for heating. ▪ Any kind of stroke, but typically less than 30mm. ▪ No dynamic requirements. ▪ Actuation force up to 200 MPa (full stroke) or 350 MPa (reduced stroke) for trained NiTi actuators. ▪ Translational movement. ▪ Fatigue cycles up to 0.5×10^6	▪ Large macroscopic displacement out of a relatively small microscopic strain, but the stress distribution over the cross-section of the spring is not constant. ▪ Need greater material volume to generate the same force (low efficiency than wire). ▪ Poor dynamic response (low bandwidth) due to the larger material (low surface area-to-volume ratio). ▪ Only the outer surface actually contracts, but the inner surface acts as both heat dissipater and opposing force to the desired direction.

Regarding the working conditions of SMA wire in linear actuation, the wire can be used under constant load, constant displacement or in a simultaneous load-displacement case.

Figure D3 shows the constant load configuration.

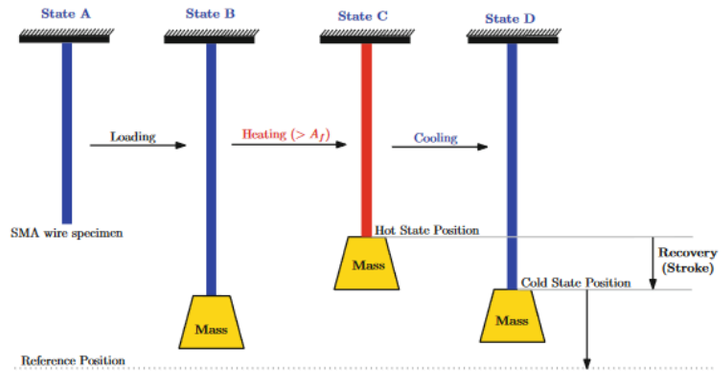

Figure D3: Schematic of Shape Memory Alloy response to heating and cooling under constant load(Rao et al., 2015)

Figure D4 shows SMA wire loading responses linearly approximated at three different temperatures above Af and a detwinning response at temperatures below Mf.

If an SMA wire, under constant external load, is heated from its martensitic state, it contracts to its austenitic state, creating a length displacement that is referred to as stroke. The net stroke under the same external load can be varied by changing the temperature up to which the wire is heated. The circular points on the responses between the cold martensitic state and hot austenitic state illustrate the effects of changes in operating temperature on the stroke.

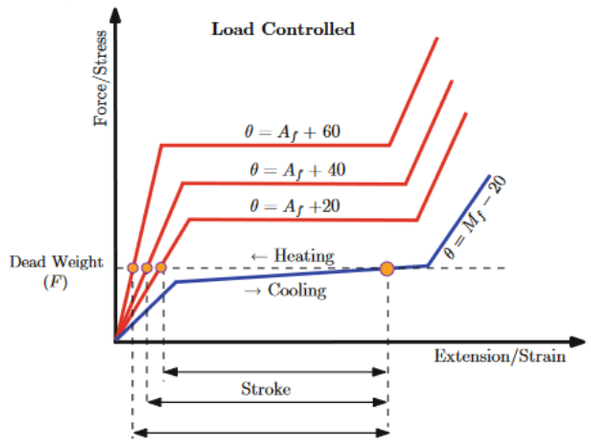

Figure D4: Linearised SMA wire response in its austenite and martensite state under constant load (Rao et al., 2015)

Similarly, in a displacement-controlled setup, an SMA wire under constant strain/deformation can provide a differential recovery/pull force under different operating temperatures. As shown in Figure D5, the net recovery pull force between the martensitic and austenitic states can be varied by changing the temperature up to which the wire is heated.

However, SMA wires are rarely used in this configuration as it does not produce any mechanical labour.

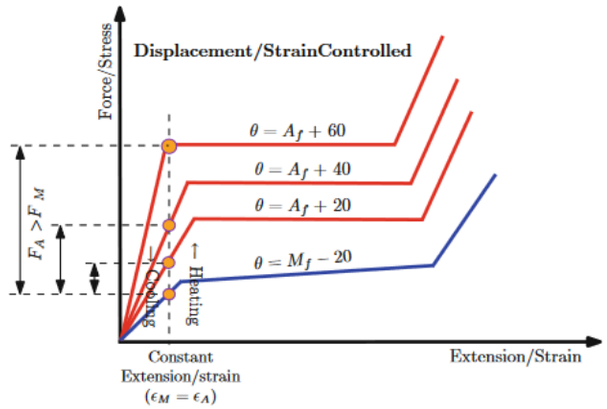

Figure D5: Linearised SMA wire response in its austenite and martensite state under constant strain (Rao et al., 2015)

More often, SMA wires are coupled with other passive structural members to reset the SMA wire back to its original state when cooled. For example, a simple arrangement of SMA wire and bias spring combination is shown in Figure D6, where the SMA wire must overcome the bias spring stiffness for the system to actuate.

When the temperature of the system is raised above Af, the system will acquire a position B where the SMA wire is in its austenitic state, causing a recovery pull force which forces the extension of the bias spring. State B can either be C or D depending on the temperature at which the SMA wire is heated above Af. Upon cooling to temperatures below Mf, the system returns back to position B, i.e. the original state, where the extended bias spring overpowers the stiffness of the martensitic SMA wire.

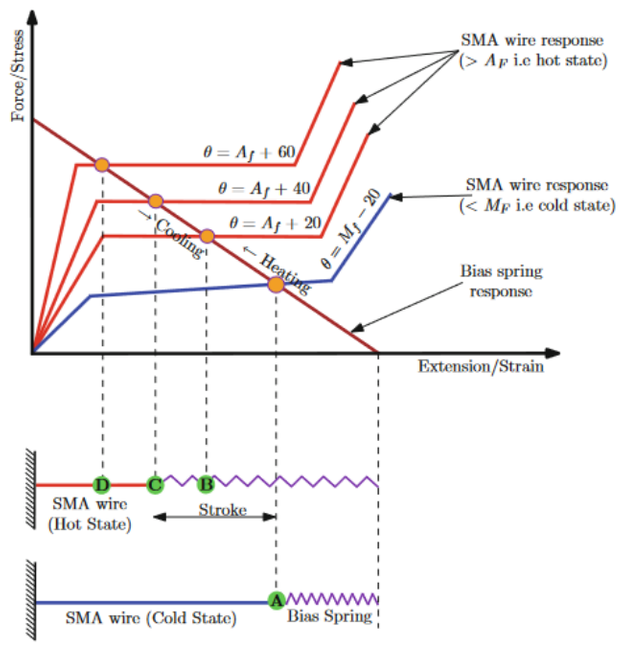

Figure D6: Linearised SMA wire response against a biased spring in its austenite and martensite state (Rao et al., 2015)

From the various combinations of loading conditions, the one that is able to output the higher strokes is the constant load. This is explained by the stress-strain curves that characterise SMA wire behaviour in Figure D3.

As seen, in a constant stress situation, when the temperature of the SMA wire is increased, the pair stress-strain point moves to the left in a horizontal line. Since the gap between lines at low temperatures is lower, the strain verified is smaller. However, at a certain stress value, the gap is larger, allowing for higher strains. In addition, increasing the constant load and looking now at the top of the curves, this stroke is lower again. Highlighting that there is an optimal load window for increased strains.

The ultimate working window is the one optimising output work given by W= F*Δx without compromising the lifespan of the wire.

For reference, Table D3 shows the relationship between the experimental heating pull force and cooling pull force and the diameter of the NiTi wire.

Table D3: Experimental responses of different diameter Nitinol wires (Rao et al., 2015)

Diameter (mm)	Resistance $\left(\frac{\Omega}{m}\right)$	Heating pull force (N)	Current estimate for 1s (mA)	Cooling pull force (N)
0.15	55	3.14	410	1.26
0.2	29	5.58	660	2.24
0.25	18.5	8.73	1050	3.49
0.31	12.2	12.55	1500	5.02
0.38	8.3	22	2250	8.83
0.51	4.3	34.91	4000	13.96

SMA Takeaways

- Shape Memory Alloys convert heat into mechanical labour in the phase transformation process that occurs between the Martensite phase ending temperature (Mf) and the Austenite phase ending temperature (Af).
- Nickel-titanium alloys are characterised by their strength, fairly widespread availability, and corrosion resistance.
- SMA actuators are more efficient and have less phase transformation fatigue when working under normal tension.
- The straight wire configuration excels at normal tension, is the most cost-effective and available configuration and has a good surface-area-to-volume ratio.
- The strains are greater at a constant load working condition.

Appendix E – Concept Selection

Goal and Solution Scope

Design an affordable, robust, and scalable SMA-driven solar-heated water displacement pump that can be implemented in the identified regions lacking access to safe drinking water, supplying water to people who have access to an improved water source, but that is not accessible on their premises.

To achieve this, the design challenge can be broken down into the sub-challenges of designing a system that:

1. Harnesses solar energy – maximising the effectiveness-to-cost ratio;
2. Converts the harnessed heat into usable mechanical energy by means of Shape Memory Alloy;
3. Uses this mechanical energy to power a water pump that meets the pumping needs of the implementation sites.
4. Integrates all these subsystems in a standalone solution that is desirable, feasible and viable.

For, it should meet the following requirements:

Requirements

- Power the Local Water Transportation Needs
- Standalone Solution
- Self-starting
- Affordable Installation and Operation
- Robust and Reliable
- Adaptable, Scalable and Versatile
- Wide Operating Working Window
- Sustainable and Environmentally Friendly (non-hazardous, non-toxic).
- Easy to Install
- Easy Maintenance
- Long Life – Minimal thermal fatigue or deterioration.

Conceptualisation – Wishes and Inspirations

The pump was idealised to solve the dire humanity problem and answer the urgent call for action for the specific context of Sub-Saharan Africa and for the implementation in the communities where people have to walk to collect water daily and where the existing infrastructure may be null. Thus, the pump must be a standalone solution without or with minimal reliance on external resources.

In these communities with minimal financial resources, affordability is a must. Only an affordable installation with minimal associated operational costs can make water accessible for all. Thus, the whole system has to be as cheap as possible.

Additionally, in the most affected regions of the world, technology and tools for maintenance can be almost null. As a result, robustness and reliability are as essential as making use of accessible materials and simple geometries, so less technical expertise or complex spare parts are required.

The system is envisioned to make the most of the excessively abundant solar exposition of the African continent to refresh the population with one of their most basic needs.

There was never an illusion of the complexity of the task at hand. However, it can be solved with one small volume of water at a time. As these regions have hours and hours of solar exposition every day, the system pumps for hours a day. Thus, not much water has to be pumped at every cycle. The crucial aspect is to pump regularly while the sun is shining, and the compounding effect will ensure that everyone's daily needs are met.

Thus, like a human heart – which is also a displacement pump – that always pumps blood even without awareness and worries, the solar-heated water pump would harmoniously ensure the vital water supply to the communities in need without the need for vigilance.

Concept 1

Concept 1 is a standalone diaphragm displacement pump with the SMA integrated into the diaphragm membrane (Figure E1).

This concept is designed to be self-starting, with the diaphragm membrane having the solar collector function as well.

Within the membrane, there are SMA tubes that are pre-trained to operate the pump over 3 stages:

Stage 1: increase the volume of the pump when the SMA temp is hot enough.

Stage 2: at this point, the pump is expanded, drawing water into its chamber. This water runs through the SMA tubes cooling them.

Stage 3: with the SMA at the martensitic phase, the biased spring overcomes the SMA force, pumping the water out. When the pump's volume is fully compressed, stage 1 begins as the diaphragm conducts heat to the SMA tubes, making it expand again.

Advantages of this concept include the fact that it is self-starting and a standalone design. However, certain drawbacks need consideration: The SMA tubes, which are essential components of this system, are notably more expensive and may exceed the budget constraints of the project (Figure E2). Additionally, the SMAs would work under bending, which is not the most efficient working condition.

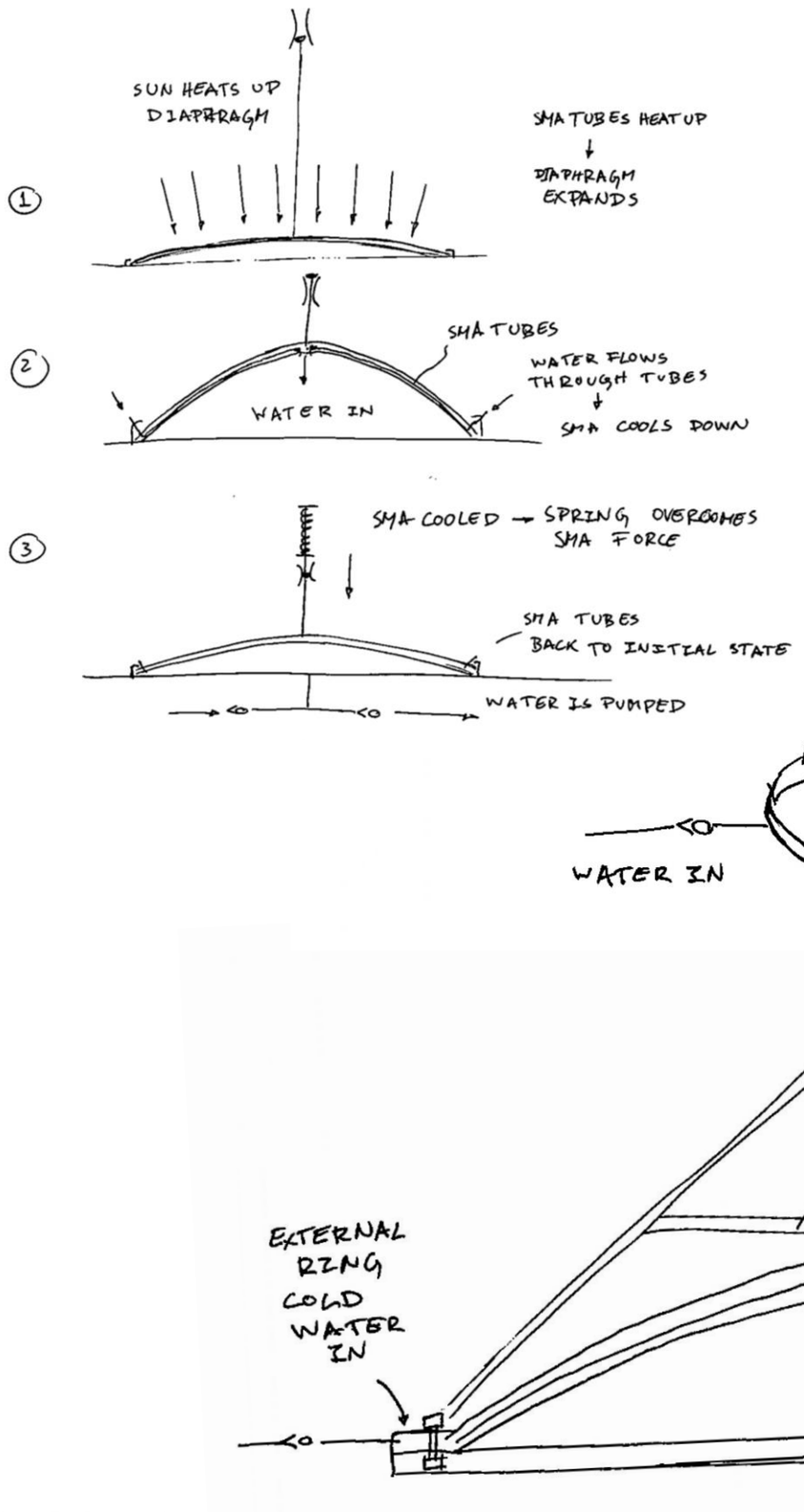

Figure E1: Concept 1.

NITI • NITINOL SMA TUBE; 2.1MM ID, 2.7 OD, AF 70°C

€218,95

Length

100 mm | 150 mm | 200 mm | 250 mm | 300 mm | 350 mm | 400 mm
450 mm | 500 mm | 550 mm | 600 mm | 650 mm | 700 mm | 750 mm
800 mm | 850 mm | 900 mm | 950 mm | 1000 mm | 1014 mm | 1030 mm

Quantity

- 1 +

Figure E2: Cost example of SMA in the tube shape.

Concept 2

Concept 2 is again a displacement pump actuated by SMA wires that are alternatively heated and cooled down through hot and cold water flows (Figure E3).

The heat source is the heated water inside the sun collector. The cold water source can be the pumping water itself or a closed circuit cooled by the pumping water.

These water flows are electronically controlled. The control system is powered by a small photovoltaic panel that harnesses enough energy to power the DC pumps and the valve.

Despite having an electronic control system, the pump is still powered by the contraction and expansion of the SMA wires. These wires are inside cooling lines, meaning that, with the alternate hot and cold flow, their temperature and, thus, phase can be controlled

When the hot water flows through the wires, the SMA contracts, pumping water out. Similarly, when the cold water flows through the wires, the SMA relaxes, and the biased springs move the piston up again, drawing new water into the chamber.

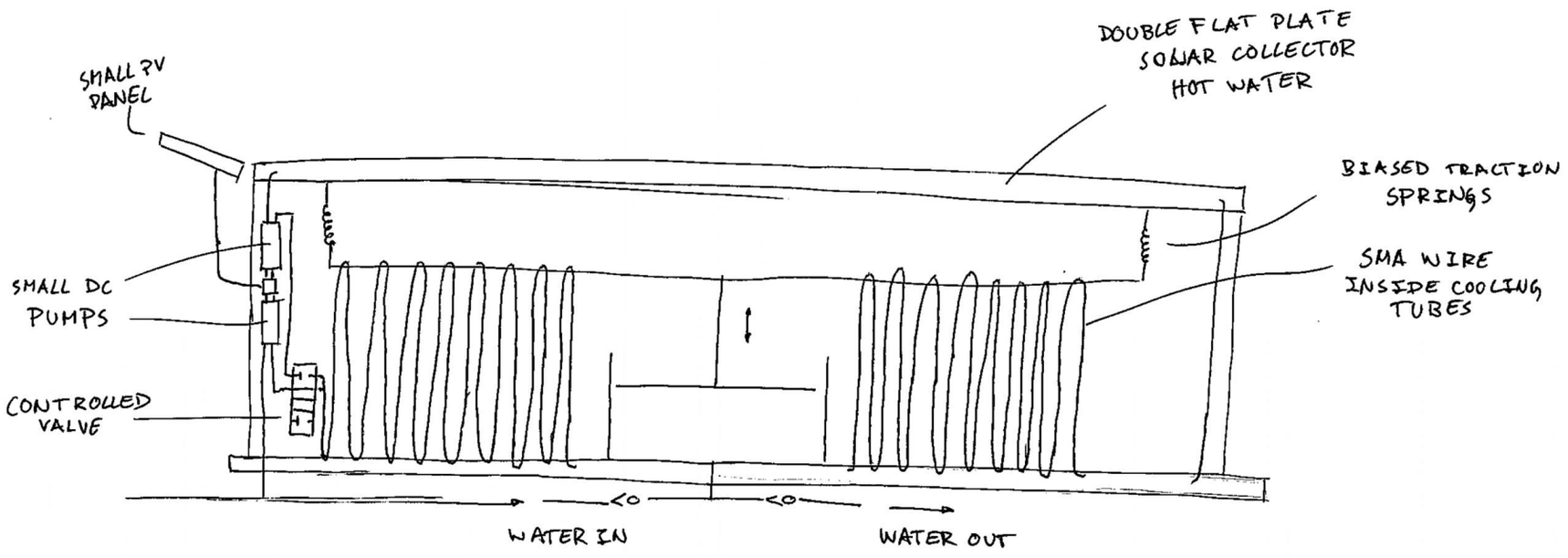

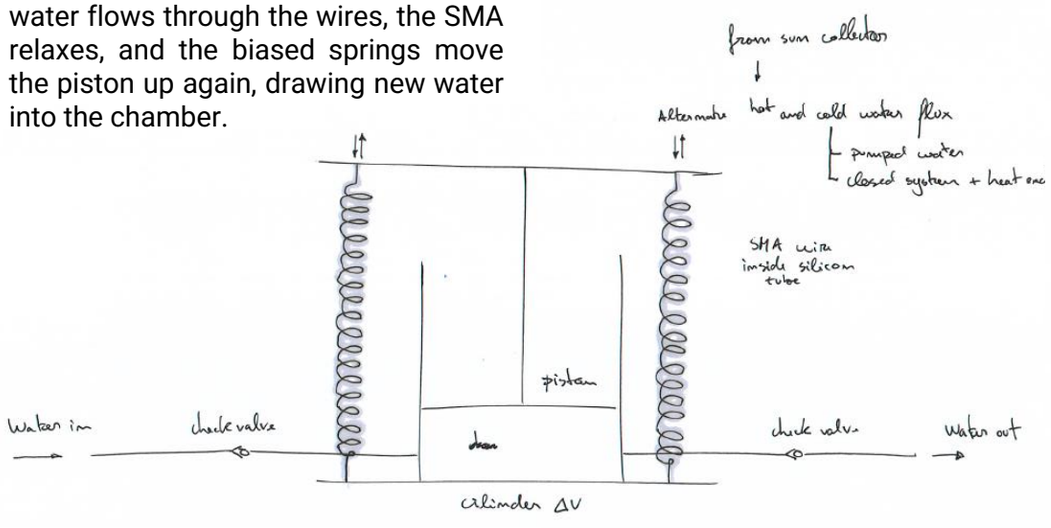

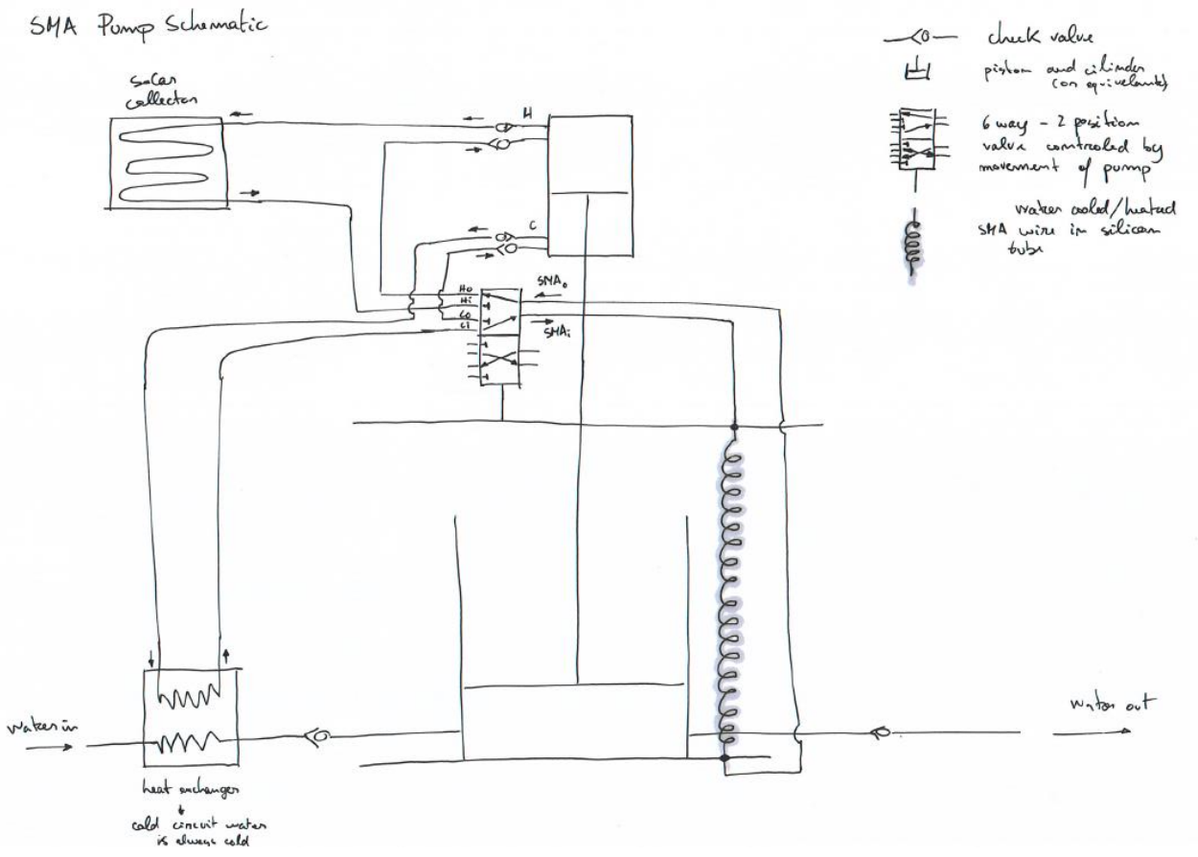

Figure E3: Concept 2.

Concept 3

Concept 3 is a disaggregated pumping system (Figure E4). This approach allows for the optimisation of each variable of the system separately, as it is easier to ensure that every component can work under its optimised working window.

This concept includes a solar collector that builds up heat that is directly transferred to the SMA wires inside it.

These SMA wires work under traction solely. Meaning its elongation and maximum traction tension are also controlled so it always works within its fatigue or mechanical limits.

When the SMA wire is heated up, it contracts, pushing the pump's piston and pumping the water out. At the last moment, the separate flush pump flows cold water through the SMA wire, which releases the tension. As the SMA wire is connected to a traction spring, it elongates, and the piston of the pump is moved again so new water flows in. At this point, the SMA starts being heated up again, making it compress and restarting the cycle.

One of the main advantages of this configuration is that each individual subsystem can be separately designed. This means the whole system can be optimised and easily adapted to the specific needs of the application site. Another advantage is that the SMA wire works under very controllable situations, meaning its working life can be extended.

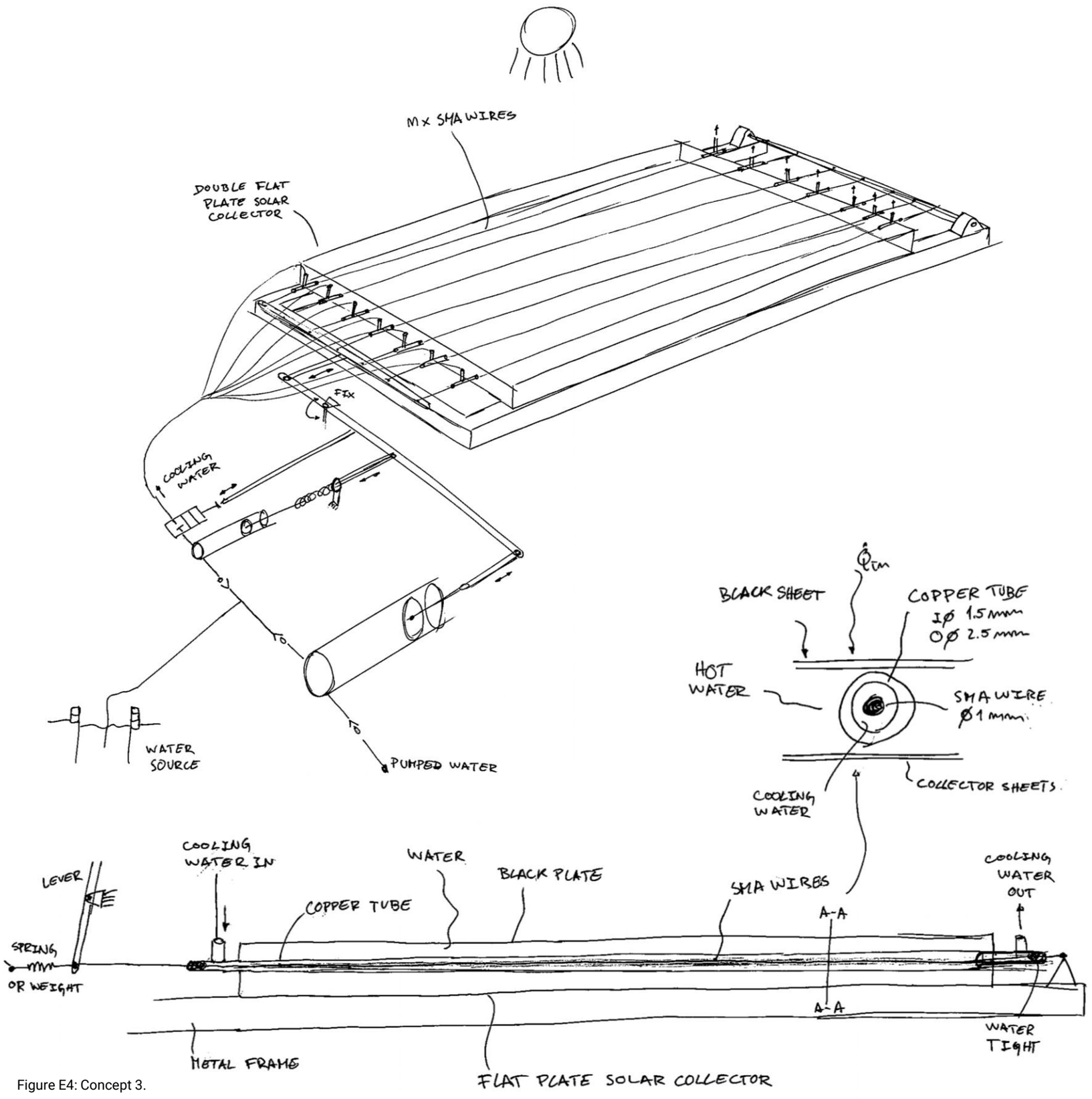

Figure E4: Concept 3.

Concept Selection

Considering the disadvantages and drawbacks of the first two concepts, namely the increased costs, reduced efficiency and lifespan and the need for external controlling systems, it was decided to go with the most valuable concept proposition that overcomes these limitations – concept 3.

This is a very promising concept that is believed can solve successfully the assignment of this thesis and meet the requirements for the pumping system, such as self-starting, affordability, and ease of manufacturing. In fact, if this working principle hypothesis is proven feasible, the pumping system will be a self-starting standalone solution that has the potential to meet all the requirements.

Appendix F – Dimensioning of the Pump

The dimensioning of the pump follows a systematic and logical step-by-step procedure:

1. Quantify water needs

The first step is to quantify the volume of water required to meet the needs of local communities to be covered by the pump.

2. Identify water source

Identify the safe drinking water source from which the pump will extract water (Figure F1).

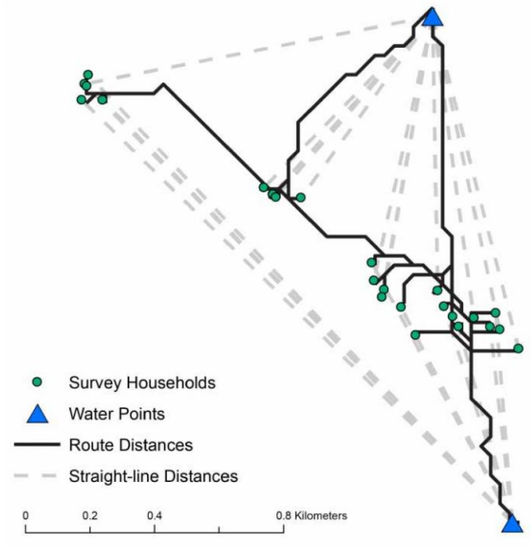

Figure F1: Example of mapped water sources and households in a village in Nampula province, Mozambique (Ho J.V.et al., 2014).

3. Determine the piping network

Design the piping network necessary to distribute water effectively from the identified water sources to the targeted communities' premises.

4. Calculate the pump head

Calculate the pump head and required water volume at each exit point, considering the elevation gains and head losses in the piping network.

5. Calculate required energy

With the pump head and water volume known, the total energy required per day can be calculated.

6. Calculate the solar collecting area

For the specific location, calculate the solar collecting area needed to harness the previously calculated required daily energy during solar exposure hours. For this calculation, the daily average solar irradiance levels can be determined using the global data layers that are available from (The World Bank, 2019) or downloadable and visualised with Google Earth software (Figure F2).

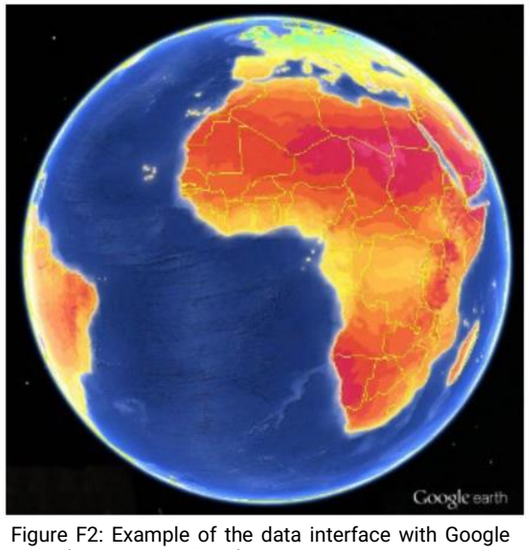

Figure F2: Example of the data interface with Google Earth (Ho J.V.et al., 2014).

This database provides all the required data regarding solar radiation for the correct dimensioning of the system, including irradiation levels, optimal tilt angles, and variances throughout the year per country (Figure F3). Thus, with the performance and efficiency of the solar-heated water pump system known, the collector area and the required number and length of Shape Memory Alloy wires can be determined.

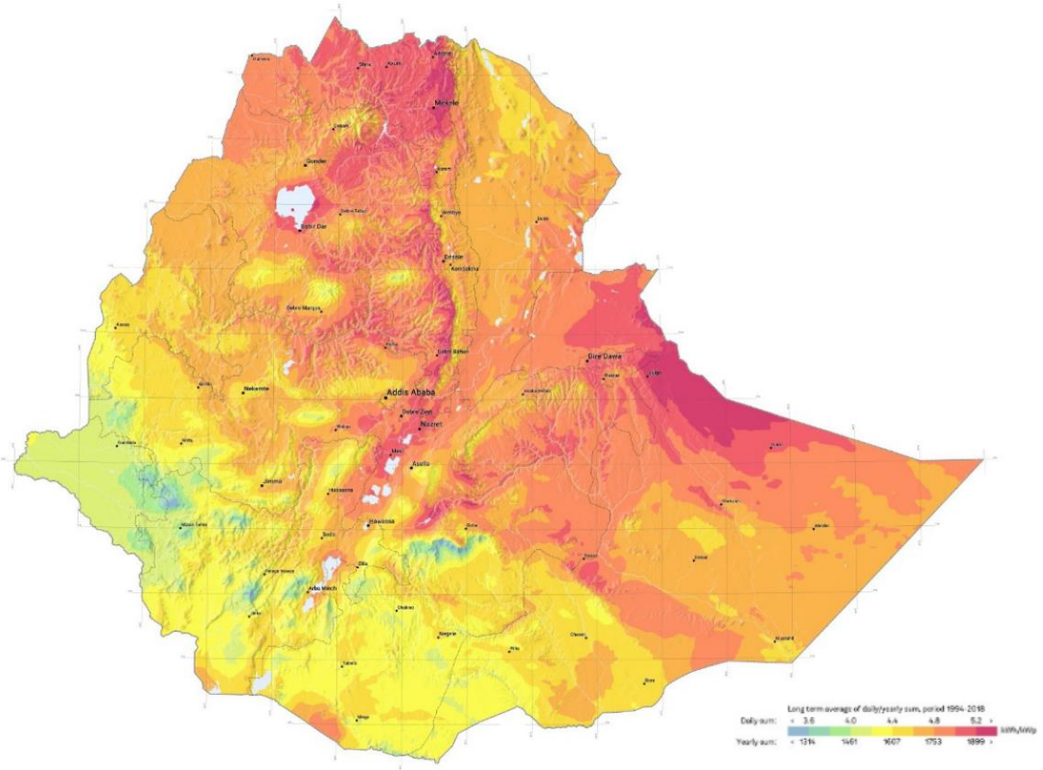

Figure F3: Example of a country (Ethiopia) PVOUT map (World Bank Group, 2020).

7. Dimension the displacement pump

The last step is the dimensioning of the positive displacement pump and the parametric geometry of the system. Having the Shape Memory Alloy wires defined, the mechanical labour produced per cycle must be broken down with the proper lever breakdown ratio (Figure F4). In addition, the correct piston area and pump volume must be dimensioned to meet the pump head and daily volumes defined in the previous steps.

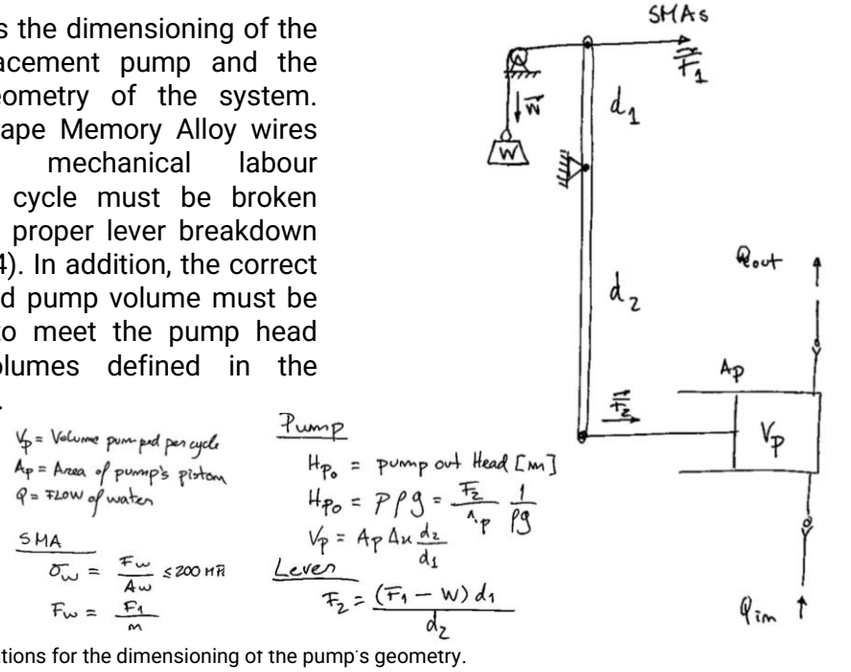

Figure F4: Considerations for the dimensioning of the pump's geometry.